Trinity College Dublin
Coláiste na Tríonóide, Baile Átha Cliath
The University of Dublin

Resting-state electroencephalographic biomarkers for tracking cognitive network dysfunction in Amyotrophic lateral sclerosis

A Thesis Submitted to School of Medicine, Trinity College Dublin,

the University of Dublin, in partial fulfilment of the requirements for the degree of Doctor of Philosophy, 2024

By

Marjorie Metzger

BSc, MSc

Supervised by:

Assistant Prof. Bahman Nasseroleslami

Prof. Orla Hardiman

Declaration, online access and general data protection regulation

I declare that this thesis has not been submitted as an exercise for a degree at this or any other university and it is entirely my own work.

I agree to deposit this thesis in the University's open access institutional repository or allow the Library to do so on my behalf, subject to Irish Copyright Legislation and Trinity College Library conditions of use and acknowledgement.

I consent to the examiner retaining a copy of the thesis beyond the examining period, should they so wish (EU GDPR May 2018).

Marjorie Metzger,

September 2023

Summary

Amyotrophic lateral sclerosis (ALS) is a devastating neurodegenerative disorder primarily characterized by the progressive degeneration of motor neurons. However, the understanding of ALS has evolved beyond its traditional characterisation as solely a motor disorder. It is now recognized as a spectrum disorder, ranging from classic ALS with no cognitive or behavioural changes to ALS with comorbid cognitive or behavioural impairment that may or may not reach the threshold for a diagnosis of ALS-frontotemporal dementia (ALS-FTD). This evolving perspective highlights the complexity of ALS and its diverse clinical presentations.

Neuroimaging and neurobiology studies have revealed that ALS symptoms and their progressions are influenced not only by motor neurons but also by wider dysfunction and atrophy in brain networks. Analysing the spectral, spatial and temporal patterns of brain network dysfunction in ALS and how they relate to clinical presentation can enhance the assessment of disease progression and provide a quantitative foundation for disease stratification. The incorporation of electrophysiological measurements into clinical practice has the potential to predict individual prognoses, to enhance the design of clinical trials by allowing the stratification of patient groups and to offer more objective, quantitative assessments of drug effects based directly on the network disruptions observed in ALS.

In this project, high-density electroencephalography (128-channels) was recorded at rest to interrogate ALS-related cognitive network dysfunction. First, given the prior evidence of non-motor network dysfunction in resting-state EEG and its correlation with cognitive decline, a longitudinal assessment of spectral EEG measures was conducted. This aimed to assess the persistence of ALS-related network patterns over the course of the disease and their association with distinct cognitive phenotypes. Second, clustering techniques were applied to the EEG spectral power trajectories, aiming to identify stable subgroups among ALS patients. These trajectories were correlated with clinical and neuropsychological evaluations to evaluate the effectiveness of network-based measures in understanding disease progression, survival outcomes, and functional decline. Third, microstate analysis was applied to identify and analyse transient, recurrent, and quasi-stable brain states, which are hypothesised to reflect synchronised activity within functional networks. Changes in microstate parameters were explored as potential indicators of modulations in the temporal dynamics of brain networks, potentially associated with cognitive and behavioural impairment. Last, patterns of frequency-specific power and phase-coupling in resting-state EEG were analysed, using a combined Hidden Markov Model and multivariate autoregression approach, to uncover temporal

disruptions in neural activity and functional connectivity within specific brain regions. The identification of spectrally distinct episodes in resting-state activity allowed for the provision of reliable indicators of ALS-related impairment specific to particular brain networks.

This project revealed significant longitudinal changes in neural activity, particularly in the fronto-temporal region, with a decline in lower-frequency (θ-band) and an increase in higher-frequency (γ-band) spectral power. Different ALS subgroups were characterized based on cognitive and behavioural profiles, showing distinct patterns of spectral EEG measure changes associated with cognitive decline, behavioural impairment, and motor decline. Survival was strongly linked to longitudinal changes in functional connectivity between specific brain regions in all subgroups. Clustering of longitudinal neural activity trajectories supported the existence of stable clusters corresponding to clinical profiles. Notably, differences in survival and functional decline were observed between clusters, highlighting the heterogeneity of ALS progression and the importance of studying long-term neural activity patterns in specific subgroups to understand disease advancement, survival outcomes, and functional deterioration.

Despite the identification of abnormal spectral measures in both sensor and source space, which persisted longitudinally, the temporal dynamics of brain networks in ALS remain poorly understood. This research studied the temporal aspects of brain network activity using EEG microstate analysis, revealing that properties of EEG microstates could offer valuable prognostic insights into ALS, particularly regarding cognitive decline. Differences in microstate properties were observed between ALS and healthy-control groups, suggesting dysfunction within somatosensory and attention networks. Moreover, correlations between microstate properties and clinical measures indicated their potential as prognosis biomarkers for ALS and in particular cognitive decline. Additionally, distinct transient brain states with unique spectral characteristics were identified in resting-state EEG. Individuals with ALS exhibited altered dynamics in one brain state associated with the posterior default mode network. These findings demonstrate the importance of dynamic analyses in understanding disruptions within neural networks related to ALS, holding clinical significance for understanding EEG signal alterations in specific functional aspects of the disease.

This thesis focuses on resting-state EEG measures to detect longitudinal neural activity patterns linked to cognitive-behavioural impairments in ALS. Additionally, this work examines patterns, observed in both sensor and source levels, which capture the temporal dynamics within EEG signals. These measures serve to quantify cognitive network disruptions in ALS and have the potential for further development to enhance patient care, assess drug effectiveness, and enable stratification for clinical trials and treatments.

Acknowledgement

I wish to express my deepest appreciation to my supervisors, Dr. Bahman Nasseroleslami and Prof. Orla Hardiman. Dr. Nasseroleslami's unwavering guidance, constant support, and encouragement have been invaluable. His keen oversight has undoubtedly contributed to the accuracy of the analyses presented here. I sincerely extend my gratitude to Prof. Orla Hardiman for her unwavering determination and visionary leadership, which have consistently set a remarkable example and propelled our research to new heights.

I thank the Thierry Latran Foundation for their financial support. Participating in their annual meetings has been both an honour and an interesting academic experience.

I am also indebted to my colleagues from the EXG group and the extended Academic Unit of Neurology. I was very lucky to be able to follow up on the work of Mr. Stefan Dukic and base my projects on such competent and well managed code. His availability and advice were a guiding light. To Mr. Vlad Sirenko, whose project was linked with the Chapter VI of this thesis, and to my colleagues from the EXG team especially Dr. Lara McManus, Dr. Roisin McMackin, Dr. Amina Coffey, Ms. Eileen Rose Giglia, Mr Saroj Bista, Mr. Matthew Mitchell, Mr. Prabhav Mehra, Ms. Serena Plaitano, Ms Adelais Farnell Sharp, it has been a pleasure working with you.

I extend my appreciation to my colleagues from the extended Academic Unit of Neurology, particularly Dr. Emmet Costello and Mr. Colm Peelo, for providing the neuropsychological scores and for their patient responses to my numerous psychology-related inquiries. I would also like to acknowledge everyone who collected data at the Irish National ALS Clinic in Beaumont Hospital and the Irish registry managers for their dedication in providing high-quality data to research. To all of you, past and present colleagues, you have made these four years fantastic. I am grateful for the proofreading, the advice, all the shared meals and moments of laughter (special shoutout to everyone enrolled in the racket's team!).

During my third year, I had the privilege of working as a demonstrator for Dr. Giovanni Di Liberto. I learnt a lot from this role and would like to thank him for his guidance. He may not remember but his insights on negative results left a lasting impact on my approach to research.

I am deeply thankful to all the participants who generously contributed their time and wisdom, inspiring me throughout this journey.

A special mention to the climbing squad – you kept me grounded during these continuous research efforts. And to all the ‘Gals’ who instantly made me feel at home in Dublin! To my

friends, whether near or far, who have been an incredible source of support, both in person and through heartfelt phone calls and messages.

Ji, your unwavering support during the thesis writing process has been a pillar of strength. Thank you for believing in me even when I doubted myself.

Et un énorme merci à ma famille pour leur soutien sans faille. Je ne pourrais jamais vous remercier assez pour tout ce que vous avez fait pour moi. Je suis incroyablement chanceuse de pouvoir compter sur vous.

Contents

List of figures

List of tables

Outputs

1. Oral presentations regarding this thesis

Metzger M., Dukic S., McMackin R., …, Nasseroleslami B., Dynamic analysis of brain states reveals altered functional networks in ALS: Insights from high-density Resting-State EEG. **20 min presentation** – *34th International Motor Neuron Disease Association (MNDA) symposium 2023*

Metzger M., Dukic S., McMackin R., …, Nasseroleslami B., Classification of ALS patients based on resting-state EEG trajectories: Clinical relevance and network progression. **10 min presentation** – *European Network to Cure ALS (ENCALS) 2023*

Metzger M., Dukic S., McMackin R., …, Nasseroleslami B., Abnormal EEG microstate characteristics during rest in ALS disease. **20 min presentation** – *Visiting researcher, Sheffield University, 2023*

Metzger M., Biomarqueurs électroencéphalographiques pour repérer les dysfonctionnements des réseaux cognitifs causés par la Sclérose latérale amyotrophique. **3 min presentation** – *Competition 'Ma thèse en 180s' Irlande 2023*. 3rd Prize.

Metzger M., Prison Break. **3 min presentation** – *Health Science Research Blitz 2023, Trinity College Dublin*. 'Most engaging' Prize.

Quantifying the unquantifiable (On behalf of Prof. Orla Hardiman). **20 min presentation** – *The Thierry Latran Foundation Annual Meeting 2021*

Metzger M., Dukic S., McMackin R., …, Nasseroleslami B., A longitudinal study of functional network disruption in Amyotrophic Lateral Sclerosis. **30 min presentation** – *Irish Electrophysiology Research Clinic 2020*

2. Poster presentations regarding this thesis

1. **Metzger M.**, Dukic S., McMackin R., …, Nasseroleslami B., Cognitive phenotypes in ALS relate to distinct longitudinal changes of functional networks disruption: a resting-state EEG study, *33rd International Motor Neuron Disease Association (MNDA) symposium 2022*

2. **Metzger M.**, Dukic S., McMackin R., …, Nasseroleslami B., Altered cross-sectional and longitudinal resting-state EEG microstates in ALS, associated with distinct sources of brain activity, *European Network to Cure ALS (ENCALS) 2022*

3. **Metzger M.**, Dukic S., McMackin R., …, Nasseroleslami B., Abnormal microstate resting-state EEG characteristics in ALS disease, *European Network to Cure ALS (ENCALS) 2021*

4. **Metzger M.**, Dukic S., McMackin R., …, Nasseroleslami B., Abnormal microstate resting-state EEG characteristics in Amyotrophic lateral sclerosis, *43rd Annual International Conference of the IEEE Engineering in Medicine and Biology Society 2021*

5. **Metzger M.**, Dukic S., McMackin R., …, Nasseroleslami B., Longitudinal changes of functional networks disruption in ALS: a resting-state EEG study, *31st International MNDA symposium 2020*

I. Introduction

1. ALS disease

Amyotrophic lateral sclerosis (ALS) is a progressive and fatal neurodegenerative disease of the central nervous system (CNS). Despite important research efforts and recent advances, ALS still has no effective treatment. Life expectancy is on average 30 months after symptoms onset (Hardiman, Al-Chalabi, Brayne, et al., 2017).

2. Epidemiology

The disease is the most common form of motor neuron disease (MND) but is still rare with a crude incidence rate of 2-3 cases per 100 000 in Europe (Hardiman et al., 2011; Hardiman, Al-Chalabi, Brayne, et al., 2017). The low prevalence of only 7-9/100 000 is due to the short survival time (Hardiman, Al-Chalabi, Brayne, et al., 2017). Despite relatively stable incidence rates in Europe, a lower average incidence rate of 1.75/100 000 was observed worldwide, by meta-analysis (Marin et al., 2017). North Africa and Asia appeared to have much lower average incidences (<1/100 000) than in Europe (or in populations with a majority of European descendants) (Feldman et al., 2022; Marin et al., 2017).

An increase in incidence is expected with the ageing of the population. Some studies already suggested an increase in incidence in the last decades but are counterbalanced by studies reporting stable incidence. The observed increase could be explained by adjusted diagnosis criteria and improved recognition of the disease, especially in the older population (Feldman et al., 2022; Hardiman, Al-Chalabi, Brayne, et al., 2017). The prevalence is also anticipated to increase thanks to improved treatments and support.

Men are overall at a higher risk of developing the disease with an evaluated male-to-female ratio of 1.3-1.4 (Feldman et al., 2022; Marin et al., 2017). The population aged, 60 and over, has also been observed to be at higher risk; the age of onset being proportional to the life expectancy (Byrne, Jordan, et al., 2013).

2.1. Clinical presentation

The clinical presentations of ALS are highly heterogeneous, not only in terms of age of onset but also site of onset, rate of disease progression, motor/respiratory symptoms and presence of cognitive/behavioural impairments.

ALS is characterised by the involvement of both upper and lower motor neurons (Hardiman et al., 2011). The progressive neurodegeneration affects the brain stem, cervical, thoracic and lumbar components of the central nervous system (Figure 1). Patients experiment progressive

muscle weakness or stiffness causing a range of symptoms including impaired limb movement, dysphagia, dysarthria and ventilation issues (Feldman et al., 2022; Hardiman et al., 2011). Failure of the respiratory function leads to death in most cases (Hardiman et al., 2011). After a focal onset of muscle weakness, it commonly spreads to adjacent body parts.

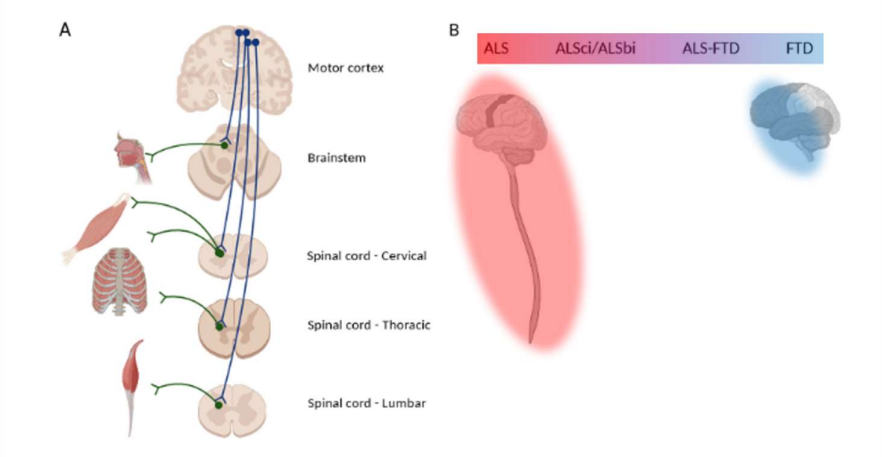

Figure 1: A. Schematic representation of upper and lower motor neuron pathways. UMN, in blue, relay signals from the motor cortex to LMN, in green, which in turn relay signals to the muscles. In ALS disease, both UMN and LMN progressively degenerate. MN present in the brainstem innervate neck muscles; their degeneration causes speech and swallowing impairments. MN connecting in the cervical segment of the spinal cords communicate with the upper limbs and respiratory muscles. MN in the thoracic and lumbar segments respectively mostly innervate respiratory and lower limbs muscles. B. Amyotrophic lateral sclerosis – frontotemporal dementia spectrum. FTD is on one end of the spectrum with pure fronto-temporal degeneration and only cognitive and behavioural impairments. ALS is on the other end with only motor and/or respiratory symptoms, caused by UMN and LMN degeneration. Patients are classified as ALS-FTD if they meet both the criteria for ALS and FTD classification. Some patients present with cognitive or behavioural impairment without meeting the criteria for an FTD diagnosis, it is defined as ALS cognitive impairment (ALSci) or ALS behavioural impairment (ALSbi). Created with BioRender.com

The most common sites of onset are the spinal cord and bulbar region (Feldman et al., 2022). In Ireland, from 1995 to 2010, 58.4% of spinal (cervical and lumbar), 36.5% of bulbar and 5.1% of generalised onsets were observed (Rooney et al., 2013). Although, a geographical discrepancy in ALS phenotypes may exist (Hardiman, Al-Chalabi, Brayne, et al., 2017). Respiratory onset is usually rarer and happens mostly in men (Feldman et al., 2022). Growing evidence shows that cognitive and behavioural symptoms sometimes even precede motor or respiratory impairment (Mahoney et al., 2021; Pender et al., 2020). Cognitive and behaviour changes may represent potential early markers of the disease.

A few years ago, the Strong diagnosis criteria were revised to recognise the neuropsychological deficits in ALS (Strong et al., 2017). The definition of ALS has been expanded to the concept of ALS fronto-temporal (ALS-FTD) spectrum (Figure 1). Around 15% of ALS patients are also diagnosed with FTD (Feldman et al., 2022; Pender et al., 2020). Most patients do not meet the criteria for dementia, but up to 50% of ALS patients develop cognitive or behavioural impairments, associated with changes in non-motor networks (Al-Chalabi et al., 2016). The

revised Strong criteria, therefore, describe the presence of such cognitive or behavioural impairment, respectively as ALSci and ALSbi.

2.2. Risk factors

2.2.1. Genetic factors

Genetic factors have been observed to play an important role in the development of ALS disease.

Familial ALS (FALS) represents around 20% of the cases (Ryan et al., 2018). The estimation of FALS incidence however varies (5-30%) depending on the degree of relatives and the extent of endophenotypes considered (Feldman et al., 2022; Ryan et al., 2018). Frontotemporal dementia (FTD) is usually considered on one end of the ALS-FTD spectrum. Additionally, other neuropsychiatric disorders, like schizophrenia, have been shown to occur at a higher rate in ALS patients' relatives than in controls (Byrne, Heverin, et al., 2013; Hardiman, Al-Chalabi, Brayne, et al., 2017). Including such endophenotypes in the definition of FALS is likely to cause an increase in detection and may represent at best the genetic architecture of the disease. A polygenic overlap between schizophrenia and ALS disease has been suggested by a genome-wide association study (Hardiman, Al-Chalabi, Brayne, et al., 2017; McLaughlin et al., 2017). Nonetheless, the uncertainties bounded by family health histories plead in favour of genetic testing.

Across patients without any FALS history, around 15% carry ALS-associated genes (Feldman et al., 2022; Goutman et al., 2022). The bulk of the current identified genetic risks relies on monogenic inheritance, with more than 40 disease-associated genes discovered (Feldman et al., 2022). The most observed mutations so far are C9orf72, SOD1, TARDBP and FUS. SOD1 has been associated with motor degeneration, while C9orf72 seems to have stronger links with cognitive and behavioural impairment (Goutman et al., 2022). Both FUS and TARDBP mutations are among those connected with dementia (Goutman et al., 2022). The heritability character of the disease is, however, probable to be oligo- or polygenic. Due to the rare character of the disease, only international consortia have the potential to deliver answers to those questions.

2.2.2. Environmental factors

Despite their growing potential, genetic studies do not explain fully the apparition of the disease. The environment is hypothesised to have a similar influence on ALS risk. The answer to the cause of ALS may partially lie in epigenetic changes (Feldman et al., 2022). Numerous

studies examined potential environmental factors like environmental toxins (Lagrange et al., 2022), medical events such as brain trauma (Goutman et al., 2022) or physical activity. In all likelihood, a combination of genetic risks and lifelong influence of environmental factors causes ALS, as suggested by the gene-time-environment hypothesis (Al-Chalabi & Hardiman, 2013).

2.3. Pathophysiology

ALS disease is characterised by the degeneration of both upper and lower MN. Such abnormal neuronal death is caused by the presence of inclusion bodies. Different cellular and molecular patho-mechanisms have been investigated as a cause of this aberrant protein aggregation. Disrupted physiological processes include: RNA metabolism, homeostasis of the proteins, cellular transport, mitochondrial function and immune mechanisms (Feldman et al., 2022).

The above-mentioned C9orf72, TARDBP and FUS mutations are involved in RNA alterations (Goutman et al., 2022). The most discussed mutant protein is the TAR DNA binding protein 43 (TDP-43). Indeed, around 97% of ALS patients display characteristics of TDP-43 proteinopathy, with cytoplasmic inclusions of the protein (Hardiman, Al-Chalabi, Chio, et al., 2017). A prion-like propagation of the disease has been hypothesised (Goutman et al., 2022; Koopman, 2022), and would be coherent with the stage-related spreading of TDP-43 inclusions. FTD patients show similar signs of TDP-43 deposition; a similarity which argues in favour of the ALS-FTD spectrum (Scotter et al., 2015). Besides, the spreading of TDP-43 pathology was associated with cognitive decline (Lulé et al., 2018), and in a post-mortem study, the type of cognitive impairment was predictive of the non-motor regions where the TDP-43 aggregated (Gregory et al., 2020).

Multiple ALS mutations, such as TARDBP, C9orf72 and SOD1, play a role in altered proteostasis (Feldman et al., 2022; Goutman et al., 2022). TDP-43 inclusion bodies, as well as FUS and C9orf72 mutations, cause defective transport between the nucleus and the cytoplasm. The inclusion bodies and mutations such as SOD1, induce mitochondrial dysfunction which leads to oxidative stress.

Disrupted inflammatory mechanisms have also been observed in ALS patients, with an initial protective response followed by cytotoxicity (Feldman et al., 2022). Different levels of immune cells in the blood, infiltrated immune cells in the CNS and abnormal production of cytokines (including interferon γ) are all patho-mechanisms present in patients (Goutman et al., 2022).

The discovered molecular steps are likely to be interconnected and interdependent. Despite important progress in unravelling the physiological mechanisms of the disease, the pathological pathways remain incompletely understood. Enhancing the assessment of the spectrum of symptoms associated with the disease, which encompasses not only the deterioration of motor and respiratory functions but also cognitive and behavioural deficits, could play a crucial role in elucidating the underlying mechanisms of the condition.

3. Cognitive impairment in ALS disease

3.1. Late discovery of the cognitive aspects of the disease

Originally, introduced by Jean-Martin Charcot in 1874, the term 'Sclérose latérale amyotrophique' or ALS, initially described a disease with purely motor symptoms (Charcot, 1874). Cognitive impairments only became apparent in the late twentieth century with the emergence of extra-motor neuroimaging evidence, large-scale epidemiologic results and robust neuropsychological assessments (Pender et al., 2020). Before, cognitive or behavioural impairments were masked by more apparent motor neuron symptoms (notably bulbar symptoms) or classified as emotional consequences of motor impairments. Since 2017, FTD is now officially associated with ALS in the ALS-FTDS (Strong et al., 2017).

3.2. Clinical presentation of cognitive impairment

ALS disease and FTD share pathophysiological and genetic characteristics, and around 15% of ALS patients present with co-morbid FTD (mainly behavioural variant-FTD, bvFTD). FTD is characterised by behavioural changes (like disinhibition or apathy), language problems and organisational struggles. Psychotic episodes may happen, especially in patients with C9orf72 repeat expansion, while memory is generally preserved until the latest stages of the disease (Finger, 2016).

Amongst non-demented ALS patients, around 40% have been observed to develop mild to moderate cognitive or behavioural symptoms (Pender et al., 2020; Phukan et al., 2012). Patients with abnormal cognition (ALSci) show executive and/or language dysfunction. The revised Strong criteria define executive impairment as impaired verbal fluency or impairment in two other non-overlapping measures of executive function (including working memory, problem-solving and social cognition) (Strong et al., 2017). The hallmark of ALS executive dysfunction is verbal fluency, usually evaluated by the generation of lists of words (specified letter or semantic categories). To ensure the distinction between cognitive and motor disabilities, the task is timed and evaluated in comparison with the reading/writing of independent words.

Behavioural symptoms (ALSbi) encompass essentially apathy (in up to 60% of patients) but also mood, hygiene or eating habits changes. The revised Strong criteria for ALSbi is met if there is evidence of apathy or two other independent Rascovsky features (Strong et al., 2017).
Emotional lability also occurs in patients and is clinically defined as a pseudobulbar affect, separately from cognitive or behavioural abnormalities (Feldman et al., 2022; Pender et al., 2020). This affect has been hypothesised to occur because of disrupted mood regulation networks (Finegan et al., 2019).
Specific disease phenotypes like the presence of C9orf72 repeat expansions or a bulbar onset seem to be predictive of existing or future cognitive impairment (Feldman et al., 2022).

3.3. Assessment of cognitive impairment

Early and regular assessment of cognitive impairment is essential for a better understanding of the disease and also for the welfare of the patients and their caregivers.
The Edinburgh Cognitive and Behavioural ALS Screen (ECAS) is a validated, widely used method for cognitive assessment in ALS (Abrahams et al., 2014). This tool allows for a short, multidomain assessment and has been specifically designed to account for the ALS disabling physical symptoms. ECAS, evaluates specifically executive function, language and social cognition, as 'ALS-specific' domains, but also memory and visuospatial skills ('ALS-non-specific' domains) to remain general. Multiple forms of the questionnaire are available to limit practice effects in the case of longitudinal assessments. The ECAS cannot replace longer, detailed neuropsychological evaluations, however, it helps to identify needs and has been proven useful to clinical care (Feldman et al., 2022; Pender et al., 2020).
An ALS-FTD diagnosis requires more detailed neuropsychiatric screenings. The ALS-FTD questionnaire evaluates behavioural impairment and can identify bvFTD (Raaphorst et al., 2012).
The recently developed Beaumont Behavioural Inventory (BBI) is more sensitive to behavioural impairments (Elamin et al., 2017; Feldman et al., 2022). This screening tool focuses on behavioural changes usually observed in ALS and adapts to physical disabilities.
Behavioural assessments are even harder than cognitive evaluations and can be in some ways of limited reliability. Except for apathy, behavioural changes are reported by caregivers, with all the subjectivity it implies. Robust, quantitative biomarkers of cognitive impairment are required for prognostication and new treatment evaluations.

3.4. Progression of cognitive impairment over the course of the disease / Prognosis of cognitive impairment?

Cognitive changes can occur early in the disease, even before physical symptoms onset (Feldman et al., 2022; Pender et al., 2020). Most patients have stable cognitive performances but around one-third of ALS patients (n=146; n=19) showed a cognitive decline in neuropsychological evaluations 6 months after baseline assessment (Bersano et al., 2020; K. M. Robinson et al., 2006).

However, no actual consensus was reached on cognitive progressions in ALS patients. A recent meta-analysis study observed that only 5 out of 13 longitudinal studies detected cognitive decline (Finsel et al., 2022). The evolution of cognitive impairment possibly only happens in subgroups of patients. Worsening behavioural symptoms, for example, are commonly reported by caregivers of ALSbi patients (Bersano et al., 2020; Burkhardt et al., 2017).

Neuroimaging or pathophysiological markers of cognitive impairment could bring additional information and help entangle the debate around cognitive decline.

4. Potential biomarkers of cognitive impairment in ALS

Biomarkers of cognitive impairment in ALS would improve disease management, clinical care and prognostication. Such biomarkers could also benefit clinical trials by facilitating participant categorisation and by ameliorating the detection of potential treatment effects.

4.1. Fluid biomarkers

Cerebrospinal fluid (CSF) and plasma neurofilaments efficiently differentiate between ALS patients and healthy controls (Benatar et al., 2016). As a consequence of neuroaxonal damage, elevated neurofilament light chain (NFL) levels are observed in the CSF and blood of patients with neurodegenerative diseases such as ALS, FTD, or Alzheimer's disease (Forgrave et al., 2019; Olsson et al., 2019; Taga & Maragakis, 2018). Concentrations of CSF NFL were associated with cognitive impairment in Alzheimer's disease and FTD, although not in MND (Olsson et al., 2019).

Glial fibrillary acidic protein (GFAP), which is found in astrocytes, is another potential biomarker of cognitive impairment in ALS. Elevated levels of GFAP in the cerebrospinal fluid (CSF) or serum have been associated with cognitive impairment in ALS patients (Falzone et al., 2022). GFAP is a cytoskeletal protein and its elevation in the CSF is thought to reflect astrogliosis. This process is hypothesised to become activated as a response to the degeneration of neurons in ALS. However, GFAP is not specific to ALS and its elevation can also be found

in other neurodegenerative disorders like FTD (Falzone et al., 2022). The lack of specificity and the invasiveness of CSF procedures limit the potential of these biomarkers.

Similarly, lower levels of uric acid (a waste product of the purine metabolism) have been observed in ALS patients and other neurodegenerative diseases (Benatar et al., 2016; Taga & Maragakis, 2018). Uric acid has been extensively studied for its antioxidative properties. Emerging results are associating levels of uric acid in serum with cognitive impairment (Tang et al., 2021). Since oxidative stress is thought to participate in ALS neurodegeneration, uric acid represents a prime target for potential therapies. However, the lack of specificity or efficient distinction between ALS subphenotypes still represents an obstacle to its use as a biomarker.

Wong *et al*. recently suggested that the p75 neurotrophin receptor (p75NTR) may play a role in the development of cognitive impairment in ALS, as it is involved in the regulation of nerve cells and as higher levels of p75NTR have been reported in patients with mild cognitive impairment (Longo et al., 2008; Wong et al., 2022). Nevertheless, even though p75NTR levels are associated with motor symptoms in ALS (Benatar et al., 2016; Taga & Maragakis, 2018), its role in the development of cognitive impairment in ALS remains obscure.

4.2. Neuroimaging biomarkers

Neuroimaging techniques, such as magnetic resonance imaging (MRI), can be used to detect changes in brain structure and function in patients, which subsequently can be used to identify cognitive impairment in ALS.

Structural MRI (sMRI) can be used to detect changes in brain structure, such as changes in grey matter volume (voxel-based morphometry) and cortical thickness (structural-based morphometry). sMRI changes in ALS-FTD patients and/or patients with more subtle cognitive impairments usually include atrophy of specific extracortical regions, such as the frontotemporal area (Agosta et al., 2016; De Marchi et al., 2021; Senda et al., 2011). These regions are important for cognitive function, including memory, language, and executive function. In addition, longitudinal progression of the frontotemporal atrophy was shown (Menke et al., 2018; Trojsi et al., undefined/ed).

Diffusion tensor imaging (DTI) is often used in combination with structural MRI. This method is used to assess the integrity of white matter pathways in the brain through the measure of water molecules diffusion. Cross-sectional studies have observed widespread white matter alterations, in non-motor areas like the prefrontal cortex, in behaviourally and cognitively impaired ALS patients (Benatar et al., 2016; De Marchi et al., 2021; Illán-Gala et al., 2020).

Diffusivity changes paralleled cognitive and behavioural symptoms (Benatar et al., 2016; Femiano et al., 2018). Longitudinal progressions of such white matter abnormalities were also shown but are more divergent between studies (Burgh et al., 2020; Menke et al., 2018; Trojsi et al., undefined/ed). Although a DTI-based sequential cognitive staging was proposed (Lulé et al., 2018), more research is required to test the sensitivity and replicability of the above findings.

By measuring blood flow to different brain regions, functional MRI (fMRI) can evaluate alterations in functional connectivity between brain regions. Basaia *et al*. linked functional changes in frontal and temporal lobes respectively to behavioural and fluency impairments in individuals with ALS (Basaia et al., 2020; De Marchi et al., 2021). Another study detected different patterns of functional changes in cognitively impaired versus non-cognitively impaired ALS patients in inferior parietal and cerebellar regions. The cerebellar region, in particular, was associated with cognitive symptoms (De Marchi et al., 2021; Hu et al., 2020). An increase in functional connectivity over time was reported in the frontal lobe (frontostriatal network), which relates to declines in attention and fluency (Castelnovo et al., 2020).

Positron emission tomography (PET) imaging can detect changes in glucose metabolism (which indicates changes in nerve cell activity) or in cerebral blood flow.

Changes in metabolism were observed in extra-motor regions in ALS (Lloyd et al., 2000; Rajagopalan & Pioro, 2019) and more specifically, changes in cerebral blood flow in frontal and subcortical regions have been linked with fluency impairment (Abrahams et al., 1995; Kew et al., 1993). Nonetheless, while fluorodeoxyglucose PET is recommended for clinical diagnosis in some neurodegenerative diseases and dementias, its use was not supported for ALS or ALS-related cognitive impairment at the 2018 European Association of Nuclear Medicine panel (Nobili et al., 2018).

5. Advantages of electrophysiological biomarkers

Electrophysiological measures have advantages compared to other neuroimaging methods in quantifying network disruptions in ALS.

5.1. Easiness of recordings

EEG recordings have limited costs (maintenance and purchase) compared to other neuroimaging methods like (f)MRI, positron emission tomography (PET) or magnetoencephalography (MEG) (Baillet, 2017; DellaBadia Jr et al., 2002; Illman et al., 2020).

Besides, the level of expertise required is inferior for EEG recordings. Including more participants and a greater number of follow-up sessions is simpler in EEG research studies.

5.2. Participants' comfort

The current project focuses on surface EEG, which is non-invasive. Electrodes are only put in contact with the scalp. The participant's comfort is therefore increased, and the risk of infection is inexistent.

The sitting position maintained by participants during the EEG recordings is easier for ALS patients with respiratory issues and bulbar symptoms. Often neuroimaging methods involving scanners like MRI or PET require the participants to lie down and remain still for an extended period of time.

5.3. Quality of the recordings

Moreover, electrophysiological recordings allow for direct measurement of neuronal activity, as opposed to indirect metabolic neuroimaging methods (Menon & Crottaz-Herbette, 2005). Brain metabolism is impacted by healthy ageing or metabolic syndrome, which could bias the interpretation of functional connectivity changes caused by neurodegeneration (Kotkowski et al., 2022; Mertens et al., 2022). EEG records potential changes on the scalp that result from voltage-gated ionic conductances causing post-synaptic potentials in cortical pyramidal neurons (Kirschstein & Köhling, 2009).

As a consequence of the direct measure, EEG has an excellent temporal resolution. In this project, signals are recorded at 512Hz, while fMRI or PET imaging methods have temporal resolutions in the order of seconds and tens of seconds (Glover, 2011; G. Wang, 2019).

EEG or MEG spatial resolution is inferior to fMRI and PET neuroimaging resolutions. The resolution of PET and fMRI are generally between three to ten mm, although it can reach 0.5 mm with high field magnets (Glover, 2011). EEG/MEG resolution is usually in the order of 10-20 mm. Nonetheless, high-density EEG coupled with structural MRI and new source localisation techniques improves highly the spatial resolution (Al-Chalabi et al., 2016; Glover, 2011; Michel & Brunet, 2019).

6. Existing electrophysiological markers of cognitive or non-motor network dysfunction in ALS

6.1. TMS

Transcranial magnetic stimulation (TMS) is a non-invasive brain stimulation technique that has been used to evaluate the function of the cerebral cortex.

Agarwal and colleagues used TMS to investigate the relationship between cortical excitability and cognitive/behavioural impairment in ALS. The study found that resting-state motor threshold (RMT, threshold to obtain a motor evoked potential) was predictive of cognition impairment (assessed by Addenbrooke's Cognitive Examination scores) (Agarwal et al., 2018). Lower RMT and reduced short-interval intracortical inhibition (SICI) reflect cortical hyperexcitability and are characteristic of ALS and FTD diseases (Agarwal et al., 2021; De Marchi et al., 2021; Vucic & Kiernan, 2017). RMT has even been shown to differentiate between ALS-FTD and ALS cohorts (Agarwal et al., 2021), while reduced SICI was associated with executive dysfunction (assessed by ECAS scores) (Higashihara et al., 2021).

6.2. MEG

Magnetoencephalography (MEG) is an additional non-invasive neuroimaging technique that can measure the magnetic fields produced by the electrical activity of neurons in the brain.
MEG responses to an MMN paradigm were observed to be altered in ALS patients with severe bulbar symptoms, suggesting impaired auditory and/or memory processing (Pekkonen et al., 2004). A widespread increase in functional connectivity was also detected at rest, implying extra-motor network impairment (Proudfoot et al., 2019).
Despite the potential of MEG to provide valuable insights, results are limited probably due to the cost and limited resolution of deep brain regions.

6.3. EEG

High-density (HD) resting-state EEG allowed for the detection of connectivity changes in extra-motor regions, at sensor level, that persisted along the progression of the disease (Nasseroleslami et al., 2019). At source-level, co-modulation of γ-band oscillating signals within the frontotemporal lobe correlated with language impairment (Dukic et al., 2019).
Furthermore, task-based EEG paradigms provided quantitative measures of network disruptions which correlated with clinical measures of cognitive impairment.
Mismatch negativity (MMN) is an event-related potential (ERP) generated by an oddball sound. In ALS cohorts, an average delay in peak time was observed, which correlated with executive dysfunction measured by the Stroop task (Iyer et al., 2017). Source reconstructed MMN responses showed increased power in the left middle/superior frontal gyri and posterior parietal cortex, which correlated with cognitive flexibility and verbal inhibition impairment (measured by the Color-Word Interference Test of the Stroop task) (McMackin, Dukic, et al., 2019). Besides, a longitudinal MMN HD-EEG study noticed a progressive increase in spectral power in fronto-temporal regions (right inferior frontal gyrus and bilateral superior temporal

gyri) in ALS and interpreted it as 'cognitive network hyperactivation' (McMackin, Dukic, Costello, Pinto-Grau, McManus, et al., 2021).

Sustained attention to response task (SART) generated left posterior parietal and insular increased spectral power in the ALS group compared to the healthy-control group at P3 component of the ERP (positive ERP peak of voltage between 300-500ms after stimulus). In particular, the spectral power in the right precuneus (P3 NoGo versus Go) negatively correlated to behavioural inhibition, which may be representative of compensation (McMackin et al., 2020).

Electroencephalography is a direct measurement of the neuro-electric activity of the brain and has the potential to distinguish between cohorts with amyotrophic lateral sclerosis (ALS) and healthy controls (HC) (Dukic et al., 2019; Iyer et al., 2017; McMackin, Dukic, et al., 2019; McMackin et al., 2020; McMackin, Dukic, Costello, Pinto-Grau, McManus, et al., 2021; Nasseroleslami et al., 2019). Although previous studies have investigated network abnormalities in both the sensor- and source-space domains of ALS patients, the temporal dynamics of these atypical EEG measures are not yet well understood.

7. Potential of microstates analysis to characterise cognitive network alterations

7.1. Microstate history and definition

Electroencephalography measures the electrical activity originating from voltage-gated ionic conductances, which are only noticeable at the scalp level when there is simultaneous post-synaptic spiking of neurons with similar orientations. As the distance from the brain source increases, the recorded voltage decreases, meaning that EEG primarily captures cortical activity. One scalp electrode records activity from different brain sources (close by and remote) and a specific brain source simultaneously 'projects' to different scalp electrodes.

Considerable time and effort have been dedicated to solving the inverse problem of localising neuronal sources that are responsible for observed scalp topographies. However, comparatively less attention has been given to investigating the temporal dynamics of these signals (Michel & Koenig, 2018).

Along the time of the recordings, maps of scalp potentials (topoplots) can be extracted. While the succession of topoplots may intuitively look spontaneous and unorganised, Lehmann et al. detected a few transient, recurrent topographies which they called 'micro-states' (Lehmann et al., 1987). Their analysis was built upon the idea that brain activity can be segmented into

distinct and specific patterns. Through microstate analysis, patterns of brain activity can be identified and then time point topographies can be assigned to different clusters of microstates. These periods of stable topographies are believed to represent the synchronized activity of neural components that make up a functional network (Michel & Koenig, 2018). Changes in microstate parameters such as occurrence or duration are thought to reflect changes in the temporal dynamics of these brain networks, rather than changes in the functional connections between networks (Gschwind et al., 2016).

7.2. Modulation of microstate characteristics by neurological and psychiatric conditions

The microstates' topographies remain stable across participants and conditions. However, altered microstate temporal dynamics have been found in participants with neurological and psychiatric conditions (Al Zoubi et al., 2019; Michel & Koenig, 2018).

Schizophrenia is one of the most studied pathologies using the EEG microstate methodology (Koenig et al., 1999; Lehmann et al., 2005; Michel & Koenig, 2018; Nishida et al., 2013). Medium-size effects were observed, arguing in favour of cognitive episodes that are detected by the microstate approach and relevant in psychiatry (Michel & Koenig, 2018). The suitability of the microstate methodology was even investigated as a measure of schizophrenia treatment efficiency.

In addition, alterations in the characteristics and the temporal dependencies of microstates were detected in anxiety and mood disorders (Al Zoubi et al., 2019) and post-traumatic stress disorder (Terpou et al., 2022). Frontotemporal dementia and Alzheimer's disease were also observed to cause abnormalities in microstate patterns (Nishida et al., 2013).

In multiple sclerosis and Huntington's disease, changes in microstates have been correlated with depression, cognitive fatigue scores, and cognitive performance (Faber et al., 2021; Gschwind et al., 2016). Furthermore, recent research has suggested that resting-state EEG microstates could serve as a biomarker for Parkinson's disease (Pal et al., 2021).

Together, these findings suggest that resting-state EEG microstates have the potential to be used as a marker of cognitive impairment in various neurological and psychiatric conditions, including ALS.

II. Literature review

To advance the development of new treatments for ALS, reliable biomarkers are crucial for evaluating disease progression and treatment effectiveness (Benatar et al., 2016; Bowser et al., 2011). While motor symptoms have been extensively studied in ALS, less attention has been given to extra-motor or cognitive network dysfunction. EEG, a widely used tool in cognitive neuroscience research, has shown promise as a potential biomarker for neurological and psychiatric conditions such as schizophrenia (Javitt et al., 2020), major depression (Olbrich & Arns, 2013), and Alzheimer's disease (Poil et al., 2013).

Here, we provide an overview of current approaches for analysing EEG data to track cognitive network dysfunction. We explore the potential of emerging EEG measuring tools to complement structural and functional imaging in analysing cognitive impairment. We also highlight the need for further validation of these approaches to support the development of new treatments in ALS.

1. Existing EEG observations of extra-motor brain network impairment in ALS

Recorded scalp EEG reflects the summed synchronous postsynaptic potential of cortical pyramidal neurons with similar orientation (Teplan, 2002). Pyramidal neurons from the cortex are involved in cognitive processes and hypothesised to majorly be the source of EEG signals due to their location and orientation (perpendicular to the surface). The difference of electrical potential between the body of neuron (soma) and the apical dendrites cause the equivalent of an electrical dipole (Teplan, 2002).

1.1. Event-locked EEG

The use of EEG in ALS includes resting-state (also called continuous) and task- or stimulus-based recordings. In event-related EEG, event-related potentials (ERPs) provide insights into the time-locked response to specific stimuli, while induced oscillatory responses offer information about the modulation of ongoing oscillatory activity by cognitive processes, without strict temporal alignment to stimuli onset.

1.1.1. Time-domain – delays in ERP components in ALS

Traditionally, EEG research based on sensorimotor or cognitive tasks analyses event-related potentials (ERPs), which represent voltage changes caused by an evoked neural event (initiated by a stimulus). Several neurophysiological biomarkers candidate for cognitive impairment could be suggested based on ERP components (Raggi et al., 2010).

Notably, (active) auditory oddball paradigms elicited longer P300 (positive peak around 300ms after stimulus) latency in individuals with ALS (Gil et al., 1995; Hanagasi et al., 2002; Ogawa et al., 2009; Paulus et al., 2002). This ERP component is often used as an index of cognitive processing speed. Delays in P300 correlate with speed-associated neuropsychological scores and have been associated with dementia (Polich, 2007).

Increased delays and reduced amplitude were observed in mismatch negativity (MMN) or N2a (negative peak around 200ms after stimulus) following passive auditory oddball paradigm (Iyer et al., 2017; Raggi et al., 2008). Reduced amplitude of Processing Negativity (PN) peak (around 50ms and 500ms after stimulus) was also noted in ALS cohort in a selective attention task (Vieregge et al., 1999).

A two-phases visual memory task evoked closed to no difference in N400 peaks between new and old items presented to individuals with ALS, while differences were present in healthy-controls (Münte et al., 1998). Such difference suggested the presence of impaired memory processes in ALS.

Few longitudinal studies of time-domain ERPs have been published, although the stability of P300 properties over time in ALS has been evaluated through the lens of Brain-Computer Interaction (BCI). P300 latency increases over the progression of the disease and as it correlates negatively with BCI performance, it needs to be accounted for (Zisk et al., 2022).

1.1.2. Quantitative EEG: analysis in Frequency-domain

In addition to the ERP properties of the signal, oscillations properties are assessed by transforming the time-domain signals into frequency-domain using Fourier transform or Wavelet analysis. Typically, the signals are examined in specific frequency-bands of oscillation ranging from 1 to 100 Hz. These frequency-bands include δ (1-4 Hz), θ (5-7 Hz), α (8-13 Hz), β (14-30Hz), and γ (31-100Hz).

To further understand the neural mechanisms of cognitive impairment in ALS, researchers may evaluate how cognitive stimuli affect oscillatory activity in the frequency-domain. This is

known as event-related spectral dynamics. For example, a decrease in β-band event-related desynchronization (ERD) in scalp parietal and pre-frontal areas was observed in individuals with ALS during a sustained attention to response task (SART). Furthermore, β-band event-related synchronization (ERS) was associated with ECAS ALS-specific scores, which is a cognitive and behavioural screen designed for ALS patients (McMackin, Dukic, Costello, Pinto-Grau, Keenan, et al., 2021). These findings provide insights into how ALS affects neural processes underlying cognition and behaviour.

1.1.3. High density EEG - Source localisation

Since the 1920s when EEG was first used on the human brain, it has been widely used in research and clinical settings to study brain function and diagnose neurological and psychiatric disorders. While it fell out of favour with the development of other imaging techniques, like fMRI, recent technological advancements have made it a valuable tool once again due to improved spatial resolution (Michel & Brunet, 2019). Increased signal-to-noise ratio offers opportunity for source analysis, which can estimate the location of the brain networks producing ERP abnormalities. Specifically, high-density EEG refers to the use of EEG recordings with a larger number of electrodes placed on the scalp (usually 64 and more) compared to traditional EEG. The increased number of electrodes can provide more spatially accurate information about the location and intensity of electrical activity in the brain. Source analysis can detect abnormalities not picked up at sensor-level and provide complementary information on disrupted pathways.

In particular, people with ALS who underwent SART testing showed increased spectral power in the left inferior parietal lobule and insular cortex during the elicitation of P300 components. Additionally, spectral power in the right precuneus during P300 was related to Color-Word Interference Test (CWIT) inhibition scores in ALS. The SART electrophysiological measures were linked to specific executive function impairments, and the changes observed in ALS patients were localized to specific frontal and parietal brain structures (McMackin et al., 2020). During MMN testing, individuals with ALS displayed an augmentation of power in the left posterior parietal, central, and dorsolateral prefrontal cortices, which was associated with reduced cognitive flexibility (McMackin, Dukic, et al., 2019). Indeed, MMN occurs when a stimulus deviates from an expected pattern, reflecting the brain's ability to detect and process

changes in the environment. ALS patients also exhibited a decrease in spectral power in the inferior frontal and left superior temporal gyri (McMackin, Dukic, et al., 2019).

Task-based EEG has demonstrated its ability to effectively detect cognitive network dysfunction in individuals with ALS. This approach specifically focuses on capturing neural responses that are time-locked to specific events. However, it should be acknowledged that task-based EEG usually requires active engagement and effort from participants to complete specific cognitive, sensory or motor tasks, which can pose challenges to participants with ALS. The motor and speech disabilities associated with ALS may significantly impact the execution of specific actions required in task-based studies.

1.2. Resting-state findings in ALS – motor and extra-motor involvement

Unlike task-based EEG, resting-state EEG captures spontaneous brain activity during a relaxed state. Resting-state EEG offers several advantages over task-based EEG, particularly in the context of cognitive impairment in ALS, which has been associated with attrition rate. Participants with executive dysfunction showed a higher likelihood of dropout after 6 months (Elamin et al., 2013). Resting-state EEG is more accessible and less burdensome for participants, especially those with severe motor or communication impairments such as the locked-in syndrome (Maruyama et al., 2021; Secco et al., 2020). By eliminating the need for participants to perform specific actions or respond to sensory stimulation, resting-state EEG reduces the potential bias introduced by speech or motor disabilities.

One notable advantage is that resting-state EEG provides a more comprehensive and general overview of brain functioning. Task-based studies focus on examining targeted neural responses. Consequently, any spontaneous activity that occurs outside of the time period of interest is usually disregarded as background noise. Resting-state approach allows for a broader assessment of brain connectivity and neural interactions, potentially revealing underlying patterns or abnormalities that might be missed in task-based studies (J. Wang et al., 2013).

Resting state experiments pose challenges in controlling subject behaviour compared to task-related activity. Even with similar instructions, the subjective experience and thoughts of subjects vary greatly. This variability in cognitive state and experiences could potentially confound the results. However, controlling spontaneous thoughts might not be necessary, as random episodic spontaneous thoughts activate similar brain regions as resting state networks

(van Diessen et al., 2015). Despite the inherent heterogeneity in resting state experiments, there is evidence of consistent activation patterns in resting state networks among healthy individuals across various studies, suggesting a limited influence of external factors.

While longer recordings have been found to enhance the stability of resting state networks, it is important to consider the risk of subject drowsiness, especially in the context of ALS symptoms that can cause fatigue. Therefore, the significance of conducting shorter resting-state recordings becomes particularly relevant. It is worth noting that stability of EEG functional networks has been observed to emerge in as little as 100 seconds, emphasizing the potential feasibility of shorter recordings in capturing meaningful resting-state dynamics (C. J. Chu et al., 2012). Resting-state functional networks have been reliably identified using various neuroimaging techniques such as fMRI, fMRI-EEG, MEG, or ECoG, highlighting the validity and effectiveness of studying resting-state activity (Brookes et al., 2011; Damoiseaux et al., 2006; Mantini et al., 2007, 2007; Miller et al., 2009; Smitha et al., 2017).

The simplicity and wide range of application of resting-state EEG makes it a promising method for translating findings to clinical settings.

1.2.1. RS – sensor space: the advantage of functional connectivity to quantify impairment in ALS

Resting-state results were initially observed in sensor-space before transitioning to source-space analyses. A study from 1998 showed a decrease in α-band power in the central scalp areas during rest (Mai et al., 1998). A widespread increase in γ-band power was observed beyond central areas, in addition to a decrease in α- and θ-band over the central areas (Jayaram et al., 2015). More recently, resting-state EEG recordings have also revealed a decrease in θ-band spectral power, centred over the scalp motor areas, which persisted over the progression of the disease (Nasseroleslami et al., 2019).

In advanced stages of ALS, individuals with complete locked-in syndrome (CLIS) exhibited decreased spectral power in the α, β, and γ frequency bands specifically in the fronto/central brain regions, when compared to healthy controls (Maruyama et al., 2021). The absence of motor activity may contribute to the observed decline in high-frequency brain activity but it was also hypothesized that this difference could be attributed to reduced "central arousal" or vigilance. Furthermore, the authors also drew parallels with Alzheimer's disease, proposing a potential connection between the decrease in high-frequency power and cognitive impairment.

Subsequent studies explored the connectivity among different brain regions by examining signal coherence, as a representation of cortical function. ALS patients have exhibited an increase in θ-band connectivity between scalp central areas, as well as an increase in connectivity between γ-band signals from the frontal and parietal scalp areas (Iyer et al., 2015; Nasseroleslami et al., 2019). Connectivity changes appeared more salient than the observed changes in spectral power and persisted over the course of 16 months (Nasseroleslami et al., 2019). These findings offer valuable insights into the neural changes associated with ALS, as they demonstrate persistent network changes not only in the motor or central areas, which are the focal points of structural changes in ALS, but also in the frontal areas, which are more closely associated with cognitive functions.

1.2.2. RS- source space: Changes in co-modulation with frontal lobe signals associated with executive function and language impairment

Intrinsic properties of the oscillatory signals, such as spectral power, coherence, and synchrony, have been linked to neurological disorders. By examining changes in spectral power and connectivity, researchers can gain insights into the underlying neural processes that are affected by ALS. In source-space, a reduction in β-band spectral power and synchrony was detected within the sensorimotor network in individuals with ALS (n=74). This decline in β-band synchrony within the motor network was found to be linked to structural changes observed through MRI scans as well as motor impairment (Dukic et al., 2019). It is worth noting that β-band EEG signals are typically associated with the planning and execution of motor tasks, but their synchrony across the motor cortex appears to be altered in resting-state conditions as well.

Alterations in co-modulation (or Amplitude Envelope Correlation, AEC) were observed within the fronto-parietal network (θ-band) and the fronto-temporal network (γ_l-band), and these changes were respectively associated with executive and language composite scores (Dukic et al., 2019). Another study (n_{ALS} = 21) detected decreased α-band AEC in motor, frontal and temporal brain regions (Fraschini et al., 2018). However, the evolution of these findings throughout the progression of the disease still necessitates further investigation.

1.2.3. Limitations of current RS EEG candidate biomarkers of cognitive impairment in ALS

As mentioned above, RS EEG present advantages over event-related EEG. Current RS EEG biomarker candidates for cognitive impairment in ALS show good discriminatory power, with

AUROC of up to 0.73 (Dukic et al., 2019; Nasseroleslami et al., 2019).Cognitive and behavioural impairment in ALS can evolve over time but existing candidate biomarkers based on spectral measures have not been evaluated longitudinally. Biomarkers that track disease progression and cognitive decline longitudinally are needed for comprehensive disease monitoring and management. Additionally, a RS EEG measure of functional connectivity (AEC) have been associated with ECAS executive and language subscores (Dukic et al., 2019) but new EEG biomarker candidates have the potential to cover additional domains of cognitive and behavioural impairment. This is particularly pertinent given the potential of dynamical analysis to identify other abnormalities of neural processes related to neurological or psychiatric conditions (Michel & Koenig, 2018; Tarailis et al., 2023).

Few studies evaluating the potential of new EEG biomarkers in ALS included sensitivity and specificity analyses. For instance, the β-band clustering coefficient of partial directed connectivity in nodal analysis demonstrated a sensitivity of 58% and specificity of 100% (Iyer et al., 2015). This highlights the importance of, not only finding new biomarker candidates per se, but also for multi-modal or integrative biomarkers, as demonstrated in other neurodegenerative diseases with cognitive impairment. For example, a study on the prediction of progression to Alzheimer's disease from mild cognitive impairment showed improved performance by integrating six EEG biomarkers (sensitivity of 88% and specificity of 82%), compared to the best individual biomarker (Poil et al., 2013). Similarly, another study combining 25 resting-state EEG features achieved flawless classification of 61 patients with probable Alzheimer's disease, Parkinson's disease dementia, dementia with Lewy bodies, and FTD-bv (Garn et al., 2017).

2. Potential of resting-state EEG dynamic analyses to evaluate cognitive network dysfunction in ALS

High-density EEG has emerged as a robust tool that offers spatio-temporal information regarding functional brain networks. While specific brain regions or networks have been associated with cognition, dynamic interactions in large-scale brain networks are also essential to cognitive processes and overall brain coordination (Bressler & Menon, 2010; Stam, 2005).

2.1. EEG microstates – sensor space

The utilisation of microstate EEG, as an additional approach, offers valuable complementary insights to functional connectivity. An increasing number of studies have demonstrated the sensitivity of microstate properties to neurological and psychiatric disorders, particularly those associated with disturbances in cognitive and behavioural processes (Al Zoubi et al., 2019; Dierks et al., 1997; Nishida et al., 2013; Tarailis et al., 2023; Terpou et al., 2022).

2.1.1. Transient, quasi-stable and recurring states of the brain

Microstates correspond to quasi-stable and recurring configurations of scalp electric fields that persist for a duration of a few tens of milliseconds. The concept of microstate originated from the initial observation that, within the EEG time series, the electrode positions of maximal and minimal potentials remain stable before swiftly transitioning to new positions that remain stable again (Lehmann et al., 1987). Polarity inversions (shift in the signs of the extrema) are observed during the stable periods as they follow the oscillations of the EEG signal. Oscillations of the same brain sources would cause an inversion of the polarity of the scalp electric field (Michel & Koenig, 2018). The absence of stable microstates in white noise with a Gaussian distribution (spatially unstructured data) or in time-shuffled EEG (temporally unstructured data) supports the notion that stable microstates are an intrinsic property of EEG signals and not the result of the specific processing methodology employed (Wackermann et al., 1993).

Statistically grouping EEG topographies with high spatial similarity, rather than considering extrema positions alone, allows for the identification of representative topographies that best represent the variance in the timeseries in a global approach (Pascual-Marqui et al., 1995). Through clustering, researchers have consistently identified four to seven distinct classes of microstates across different participants and conditions, which account for 66% to 88% of the overall variance in the EEG signal (Tarailis et al., 2023). Each microstate class is postulated to represent a fundamental "building block" of the spontaneous thought process (Lehmann et al., 1998). The original EEG timeseries can be decomposed into non-overlapping segments of the identified microstate classes (Michel & Koenig, 2018). Considering that functional states are believed to involve widespread brain activity, it is crucial to regard the scalp field as a whole. The reappearance of the same field configuration might arise from the involvement of identical neural sources, thereby reflecting the activation of the same functional network.

2.1.2. Neurophysiological basis of EEG microstates and their transitions

The mechanisms driving microstates and their transitions are complex and not fully understood, but several hypotheses have been proposed. Microstates are believed to reflect synchronized activity among large-scale neuronal networks. Synchronized firing of neurons within these networks generates macroscopic electrical fields that can be detected by EEG. Specifically, microstates are hypothesised to be generated by spatially distinct sources associated by phase synchrony (Seeber & Michel, 2021). Additionally, variations in cortical excitability, influenced by neurotransmitter levels such as noradrenaline, acetylcholine, dopamine, serotonin, or neuropeptides, may impact microstate dynamics. For example, oxytocin was demonstrated to impact microstate variations, especially their durations (Schiller et al., 2019). Thalamocortical networks have also been implicated in generating and modulating synchronized neural oscillations detected by EEG (Lopes da Silva, 2013), with observations of associations between microstates and thalamic nuclei reported in fMRI-EEG studies (Michel & Koenig, 2018; Schwab et al., 2015). Microstates were hypothesised to correspond to different states of thalamocortical network activity, with transitions between microstates reflecting shifts in the functional connectivity within these networks, potentially including cortico-cortical networks as well.

Although the exact mechanisms driving microstate transitions are unclear, studies have shown that transition probabilities are non-random, except in the case of Alzheimer's disease, which introduces randomness (Nishida et al., 2013). Regarding the timescale correspondence between EEG microstates (approximately 80ms) and fMRI (5-10s), research by Van der Ville et al. revealed a scale-free or 'fractal structure' of microstate dynamics, along with long-range dependencies dependent on microstate temporal characteristics (Gschwind et al., 2015; Ville et al., 2010). However, this scale-free characterisation and long-range dependencies were later discussed and a limit to the memory range (<1s) was suggested, considering the decay of the autoinformation function of the sequence of microstates (von Wegner et al., 2017).

The discrete nature of microstates has also been debated, with suggestions of a more continuous process (Mishra et al., 2020). While the dominance of a microstate over a specific duration is acknowledged, the microstate transitions and their underlying biomechanisms are proposed to follow continuous trajectories.

Overall, microstate dynamics likely arise from the interplay of multiple neurophysiological mechanisms, including neuronal synchronization, thalamocortical interactions, cortical excitability, neuromodulation, and others. Further research is needed to elucidate the specific contributions of these mechanisms to the generation and regulation of EEG microstates.

2.1.3. Localisation of the brain sources generating microstates

fMRI-EEG: multi-modal recordings

To investigate the potential relationship between resting-state EEG microstates and fMRI resting-state networks (RSN), several studies have simultaneously recorded EEG and fMRI data (Abreu et al., 2021; Britz et al., 2010; Hunyadi et al., 2019; Musso et al., 2010a; Yuan et al., 2012). However, the differences in methodologies employed in these studies make direct comparisons challenging (Michel & Koenig, 2018).

While most studies used a standard spatial clustering algorithm (Bréchet et al., 2019; Britz et al., 2010; Musso et al., 2010a), some studies employed ICA (Yuan et al., 2012) or HMM (Hunyadi et al., 2019) to identify these brain states. Moreover, the number of EEG microstates identified varied across studies, ranging from 4 to 16. In one study by Britz et al. (n= 9), the four canonical microstates were associated with auditory, visual, salience, and attention networks by convolving the microstate time courses with the hemodynamic response function and comparing them with fMRI ICA components (Britz et al., 2010).

The one-to-one correspondence between microstates and resting-states networks has however been questioned. Two studies (n=24, n=9) associated microstates maps with a combination of fMRI resting-state networks and vice-versa, which appears to more accurately represent the dynamics of brain states (Hunyadi et al., 2019; Yuan et al., 2012).

EEG microstates have consistently demonstrated a relationship with fMRI resting-state networks. The lack of a one-to-one association may be attributed to the disparity in temporal resolution between fMRI and EEG. In order to preserve the temporal resolution of EEG, several studies have employed EEG-based source localization methods to estimate the brain sources of the microstates (Michel & Koenig, 2018). These source estimations rely on a linear inverse solution applied directly to the EEG signals.

For instance, Bréchet et al., (n=15) extracted 6 microstates from task-initiated EEG data using standard spatial clustering and subsequently estimated the sources of each microstate using LAURA linear distributed inverse solution. They detected fMRI connectivity networks using fractional amplitude of low frequency fluctuations (fALFF) in consecutive fMRI recordings and reported anatomical overlap between fMRI connectivity networks and EEG microstates sources (Bréchet et al., 2019). Other studies independently analysed EEG recordings without association with fMRI data (Bagdasarov et al., 2022; Bréchet et al., 2020; Custo et al., 2017; Liu et al., 2021; Milz et al., 2017; Pascual-Marqui et al., 2014). Initially, Pascual-Marqui et al. applied eLORETA to estimate the source localisation of each microstate. By averaging the activity across participants (n=109), they observed a significant spatial overlap among microstates. The same group observed that microstate topographies were mainly influenced by alpha-band activity (Milz et al., 2017). They postulated that microstate transitions might reflect inhibitory functions, given that alpha oscillations are known to reflect inhibitory control. Moreover, they suggested that a diverse set of brain regions, rather than specific ones, could generate the same microstate class, which poses challenges for source localization. Custo et al, similarly reported a substantial overlap among the sources of seven microstates, identified using a 2-steps GLM approach, which they referred to as ‘common hubs’ (Custo et al., 2017). The identified microstate-specific brain regions additionally overlapped with the fMRI-EEG results of Britz et al (Britz et al., 2010).

More recent studies have explored the sources of microstates in various conditions, brain states, and during child development. In individuals with methamphetamine use disorder, the distribution of EEG power density during specific microstates is disrupted (Chen et al., 2020). For individuals with absence epilepsy, distinct microstate sources and parameters have been observed before and after seizures, suggesting a spatial and temporal recovery following the seizure (Liu et al., 2021). Bréchet et al. associated a particular class of microstates with the experience of dreams and investigated their source localization (Bréchet et al., 2020). Bagdasaro et al. observed changes in microstates C and D associated with age and sex in children aged 4-8. They identified the brain sources responsible for these microstates as partially located in the dorsal fronto-parietal network or dorsal attention network, and in the 'midcingulo-insular' or salience network, respectively (Bagdasarov et al., 2022).

2.1.4. Microstates and cognitive impairment

Functional interpretation of microstates

Combining results from source localisation and paradigm studies, leads to possible interpretation of the functional network /significance of each 'canonical' microstate.

Initially, microstate A was primarily associated with activation in the auditory network (Britz et al., 2010; Custo et al., 2017; Michel & Koenig, 2018). However, it has also been found to be linked to visual processing, particularly due to its higher coverage during visualisation rather than verbalisation tasks (Milz et al., 2016). In the recent systematic review by Tarailis et al, an association with the level of brain arousal or alertness was additionally suggested based on more recent findings (Tarailis et al., 2023).

Microstate B has predominantly been associated with the visual network based on source localization and paradigm-based studies (Bréchet et al., 2019; Britz et al., 2010; Custo et al., 2017; Michel & Koenig, 2018). Furthermore, an increased transition probability between microstate class B and microstate class C has been observed during an autobiographical memory task, possibly related to self-visualization (Bréchet et al., 2019).

Microstate C topography tends to differ between studies and is sometimes reported as split between two different microstates with high spatial correlation, in studies with more than four microstate classes (Custo et al., 2017; Michel & Koenig, 2018; Tarailis et al., 2023). Britz et al, interpretated microstate C as originating from the salience network using combined EEG-fMRI recordings (Britz et al., 2010). Source localisation studies observed a similar overlap with the DMN but rather related microstate C with self-reflection and internal mentation (Bréchet et al., 2019; Custo et al., 2017).

The findings from studies investigating brain activity during microstates predominantly indicate an association between microstate D and the dorsal frontoparietal or dorsal attention network (Bréchet et al., 2019; Britz et al., 2010; Custo et al., 2017; Pascual-Marqui et al., 2014). Notably, microstate D was found to be less prevalent during hypnosis (Katayama et al., 2007) or during an undirected mentation, as applied in transcendental meditation (Faber et al., 2017). These observations suggest that microstate D is associated with executive functioning, like attention reorientation.

Although the specific brain regions generating microstates lack replicability, possibly due to methodological differences and temporal overlap, it seems evident that microstate classes A

especially and microstate B, in a lesser extent, are associated with more fundamental somatosensory functions, while classes C and D are linked to higher-order cognitive functions, as highlighted by Michel and Koenig (Michel & Koenig, 2018).

Fluctuations in microstate properties in neurological and neuropsychological conditions

To further establish the association of classes C and D with cognition, the influence of neuropsychiatric conditions like schizophrenia or frontotemporal dementia on the balance between microstate classes C and D has been observed (Nishida et al., 2013). Notably, a comprehensive meta-analysis spanning 15 years of research in schizophrenia revealed that microstate properties demonstrate larger effect sizes compared to spectral measures (Rieger et al., 2016). Although task-based averaged ERP analysis remains superior in identifying impaired brain processes in schizophrenia, microstate analysis offers distinct advantages when studying resting-state. Resting-state analysis are particularly relevant in specific cases, such as those affected by locked-in syndrome, while also enhancing our overall understanding of a condition.

In bipolar disorder during the euthymic mental state, alterations in microstate class B properties have been observed, showing correlation with symptoms of dissociation and anxiety (Damborská et al., 2019; Vellante et al., 2020). However, the findings yielded contradictory results, with one study suggesting an increase in microstate B presence while the second indicates a decrease.

In Alzheimer's disease, random patterns of microstate transitions have been observed, which do not occur in healthy controls (Nishida et al., 2013). There has also been a reported decrease in microstate stability (Dierks et al., 1997), and recently, a combination of EEG spectral measures and microstate complexity (new measure of transitioning between microstates) has enabled the classification of individuals with Alzheimer's disease versus healthy controls and the prediction of mild cognitive impairment progressing to Alzheimer's disease (Tait et al., 2020). These findings suggest that EEG microstate analysis has the potential to become a functional biomarker for Alzheimer's disease.

Similarly, microstate properties have been proposed as a biomarker for Parkinson's disease (Pal et al., 2021). The transition between microstate classes has been observed to correlate with cognitive impairment as assessed by the Mini-Mental State Examination (Hanoglu et al., 2022), while the occurrence of microstate C and the duration of microstate B have been found

to correlate with cognitive decline as measured by the Montreal Cognitive Assessment (C. Chu et al., 2020)

Microstates, which represent patterns of topographies, hold significant potential in tracking cognitive network dysfunction.

2.2. Temporal patterns of spectral power and functional connectivity

Resting-state EEG connectivity measures have demonstrated superior discrimination between individuals with ALS and those without, in comparison to time-domain measures (Dukic et al., 2019). Consequently, investigating dynamical patterns of connectivity becomes particularly intriguing. Phase synchrony, a measure of functional connectivity, holds particular relevance as it is hypothesised to serve as a coordination and regulation mechanism for cognitive processes (Cohen, 2019). Studies have revealed its importance in cognitive functions such as working memory and attention tasks (Hinault et al., 2020; Varela et al., 2001).

The spectrally-distinct episodes observed in resting-state recordings (Dukic et al., 2019; Nasseroleslami et al., 2019) serves as evidence that dynamic analysis of spectral power and connectivity measures can provide reliable domain-specific indicators of impairment in ALS.

2.2.1. Microstates in time-frequency domain

Brain microstates represent the concept of transient, yet repetitive occurrences of relatively stable topographies, associated with (one or more) brain sources. The Topographic Time-Frequency Decomposition (TTFD) of EEG signal, proposed by Koenig et al., combines time-domain topographies with time-frequency (TF) decomposition of the signal, using complex Gabor wavelets (Koenig et al., 2001). This is achieved by generating time-frequency planes, resulting in a topographical representation in the time-frequency domain. In a similar manner to microstate analysis, a clustering approach can be used to identify the most dominant time-frequency topographies.

This method has proven its efficacy in predicting fMRI dynamic functional connectivity (dFC) states more accurately than spectral power alone. Abreu et al. demonstrated that four time-frequency microstates derived from TTFD outperformed spectral power in predicting fMRI dFC states, achieving an accuracy of 90% compared to 20% with spectral power (Abreu et al., 2021). This highlights the relevance of time-frequency EEG microstates in comprehending brain network dynamics. More specifically, TF microstates (B, C and D) were associated with specific thalamus subnuclei activity as captured by simultaneous EEG-fMRI recordings

(Schwab et al., 2015). Thalamus control over functional cortical connectivity has been hypothesised to play a key role in attention and cognitive function (Schmitt et al., 2017), which may relate to the association of EEG microstates with cognitive mechanisms such as attention, memory or executive function.

2.2.2. *Dynamic analysis of spectral power and functional connectivity*

Vidaurre et al. have documented instances of transient, recurring events, in which spectral MEG measures such as spectral power and phase-based connectivity exhibit stability (Vidaurre et al., 2016; Vidaurre, Hunt, et al., 2018). Using an algorithm based on the Hidden Markov Model, they inferred spectral power and phase synchrony (in function of the frequency) for short period of time which may represent a stable HMM state or brain network. They then estimated how well the parameters can explain each time point to determine whether timepoints belong to the same state. Spectral, temporal and spatial information are all included in the resulting models. The source-localised power and connectivity features of the identified HMM states enabled the authors to link some states with functional sensory, motor and cognitive networks.

Expanding on this methodology, Fauchon et al. (Fauchon et al., 2022) applied the same method to neuropathic pain, revealing abnormal patterns in the HMM MEG states associated with the sensorimotor and ascending nociceptive pathways, as well as the frontal attentional network when compared with healthy controls. Similarly, Zhang et al. investigated patients with major depression, using the same method, and observed alterations in the default mode network (DMN) and increased occupancy (or neural activity) in the fronto-temporal network among suicide attempters, as compared to non-suicidal patients (Zhang et al., 2022). Furthermore, the same research group successfully combined MEG with intracranial EEG, establishing a relationship between intracranial EEG power changes and MEG HMM brain states (Zhang et al., 2021).

Growing evidence indicates that the whole-brain network can be decomposed into functional resting-state subnetworks consisting of spatially distributed brain regions (Damoiseaux et al., 2006; Smitha et al., 2017; van den Heuvel et al., 2009). Previous research using fMRI has demonstrated the importance of temporal fluctuations in functional connectivity, showing specific changes during different mental states such as analgesia (L. F. Robinson et al., 2015),

as well as in neurological and psychiatric conditions such as schizophrenia, major depression, and Alzheimer's disease (Hutchison et al., 2013).

The development of new analysis methods for M/EEG holds the promise of enabling the identification of resting-state functional networks, similar to those well-established in fMRI literature.

III. Aims and objectives

1. Aims

ALS is a neurodegenerative disease that affects both motor and non-motor neural networks. To effectively monitor the cognitive network dysfunction in ALS, there is a certain need for reliable biomarkers. Resting-state EEG has emerged as a promising tool for detecting neural network disruptions in ALS due to its non-invasive and low-cost nature.

Previous resting-state EEG studies have shown non-motor neural network dysfunction in ALS (Nasseroleslami et al., 2019). Potential neurophysiological biomarkers that characterize these disruptions have already been described. By using source-space reconstructed resting-state EEG, functional connectivity differences have been observed between ALS and healthy control (HC) cohorts, which correlated with MRI structural changes and cognitive decline (Dukic et al., 2019). Resting-state EEG connectivity measures also formed stable clusters, which can serve as novel ALS phenotypes (Dukic et al., 2022). By identifying these phenotypes, clinicians can better tailor treatments and monitor disease progression. In summary, resting-state EEG is an advantageous tool for detecting and characterising cognitive network dysfunction in ALS. Using this promising method, the current work aimed to:

Aim 1: Characterise cognitive phenotypes in ALS by distinct longitudinal changes of functional network disruptions

Aim 2: Classify ALS patients based on resting-state EEG trajectories: clinical relevance and network progression

Aim 3: Develop new biomarkers of cognitive-behavioural impairment based on dynamic resting-state episodes in sensor-space

Aim 4: Develop new biomarkers of cognitive-behavioural impairment from spectral power and connectivity changes, using dynamic analysis of resting-state data

2. Hypotheses and Objectives

2.1. Aim 1: Characterise cognitive phenotypes in ALS by distinct longitudinal changes of functional network disruptions

Rationale: The acknowledgement of the wide-ranging and diverse nature of neuropsychological impairments has been instrumental in pinpointing the existence of the ALS-FTD spectrum, which in turn has resulted in the development of the revised Strong diagnosis criteria (Strong et al., 2017). About 40% of patients exhibit cognitive or behavioural abnormalities, and an additional 14% develop dementia. Given the clinical heterogeneity inherent to the disease, the process of diagnosis and prediction of prognoses, as well as determining the efficacy of palliative treatment, can be challenging. Resting-state EEG has already detected non-motor network dysfunction in ALS patients that persisted over time in sensor-space (Nasseroleslami et al., 2019). In addition, changes in RS EEG functional connectivity have been observed between ALS patients and healthy controls that are correlated with cognitive decline (Dukic et al., 2019).

Hypothesis: Distinct longitudinal changes of functional network disruption would correspond to distinct cognitive phenotypes

2.2. Aim 2: Classify ALS patients based on resting-state EEG trajectories: clinical relevance and network progression

Rationale: Longitudinal resting-state EEG spectral measures can offer valuable biomarkers to evaluate the dysregulation of cognitive-behavioural brain networks in ALS. The goal is to define stable subgroups of ALS patients based on trajectories of resting-state spectral EEG measures over time and to determine whether such clusters can be linked to clinical cognitive presentation. Relations between resting-state EEG trajectories and comprehensive clinical neuropsychological evaluations should allow creation of a comprehensive, network-based measure of impairment suitable for clinical trials. Analyzing patterns of brain activity trajectories could provide valuable insights into disease progression, survival outcomes, and functional decline. EEG-based subgrouping of individuals with ALS may contribute to a better understanding of ALS mechanisms and inform more personalised approaches to treatment and patient care.

Hypothesis: This data-driven approach would generate a, longitudinally tested, set of measures, facilitating the development of a network-based measure of impairment suitable for

clinical trials and enhancing our understanding of ALS mechanisms for personalized treatment and care.

2.3. Aim 3: Develop new biomarkers of cognitive-behavioural impairment based on dynamic resting-state episodes in sensor-space

Rationale: Previous studies have explored abnormal connectivity in ALS using EEG measures (Dukic et al., 2019; Nasseroleslami et al., 2019), but the temporal dynamics of these measures are not well understood. Analysing multi-channel EEG signals can help identify transient, recurrent, and stable brain states. This approach, known as microstate analysis, identifies similar activity patterns and assigns each time point to a specific microstate, hypothesised to represent the synchronized activity of neural elements in a functional network (Michel & Koenig, 2018). Changes in microstate parameters reflect modulations in the temporal dynamics *of* brain networks rather than changes in connectivity *between* networks (Gschwind et al., 2016). Microstate analysis is an established method that has revealed altered temporal dynamics in participants with neurological and psychiatric conditions, despite the stability of canonical microstate prototypes across participants and conditions (Al Zoubi et al., 2019; Michel & Koenig, 2018; Nishida et al., 2013).

The culmination of prior research on resting-state EEG and the identification of specific cognitive episodes within resting-state activity serve as compelling evidence that the analysis of RS EEG signals can yield reliable measures of cognitive dysfunction.

Hypothesis: Data generated from cognitive episodes of resting-state activity will provide biomarkers that strongly correlate with cognitive and behavioural impairment.

2.4. Aim 4: Develop new measures of cognitive-behavioural impairment from spectral power and connectivity changes, using dynamic analysis of resting-state data in source-space

Rationale: Another approach to studying brain network dynamics involves analysing patterns of frequency-specific power and phase-coupling. Co-modulation or synchrony between signals reflects important mechanisms of brain network coordination during motor or cognitive tasks. Differences in spectral power and functional connectivity have been observed between cohorts with amyotrophic lateral sclerosis (ALS) and healthy controls (HC). Specifically, disruptions in functional connectivity in frontal, frontoparietal, and fronto-temporal regions have been found to correlate with cognitive decline (Dukic et al., 2019).

Resting-state electrophysiology studies have revealed abnormal dynamical patterns of spectral power and/or functional connectivity in neuropathic pain (Fauchon et al., 2022), Alzheimer's disease (Núñez et al., 2021), and depression (Zhang et al., 2022). Such spatially distinct patterns are hypothesised to reflect functionally different brain networks.

The findings from resting-state EEG studies, combined with the identification of spectrally distinct episodes in resting-state activity, serve as a proof of concept that analysing spectral brain microstates in resting-state EEG can provide reliable brain network-specific indicators of impairment.

Hypothesis: data generated from spectral cognitive episodes of resting-state activity would yield new and complementary biomarkers of network impairment that strongly correlate with cognitive and behavioural deficits.

IV. General materials and methods

1. Participant recruitment

Ethical approval was obtained from the Tallaght University Hospital / St. James's Hospital Joint Research Ethics Committee - Dublin [REC references: 2014 Chairman's Action 7; 2019-05 List 17 (01)] before the start of the project and data acquisition was performed in accordance with the Declaration of Helsinki. All participants provided informed written consent to the procedures before undergoing assessment. Specific and detailed participants' demographics are included for each project in the corresponding chapter.

1.1. ALS patient recruitment

Clinicians approached patients diagnosed with ALS or ALS-FTD in the Irish National Centre of Expertise of ALS in Beaumont Hospital, Dublin, Ireland. All ALS diagnoses were based on the revised El Escorial criteria (Ludolph et al., 2015) and the Strong criteria (Strong et al., 2017). Patients were offered the opportunity to participate in research and if interested were contacted later by phone call by a member of the Neural signal analysis and neurophysiology team to get further information on the progression of the EEG experiment. Patients diagnosed with primary lateral sclerosis (PLS), progressive muscular atrophy (PMA), multiple sclerosis (MS), flail arm/leg syndromes, or with other medical morbidities/neurological

symptomatology like stroke, brain tumor or epilepsy were excluded. Consenting and suitable participants were dully informed of the longitudinal nature of the study (up to five recordings were to be scheduled every four to five months) but high dropout was expected due to the fast progression of the disease. As the disease progresses, it becomes more difficult for patients to travel to the hospital or even to stay in a sitting position for extended periods of time due notably to muscle cramps.

1.2. Controls recruitment

Aged-matched healthy controls (HC), without any neurological condition, were additionally recruited by a member of the team from an existing volunteer database (Burke et al., 2017) or through public advertising. First-degree relatives of ALS patients were excluded from the study to avoid any potential bias due to pre-symptomatic ALS or other related subthreshold clinical characteristics.

2. Electrophysiological signals

2.1. Acquisition hardware

Electrophysiological signals were recorded on a Biosemi ActiveTwo system (Honsbeek et al., 1998). The ActiveTwo system measures time-varying potential differences on body surfaces, using sintered Ag/AgCl electrodes. The active nature of the electrodes allows for reduced noise levels. A conductive gel at the interface between the electrode and the skin further limited external noise.

Eight flat-type electrodes were used to detect physiological artefacts by recording electromyograms (EMG) and electrooculograms (EOG) signals. The EEG recordings were performed using 128 pin-type electrodes, with equiradial distribution on the skull, in a positioning headcap. High-density EEG improves the ability to estimate brain regions localised activity. All recordings were protected from external electric fields by a Faraday cage. Signals were digitised at 2048Hz and transmitted to the monitoring computer through a fiber-optic cable to ensure electrical isolation and absence of interference.

2.2. Acquisition software

The signals were recorded at 512 Hz, with a low-pass anti-aliasing filter (cut-off at 104Hz), using Actiview software (Honsbeek et al., 1998). Online monitoring of signals stability and amplitude insured high quality recordings.

2.3. Data acquisition procedure

The experiments comprised resting-state EEG recordings, conducted at the Clinical Research Facility (CRF) of St James's Hospital, Dublin. Written consent was obtained from participants after a careful reminder of the voluntary nature of the study and an outline of the experiment. For the duration of the experiment, participants were seated in a high-backseat or their own wheelchair when required. Eight EMG/EOG electrodes were applied on cleaned skin, on the earlobes, the temples, the mastoids and above/below the left eye. A size-appropriate headcap was then positioned by centring the electrode A1, horizontally between the nasion and inion bones, and coronally between the two ears, to allow future comparisons between participants. The positioning of the EEG cap was secured before the appliance of electrolyte gel in each electrode holder. While inserting pin-type electrodes in their assigned holders a conductive bridge formed between the skin and the electrodes. All electrode cables were tied to the participant's chair to avoid any pulling.

Electrode offsets, measuring the difference in voltage between an electrode and the Common mode sense (CMS) reference electrode, were monitored to remain stable and between +/- 25mV. Following set-up, participants were asked to rest with eyes open (EO) and then closed (EC), always while comfortably seated. A letter X (6x8 cm^2, printed black on white) provided a gaze target. EEG signals were recorded, for six blocks of 2 min, (three for each eye condition) to ensure subject wakefulness and well-being in-between. To ensure the most advantageous combination of participant effort and research output, the resting-state recordings were part of a much larger EEG experimental procedure, which will not be detailed, as only the resting-state data were analysed for the subsequent results. It has to be noted that resting-state recordings were not conducted in a naive state, as participants typically engaged in cognitive or motor tasks prior to the recording.

2.4. Signal analysis

The EEG signals were analysed using MATLAB R2019b-R2022a software (The MathWorks, 2019), the EyeBallGUI toolbox (Mohr et al., 2017), the Fieldtrip v20190905 toolbox (Oostenveld et al., 2011) and the EEGLAB 2019 toolbox (Delorme & Makeig, 2004).

2.4.1. Preprocessing

An automatic artefact rejection method was used to reject bad epochs in the EEG signals (Dukic et al., 2017). The amplitude, the mean shift, the variance and the band-variance of spectral power were checked against a 3.5 Z-score threshold. The EEG signal was resampled at 256 Hz, band-pass (one-pass zero-phase FIR: 1-97Hz) and notch filtered (third-order Butterworth: 50Hz). An automatic algorithm [28] [29], which evaluates the correlation between EEG channels, high signal standard deviations and the ratio of high to low frequencies, was then used to detect noisy channels. The average number of removed channels was 3.9±8.6. If more than 11 channels were marked as noisy, the recording was excluded from the study. Channels that were marked for removal were interpolated from the remaining electrodes using spline interpolation (Oostenveld et al., 2011). Finally, the channels were referenced to the common average.

2.4.2. Source estimations

The EEG data were processed as described in Dukic et al. (Dukic et al., 2019). Namely, source localisation was performed using the Linearly Constrained Minimum Variance (LCMV) beamformer (Oostenveld et al., 2011) and a head model based on the ICBM152 MRI template (Fonov et al., 2009). The source-space signals were estimated in 90 brain regions from the automated anatomical labelling (AAL) atlas (Tzourio-Mazoyer et al., 2002). Using these source-localised signals, spectral measures were computed in six frequency bands usually considered in resting-state EEG studies (Dukic et al., 2017; Iyer et al., 2015), i.e. δ (2-4 Hz), θ (4-7 Hz), α (7-13 Hz), β (13-30Hz), γ_l (30-47 Hz) and γ_h (53-97 Hz). For each brain region, normalised spectral power was estimated using a Fast Fourier analysis applied on 2 s epochs. For all pairs of brain regions, functional connectivity was estimated using amplitude envelope correlation (AEC), which measures the co-modulation, and using imaginary coherence (iCoh), which measures the synchrony between two regions of interest (ROIs).

2.4.3. Longitudinal analyses

The longitudinal analyses performed on the spectral power and functional connectivity data are described in chapter V.

2.4.4. Dynamic analyses

Dynamic analyses of resting-state EEG data were conducted to establish new measures of impairment in ALS. Changes in the dynamics of EEG signals have been observed in numerous neuropsychiatric conditions (Koenig et al., 1999; Lehmann et al., 2005; Michel & Koenig, 2018; Nishida et al., 2013). Such analyses were meant to interrogate, in particular, fronto-temporal and fronto-parietal cognitive networks. To this end, we investigated transient brain states defined in time and frequency domains. Detailed descriptions can be find in chapters VII and VIII.

3. Motor and cognitive clinical scores

Most patients underwent further clinical assessments, independently from the current project, including the revised ALS functional rating scale (ALSFRS-R) (Cedarbaum et al., 1999), King's stagings, as well as ALS-specific behavioural and cognitive measurements (Traynor et al., 2003). Patients' written and informed consent, included agreement to share clinical information with the research team. Functional clinical evaluations were collected from the Irish Motor Neuron Disease Registry (O'Toole et al., 2008; Rooney et al., 2013; Ryan et al., 2018; Traynor et al., 2003) for the benefit of this research. Longitudinal Edinburgh cognitive and behavioural ALS Screen (ECAS) (Abrahams et al., 2014) and Beaumont behavioural inventory (BBI) (Elamin et al., 2017) were collected by the Academic Unit of Neurology, TCD, and made available for correlative analyses.

3.1. Survival

As part of the Irish Motor Neuron Disease Registry, ALS patients were asked an estimation of the initial date of symptoms onset. Dates of death are tracked as well to allow for survival time estimations.

3.2. ALSFRS-R

The revised ALS-functional rating scale (ALSFRS-R) evaluates a patient physical function through 12 measures rated from 0 to 4 (normal). Measures include the capacity to swallow, use utensils, climb stairs or breath and were grouped to be anatomically relevant. We defined

subgroups of the total rate, respectively of which body region or system the tasks fall in. The 'bulbar' subgroup corresponds to scores 1 to 3, 'upper limbs' to scores 4 to 6, 'lower limbs' to scores 7 to 9 and 'respiratory' to scores 10 to 12. ALSFRS-R scores were collected, for most patients participating in the study, by clinicians as part of the Irish National ALS clinic.

3.3. King's stagings

The King's clinical staging system similarly estimates the anatomical progression of the disease. Stages are defined based on the number of affected regions, from 1 (early disease) to 5 (death). When no King's staging was available, the staging was extrapolated from ALSFRS-R scores (Balendra et al., 2014).

3.4. Edinburgh cognitive and behavioural ALS screen (ECAS)

The Edinburgh Cognitive and Behavioral ALS Screen (ECAS) (Abrahams et al., 2014) is widely used to detect cognitive and behavioural changes, specifically in ALS patients. The screen consists of a quick neuropsychological assessment, usually performed by a trained professional as part of the Irish National ALS clinic. This screening tool incorporates executive, social, verbal fluency and language tasks, as ALS-specific assessments, but also memory and visuospatial tasks, as non-ALS specific. The total score ranges from 0 (poorest) to 136 (best performance). Three versions of the questionnaire (A, B and C) were used to reduce the practice effects (Costello et al., 2020; C. J. Crockford et al., 2018). Established cut-off scores based on age and education in the Irish normative population were utilised to label patients with abnormal cognition.

3.5. Pre-morbid IQ

As a further cognitive assessment, a test of pre-morbid functioning (TOPF), which is an updated version of the Wechsler test of adult reading, estimated pre-symptomatic IQ in ALS patients attending the Irish National ALS clinic (Wechsler, 2003).

3.6. Beaumont behavioural inventory (BBI)

The BBI questionnaire was specifically designed to evaluate behavioural changes in ALS while taking into account the influence of motor impairment (Elamin et al., 2017). Scores above 6 correspond to mild impairment while scores above 22 show severe behavioural changes.

4. Statistical methods

Only statistical methods repeatedly used during the project are described in this section, more specific statistical analyses are described in their corresponding result section. All statistical analyses were performed using MATLAB software (The MathWorks, 2019).

4.1. Parametric statistics

Parametric statistics assume the data follow a probability distribution with fixed parameters, often the normal distribution.

4.1.1. Linear Mixed-Effects model

Linear mixed-effects (LME) models combine 'fixed' and 'random' effects, as an extension of standard linear models. They require linearity, homoscedasticity and normality of the residuals. Mixed-effects models are well adapted for sparse or unbalanced data sets (West et al., 2007) and thus recommended for longitudinal studies with missing data. In addition, subject-specific random effects are appropriate to represent at best the phenotypic diversity of ALS disease.

4.2. Non-parametric statistics

Non-parametric statistics are defined as not requiring any 'parameter' specification, either because no distribution shape is specified or because the probability distribution is specified without its parameters. Order and ranks statistics are common examples of such statistics. In the case of a normal distribution, parametric tests usually have more statistical power. However, the non-parametric methods have the advantages of the robustness and more generally, have wider applications.

4.2.1. Non-parametric inferential statistical methods

The Mann-Whitney-U test or Wilcoxon unsigned rank test is a non-parametric test applied on independent samples (Mann & Whitney, 1947). The null hypothesis assumes the two samples have identical distributions. It can be interpretated as a test of equality of the medians.

The Wilcoxon signed rank test is another non-parametric hypothesis test, which is applied on paired observations (Mann & Whitney, 1947). It tests the null hypothesis that the median of the distribution is null.

The non-parametric equivalent of the one-way analysis of variance (ANOVA), the Kruskal-Wallis test, has also been applied.

The frequently mentioned, Spearmann's correlation, is a rank-based measure that evaluates monotonic relationships between two variables. The parametric Pearson's correlation only assesses linear relationships but is more robust to outliers.

For any statistical test, a true effect can only be accurately detected if there is enough statistical power ($1-\beta$). In this study, the statistical power or probability of correctly rejecting the null hypothesis, was estimated based on an Empirical Bayesian inference (EBI) (Nasseroleslami, 2018). The EBI toolbox initially fits an Akaike information criteria (AIC)-guided Gaussian mixed model on the Z-transformed test statistics to obtain an empirical estimation of the probability density function. Probability density functions were then similarly estimated for the null and non-null distributions, both acquired by bootstrapping. Prior and posterior probabilities were inferred from the null distribution and density functions. Type I error (α), Type II error (β) and false discovery rate (FDR) could then be evaluated by numerical integration of the density functions.

When considering multiple comparisons, the number of potential errors grows with the number of inferences. To counterbalance this issue, controlling procedures, like the Bonferroni correction (Bonferroni, 1936), have been developed. Among those, the FDR estimates the rate of false rejections. It was initially described by Benjamini and Hochberg to provide control over the number of Type I errors (false positives or α) (Benjamini & Hochberg, 1995). They later proposed an adaptive FDR with improved power (Benjamini et al., 2006). This latest version is coded in the EBI toolbox and has been used to correct for multiple comparisons during this project (Nasseroleslami, 2018).

V. Results: Cognitive phenotypes in ALS characterised by distinct longitudinal changes of functional network disruptions: a resting-state EEG study

The study described in this section has been submitted to a peer-reviewed journal:

Metzger M, Dukic S, et al., Distinct longitudinal EEG functional network disruptions characterise ALS cognitive phenotypes.

Figures, tables, results and discussion sections comes, in full, from this manuscript. Introduction and methods sections from this manuscript have been abbreviated to avoid repetition of the contents of previous chapters. The work described in this chapter is based on the cross-sectional study and data collection carried out by Mr Stefan Dukic when he was working in the Academic Unit of Neurology, TCD. Existing code was adapted and applied to longitudinal data. Further statistical analyses were developed specifically for this project.

1. Introduction

The presence of a wide a range of clinical presentations in ALS leads to uncertainties when diagnosing and predicting the disease course. There is therefore an urgent need for robust and validated phenotypic biomarkers, to improve understanding of variation in ALS progression and responses to potential therapies.(Bede & Hardiman, 2018; Nasseroleslami, 2018; Pender et al., 2020; Taga & Maragakis, 2018).

Functional and structural magnetic resonance imaging (fMRI-sMRI) have been extensively employed to identify alterations in the brain due to ALS, revealing variations in grey matter and functional connectivity among subgroups of individuals with ALS based on cognitive profiles, both cross-sectionally(Temp et al., 2021) and longitudinally(Burgh et al., 2020; Shen et al., 2018). Nevertheless, using fMRI for clinical trials presents obstacles, encompassing considerable expenses, participant unease, restricted applicability to certain groups, and temporal resolution constraints, which are not encountered in other neuroimaging modalities like EEG.

Directly measuring the function of networks which generate these cognitive and behavioural functions shows promise in the search for such biomarkers.(McMackin et al., 2020; McMackin, Muthuraman, et al., 2019) In particular, resting-state EEG offers greater accessibility and reduced participant burden, as it avoids the necessity of specific actions or responses, mitigating potential biases from speech or motor disabilities.(Maruyama et al., 2021; Secco et al., 2020) Differences between the ALS group and healthy controls that persisted longitudinally have been identified, at sensor level, in resting-state EEG measures of neural activity (from θ-band spectral power) and functional connectivity (from θ, γ_h-band coherence between signals).(Nasseroleslami et al., 2019) Furthermore, source localization of EEG signals allowed researchers to determine the specific regions within the brain that generated the electrical activities recorded on the scalp. A subsequent study observed disease-

specific patterns in the spatially mapped sources of brain activity, providing insights into the neural dynamics underlying functional impairments.(Dukic et al., 2019) Across different frequency bands, a decrease in neural activity has been shown in motor and non-motor networks (including the occipital, temporal and sensorimotor regions). Additionally, an increase in the co-modulation of signals has been observed in the central, posterior and frontal areas, while the synchrony between signals decreased in the frontotemporal and sensorimotor regions. Changes in EEG functional connectivity correlated with MRI structural atrophy in cognitive networks (frontal region), as well as clinical measures of functional cognitive impairment.

In our previous studies, we demonstrated that resting-state electroencephalography (EEG) can identify at least four specific patterns of network dysfunction. PwALS who were part of the two clusters that displayed alterations in frontotemporal networks compared to HC, also demonstrated heightened cognitive and behavioral impairment. This observation points toward a link between network dysfunction and specific neuropsychological profiles manifested by individuals. The current longitudinal study is needed to show reliability and effectiveness of these measures, paving the way for their potential development into prognostic biomarkers for ALS. The primary objectives of this study were to identify and quantify changes in functional brain networks throughout the progression of ALS in individuals with distinct cognitive profiles.

2. Methods

2.1. Ethical approval

Ethical approval was obtained from the Tallaght University Hospital/St. James's Hospital Joint Research Ethics Committee in Dublin [reference: 2014 Chairman's Action 7 and 2019-05 List 17 (01)], as described in General material and methods (Chapter IV).

2.2. Recruitment – inclusion and exclusion criteria

Exclusion and inclusion criteria are described in General material and methods (Chapter IV, section 1).

Table 1: Demographic profiles for the individuals with ALS. Up to five recording sessions were scheduled, with in-between time delays representing delays between each session. The table details the gender proportions, the average ages at

recording and, when applicable, disease durations, delays between sessions, site of onset and the number of patients with FTD comorbidity. Numbers show mean and standard deviation.

Groups	N	Male (%)	Age (years)	Disease duration [increment since T1] (months)	Follow-up intervals (months)	ALSFRS-R scores (at Tx)	Site of onset (N)			ALS-FTD diagnosis (N)
							Bulbar	*Spinal*	*Thoracic*	
Participants T1	116	74	62 ± 11	25 ± 18	/	36 ± 7	22 (19%)	86 (74%)	5 (4%)	5
Participants T2	60	77	60 ± 11	32 ± 19 [+7.3]	4.9 ± 1.2	35 ± 8	14 (23%)	43 (72%)	2 (3%)	2
Participants T3	44	80	60 ± 12	37 ± 19 [+12]	4.9 ± 1.3	33 ± 9	8 (18%)	34 (77%)	1 (2%)	2
Participants T4	22	86	61 ± 11	42 ± 24 [+17]	4.9 ± 1.1	33 ± 7	2 (9%)	19 (86%)	1 (1%)	1
Participants T5	7	57	57 ± 13	52 ± 31 [+27]	6.5 ± 2.4	33 ± 6	0	6 (86%)	1 (14%)	0

2.3. Experiment

2.3.1. Experimental design

The recruited participants attended EEG recording sessions. No blinding was performed, as the participants, experimenters or data analysists could not access the final EEG measures during experiments. EEG data from 124 individuals with ALS (male: 69.3%; age [mean ± standard deviation]: 63.13 ± 15) were recorded. The study included up to four follow-up recording sessions, with approximately 5.4 ± 2.1 months between sessions. The total number of EEG recordings was 249, of which 116 were baseline and 60, 44, 22 and 7 were follow-up 1-4, respectively. On average, the participants attended 2 ± 1.2 recording sessions.

2.3.2. Recruitment – inclusion and exclusion criteria

Exclusion and inclusion criteria are described in General material and methods (Chapter IV, section 1).

Table 1 details the demographic profile for each follow-up.

2.3.3. EEG acquisition

EEG data were collected at rest as described in General material and methods (Chapter IV, section 2).

2.3.4. Disease severity and neuropsychology assessment

Disease severity was assessed using ALSFRS-R scores (Cedarbaum et al., 1999) and King's staging system,(Balendra et al., 2014) collected from the Irish Motor Neuron Disease Registry. The assessments are described in details in General material and methods (Chapter IV, section 3). The participants' ALSFRS-R scores were recorded on average 7.4 ± 5.1 times, between 3.7 and 145 months after onset. The symptoms were evaluated at intervals of approximately 3.3 ± 3.7 months. Except for 9 participants from the EEG database, all participants had their ALSFRS-R scores registered.

To provide wider clinical profiling, the Edinburgh Cognitive and Behavioral ALS Screen (ECAS) (Abrahams et al., 2014) and Beaumont behavioral inventory (BBI),(Elamin et al., 2017) which were developed to compensate for the impact of motor impairment in ALS, were also obtained from parallel ongoing research projects in the Academic Unit of Neurology.(Costello et al., 2020, 2021) The ECAS scores were obtained up to three times, between 3.7 and 100 months after onset, with a score range of 46 to 135 (for total ECAS, with an abnormality cut-off adapted for age and level of education). Three versions of the ECAS (A, B and C) were used to reduce the practice effects.(Costello et al., 2020; C. J. Crockford et al., 2018) Behaviour was assessed using the Beaumont behavioural inventory. BBI assessments were conducted up to three times for each participant, between 2.8 and 100 months after onset, yielding scores ranging from 0 to 73 (above 6 representing mild impairment and above 22 representing severe impairment).

2.3.5. Subgrouping of participants according to their neuropsychological profiles

To analyse the effect of the cognitive and behavioural impairment on spectral EEG measures, the longitudinal trajectories were modelled separately for subgroups of individuals with ALS: cognitively impaired (ci), behaviourally impaired (bi) and non-impaired (ncbi). This discrimination by neuropsychological profiles was included with the expectation that participants with cognitive or behavioural impairment experience different progressions of neurodegeneration compard to participants with normal cognition and behaviour. The ALS group comprised a total of 124 participants, with 27 participants exhibiting cognitive impairment (ALSci), 58 participants demonstrating behavioral impairment (ALSbi), and 53

participants showing no cognitive or behavioral impairment (ALSncbi). 14 participants were part of both the ALSci and ALSbi groups due to displaying both cognitive and behavioral impairments. Abnormal cognition was determined for a participant if they were diagnosed with ALS-FTD or if their ECAS scores exceeded the abnormality cut-off scores based on age and education for the Irish population.(Pinto-Grau et al., 2017; C. J. Crockford et al., 2018; Costello et al., 2020) The assessment of abnormal behavior was conducted using the BBI, with behavioral impairment defined as scoring ≥ 6 points on the BBI scale.

2.4. Data analysis

The EEG signals were preprocessed and processed as described in Chapter IV, section 2.4.

The normalised spectral power, which measures the neural activity in a brain region, the amplitude envelope correlation (AEC), which measures the co-modulation between two regions, and the imaginary coherence (iCoh), which measures the synchrony between two regions, were all obtained from the source-localised signals.

2.5. Statistical analysis

Linear mixed-effects (LME) models, which can account for disease heterogeneous progressions, were used to track brain network patterns of participants over time. This method has been shown to be robust for sparse and unbalanced data sets and useful for longitudinal studies with missing data.(West et al., 2007) LME Models were built to estimate the progressions of the EEG measures (normalised spectral power and connectivity) and of the clinical scores (ALSFRS-R, ECAS and BBI) over time.

2.5.1. Electroencephalography

Spectral power, co-modulation and synchrony were analysed separately for each frequency band ($\delta, \theta, \alpha, \beta, \gamma_l, \gamma_h$). All models were built in MATLAB using the *fitlme* function, with the Quasi-Newton method, as the iterative algorithm to data fitting and optimising the likelihood function, and Restricted Maximum Likelihood to avoid bias in the estimated covariance parameters. F-statistics were conducted to test for significant fixed-effects. The purpose of our LME models was to check whether there is an overall main effect of time (in the entire brain) but also to estimate the rate of progression in each brain region (as random-effects).

To reduce the dimensionality and avoid over-parameterisation (when not all the linear combinations of parameters are estimable), we regrouped and contracted the measures for broader brain areas: frontal, temporal, motor, parietal, occipital and subcortical areas (see Supplementary note 1: brain networks). The subgrouping was initially based on the five anatomical lobes: frontal, temporal, centro-parietal, occipital and subcortical. Since the motor cortex is a key area of atrophy in ALS, the centro-parietal lobe was subsequently separated into the parietal lobe and the motor network.

To assess where significant longitudinal changes occurred, a bootstrapping method was performed on ROI-specific LME models (1 model per ROI): Measure ~ Time + (Time|Participant). To evaluate the null-hypothesis of no time effect on the EEG measures, the (two to five) timepoints were randomly resampled in each participant before computing a new LME model (1000 repetitions). The results of this statistical method were then corrected to account for the number of ROIs using a 10% adaptive false discovery rate (FDR) (Benjamini et al., 2006; Nasseroleslami, 2018) and applied as a mask to visualise estimated sources of neural activity changes over time.

Longitudinal trajectories of the EEG spectral power were estimated using the following model described in Wilkinson-Rogers notation:

Power ~ Time + (Time|Participant) + (Time|ROI).

The fixed-effects coefficient corresponds to the time since the onset of the disease ('Time'). The random-effects include a participant-specific factor and an ROI-specific factor. Age and gender were considered for inclusion as random-effects but were not significantly improving the models (based on a likelihood ratio test); hence, were not included. The random-effect coefficients and the residuals, associated with the EEG score of a participant, within a brain region, were checked to confirm they follow normal distributions, were independent, and had constant variance (using the Kolmogorov–Smirnov test ($q<.05$); Ljung-Box Q-test ($q<.05$); Engle's ARCH test ($q<.05$) or diagnostic plots).

To estimate the connectivity progressions, we used a similar LME model, with the same fixed-effects. It was then possible to add an interaction term to investigate participant-specific effects

on the functional connectivity within or between brain regions of interest. In Wilkinson-Rogers notation, the model is described as:

Connectivity ~ Time + (Time|Participant) + (Time|ROI) + (-1+Time|ROI:Participant).

All connectivity values were transformed using a rank-based inverse normal transformation (Beasley et al., 2009) to reduce the deviation of residuals from normality. Age and gender were again considered for inclusion as random-effects but were not significantly improving the models; therefore were not included.

2.5.2. Clinical scores

After evaluating the progression of EEG measures, we analysed the evolution of motor and cognitive clinical scores. While also considering total scores, we prioritised ALSFRS fine motor subscore as a measure of motor function, ECAS fluency subscores as a measure of cognitive impairment(Abrahams et al., 2000, 2014) and BBI scores as a measure of behavioural change. A linear function was defined to represent each clinical score (ALSFRS-R fine motor subscore, total ECAS, ECAS fluency and BBI scores) progression over time. Each score was modelled as Score ~ Time + (Time|Participant). The fixed-effects coefficients can be described as the mean intercept and slope for all participants. Similarly, the random-effects coefficients respectively described the participant-specific deviation from intercept and slope. Age, gender and education were considered for inclusion but only education was deemed relevant for the ECAS models (based on a likelihood ratio test). For the cognitive progression models, an additional term, to account for the versions of the ECAS questionnaire (A, B and C) was also added. The three alternative versions were used to reduce practice effects but, in our case, some participants performed a sequence A-A-A, while others undertook sequence A-B-C, which needed to be addressed. The ECAS model can be described as: ECAS ~ Time + Version + (Time|Subj:Study) + (Time|Education). The assumptions of normality, independence, and constant variance of the residuals were checked (using the Kolmogorov–Smirnov test ($q<.05$); Ljung-Box Q-test ($q<.05$); Engle's ARCH test ($q<.05$) or diagnostic plots).

2.5.3. Correlations between EEG and clinical measures

Following the estimation of both the linear mixed regressions of EEG measures and clinical scores (ALSFRS-R, ECAS, BBI) over time, the rank correlations between them were calculated. For each participant, the EEG spectral measure changes over time, at frequency f (δ to γ_h-bands), were estimated by the time-related participant-specific random-effect of the linear mixed model. Similarly, participant/ROI interactions were used to localise participant-specific variations in brain regions. All random-effects slope signs were adjusted according to the fixed-effect slope (or according to the sum of the fixed-effect slope and ROI-specific slope in the case of a participant/ROI interactions) to represent faster or slower changes in regard to the average changes across participants. For each participant, the clinical changes (survival or ALSFRS-R bulbar, upper / lower limbs, respiratory or total ECAS) over time were also estimated by the time-related slope of the LME model.

Correlations between EEG and clinical measures regression coefficients were computed using the Spearman correlation coefficient. The statistical power of each correlation was estimated by bootstrapping (N=2000) using the EBI toolbox.(Nasseroleslami, 2018) A 5% FDR correction was implemented for the multiple comparisons of the participant/ROI interactions correlating with clinical scores, separately for each frequency and each score of motor or cognitive decline. Correlations between EEG values and survival were corrected similarly with a 1% FDR to facilitate visualisation.

3. Results

3.1. Changes in neural activity: decrease in slow oscillations, increase in faster oscillations

We observed distinct patterns of longitudinal changes in neurophysiological measures within the entire ALS group. As indicated above, the neurophysiological measures investigated encompassed: the spectral power, reflecting the intensity of oscillations in neuroelectric activity, as well as the AEC (co-modulation of signals) and the iCoh (synchrony between signals), respectively representing an amplitude and a phase-based measure of functional connectivity between brain regions.

Across all participants, spectral power significantly increases over time in the frontal and temporal lobes in γ-band and decreases in θ-band (**Figure 2**). A detailed description of the models examining these effects can be found in Supplementary Note 2. In the following sections, the longitudinal effects in the ALSci, ALSbi, and ALSncbi subgroups were investigated to assess whether the observed frontotemporal network changes could have been driven by ALSbi or ALSci participants. A detailed description of the longitudinal effects per subgroup can be found in the Appendix – Chapter V, Note 6.

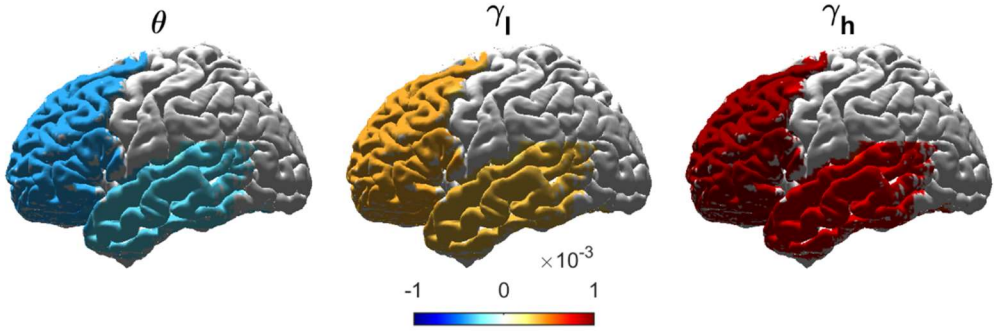

Figure 2: Changes in neural activity include a decrease in slow oscillations and increase in faster oscillations. *Longitudinal changes of EEG spectral power in ALS were measured in term of significant longitudinal spectral power variations, based on the time fixed-effect and the time ROI-specific random-effects (Bootstrapping, q<0.05). Longitudinal changes were mapped to get a spatial visualisation. The neural activity showed a significant decrease in θ-band and an increase in γ-band.*

3.2. Longitudinal changes in functional clinical measures

We observed significant changes in longitudinal functional clinical scores, including ALSFRS-R and neuropsychological scores, within the entire ALS group. These scores serve as valuable tools for assessing both the physical and cognitive progression of the disease, using established qualitative measures. Specifically, our models computed significant declines in ALSFRS-R scores ($p < 0.001$) and a slight increase in ECAS total scores ($p < 0.05$). When considering ECAS scores for the overall ALS group, a practice effect and potential non-random dropout lead to an average increase.(Costello et al., 2020) Although some participants may exhibit a decrease in ECAS scores, 80% of the individuals in our dataset did not show any cognitive impairment at any point in time. Furthermore, verbal fluency and BBI scores did not exhibit significant changes over time. For a more detailed examination of the fixed-effects coefficients and random-effects variances, please refer to Appendix – Chapter V – Supplementary note 3.

3.3. Widespread increased EEG co-modulation in cognitively impaired participants

We observed widespread significant increased (δ- and θ-band) co-modulation in ALSci (**Figure 3**). The intra-frontal (α-band) co-modulation also showed an increase for the ALSci subgroup. A detailed description of the fixed-effects can be found in the Supplementary material, Note 2.

In ALSci, we observed that changes in participants' region-specific connectivity were associated with corresponding neuropsychological changes, as assessed through three consecutive administrations of the ECAS (**Figure 3**) (details in Appendix – Chapter V, Note 3). To elaborate further, higher rates of β-band co-modulation changes in connectivity between the frontal and occipital lobes, between the frontal and temporal lobes, and between the subcortical and occipital lobes were found to be positively correlated with a more rapid decline in verbal fluency scores (correlation coefficients: $r_s > 0.5$, statistical powers: $1\text{-}\beta > 0.8$). By contrast, higher rates of changes either (i) within the motor and parietal region (β-band) or (ii) between the motor and temporal lobes (δ-band) were associated with a decreased rate of change in cognition, affecting both the ECAS total score and verbal fluency score (correlation coefficients: $r_s \leq -0.5$, statistical powers: $1\text{-}\beta \geq 0.8$).

No significant associations were found between the co-modulation in ALSci and other clinical measures (ALSFRS-R subscores or BBI scores).

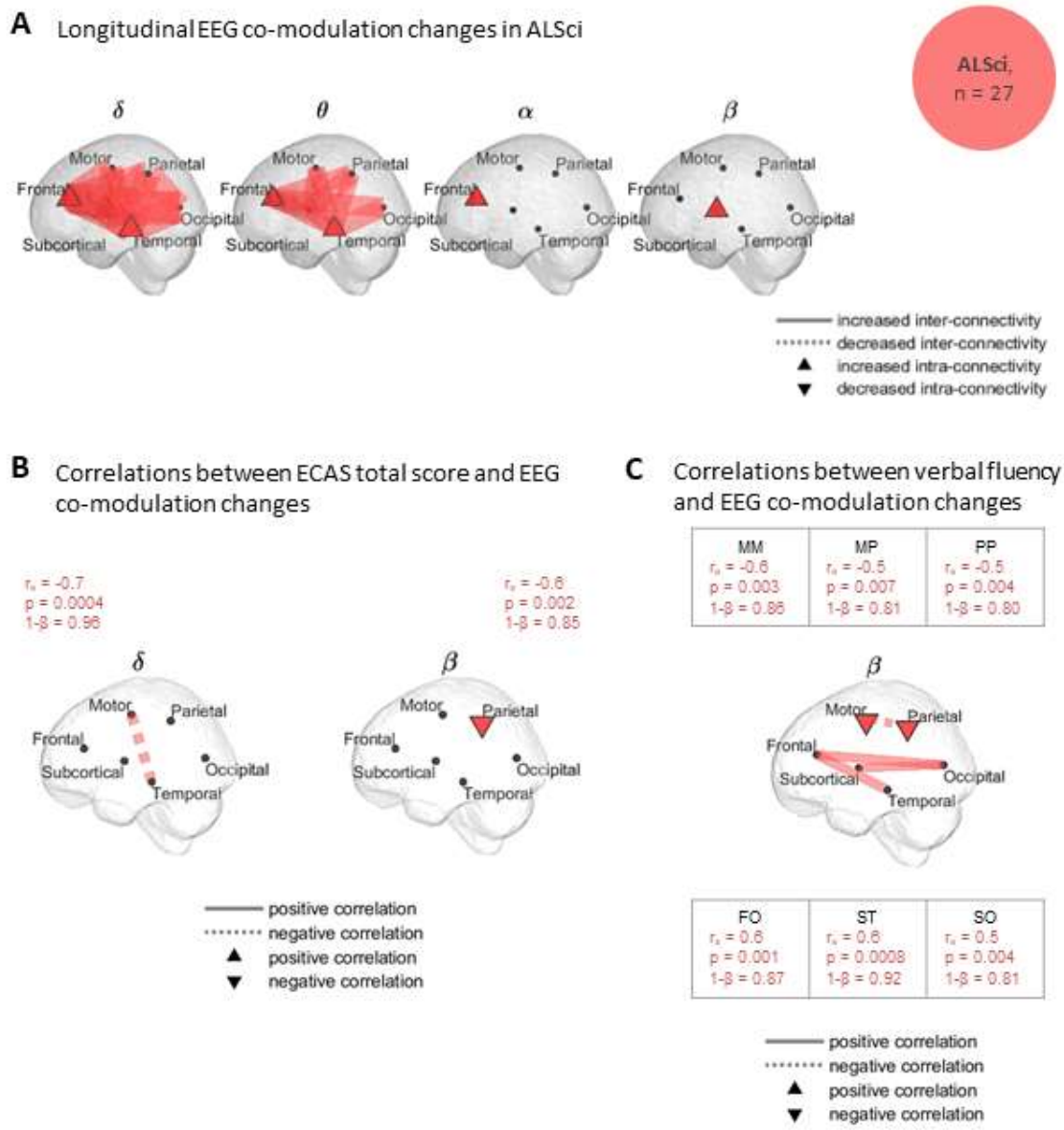

Figure 3: Widespread increased EEG co-modulation in ALSci, and associations with cognitive decline. *(A) Regions of longitudinal changes of EEG co-modulation and synchrony in ALSci group. The significant longitudinal connectivity changes were mapped to get a spatial visualisation of their magnitudes. The longitudinal variations represent the combined estimated slope (significance by bootstrapping, $q<0.1$). A widespread increase in δ- and θ-band co-modulation was observed in ALSci. The dashed lines represent a decrease while the solid lines represent an increase in connectivity. A filled node represents significant intra-region connectivity. (B-C) Regions with significant correlations between participant/ROI-specific co-modulation progressions and cognitive decline, in ALSci. For each significant correlation, the correlation coefficient, r_s, the p-value, p, and the statistical power,1-β are given. An adaptive FDR was applied to Spearman's correlation coefficients. (B) Correlations between EEG co-modulation and ECAS total score progressions. (C) Correlations between EEG co-modulation and ECAS verbal fluency changes. ALSci: individuals with ALS and impaired cognition; MM: intra-motor connectivity; MP: connectivity between motor and parietal regions; PP: intra-parietal connectivity; FO: connectivity between frontal and occipital regions; ST: connectivity between subcortical and temporal regions; SO: connectivity between subcortical and occipital regions.*

3.4. EEG spectral measures and behavioural impairment

The spectral power significantly increased in the temporal lobe (γ_l-band) in ALSbi (**Figure 4**). A detailed description of the fixed-effects can be found in the Appendix – Chapter V, Note 2. Additionally, a higher rate of change in α-band co-modulation between the frontal and parietal lobes was associated with an increased rate of changes in BBI scores (correlation coefficient: r_s = 0.4, statistical powers: 1-β = 0.9). No significant associations were found between the co-modulation and other clinical measures (ALSFRS-R subscores or ECAS scores) in ALSbi.

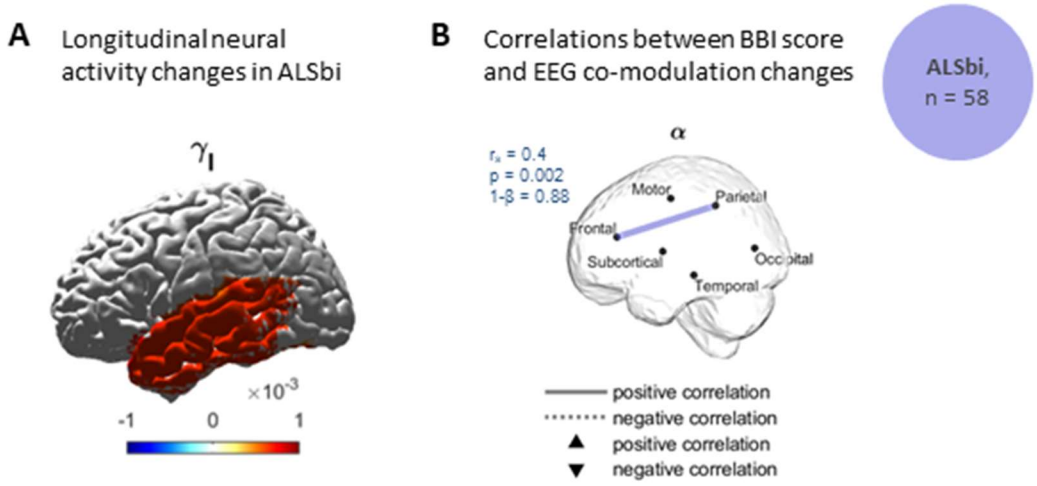

Figure 4: Increased EEG neural activity in the temporal lobe in ALSbi and associations with behavioural impairment. *(A) Longitudinal changes of EEG spectral power in ALSbi. The significant temporal spectral power variations, in terms of the time fixed-effect and the time ROI-specific random-effects (Bootstrapping, q<0.1), were mapped to get a spatial visualisation. An increase in γ_l-band co-modulation was observed in the temporal lobe for the ALSbi group. (B) Regions with significant correlations between participant/ROI-specific co-modulation progressions and cognitive decline, in the ALSbi group. A higher rate of change in co-modulation between the frontal and parietal lobes was correlated with an increased rate of change in BBI scores. For each significant correlation, the correlation coefficient, r_s, the p-value, p, and the statistical power, 1-β, are given. An adaptive FDR was applied to Spearman's correlations. ALSbi: individuals with ALS and impaired behaviour.*

3.5. Widespread decreased β-band EEG synchrony in participants with normal cognition and behaviour

In ALSncbi participants, we observed widespread significant changes in synchrony, with especially a significant decrease in β-band (q < 0.1, Figure 5). A detailed description of the fixed-effects, can be found in the appendix.

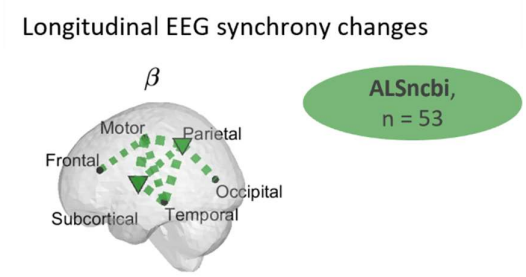

Figure 5: Widespread decreased β-band EEG synchrony in the ALSncbi group. *Regions of longitudinal changes of EEG synchrony in the ALSncbi group. The significant longitudinal connectivity changes were mapped to get a spatial visualisation of their magnitudes. A widespread decrease in β-band synchrony was observed in the ALSncbi group. The longitudinal variations represent the combined estimated slope (significance by bootstrapping, q<0.1). The dashed lines represent a decrease while the solid lines represent an increase in connectivity. A filled node represents significant intra-region connectivity. ALSncbi: individuals with ALS with normal cognition and behaviour.*

The slopes of the ALSFRS-R models (details in Appendix – Chapter V, Note 3) were used as an estimation of the speed of the disease progression per participant. We identified significant correlations of the changes in the clinical scores (progression rates) with the average brain-wide changes in neural activity (spectral power). In cognitively and behaviourally unaffected participants, the spectral power changes (θ-, γ_l-, $\gamma_h$bands) negatively correlate (q <.05) with fine motor changes over time (θ-band: r_s = -0.4, p = 0.003, 1-$\beta_{0.05}$ = 0.83; γ_l-band: r_s = -0.4, p = 0.003, 1-$\beta_{0.05}$ = 0.86; γ_h-band: r_s = -0.4, p = 0.002, 1-$\beta_{0.05}$ = 0.84). Higher rate of change in spectral power were associated with decreased rate of change in the fine motor score.

No significant associations were found between the spectral power and the other clinical measures (other ALSFRS-R subscores or neuropsychological scores) in the ALSncbi group.

3.6. Correlations between survival and changes in the EEG measures

The relationships between network changes and survival outcomes are depicted in **Figure 6**. In ALSci participants, higher rates of change in co-modulation, over the disease timecourse, between the frontal and temporal regions (β-band) or between the subcortical and parietal lobes (θ-band) were associated with poorer prognosis (p<.001, FDR at q=.01). On contrary, higher

rates of change between the motor and parietal regions or within the parietal lobe were associated with a better prognosis (p <.001, FDR at q=.01).

ALSbi participants showed a link between higher rates of change of γ_h-band co-modulation between frontal and parietal lobes and poorer prognosis (p <.001, FDR at q=.01).

In ALSncbi participants, significant negative correlations were localised between the parietal and subcortical lobes (co-modulation, δ-band). Positive correlations with survival were found between the subcortical lobe and the occipital area (β-iCoh).

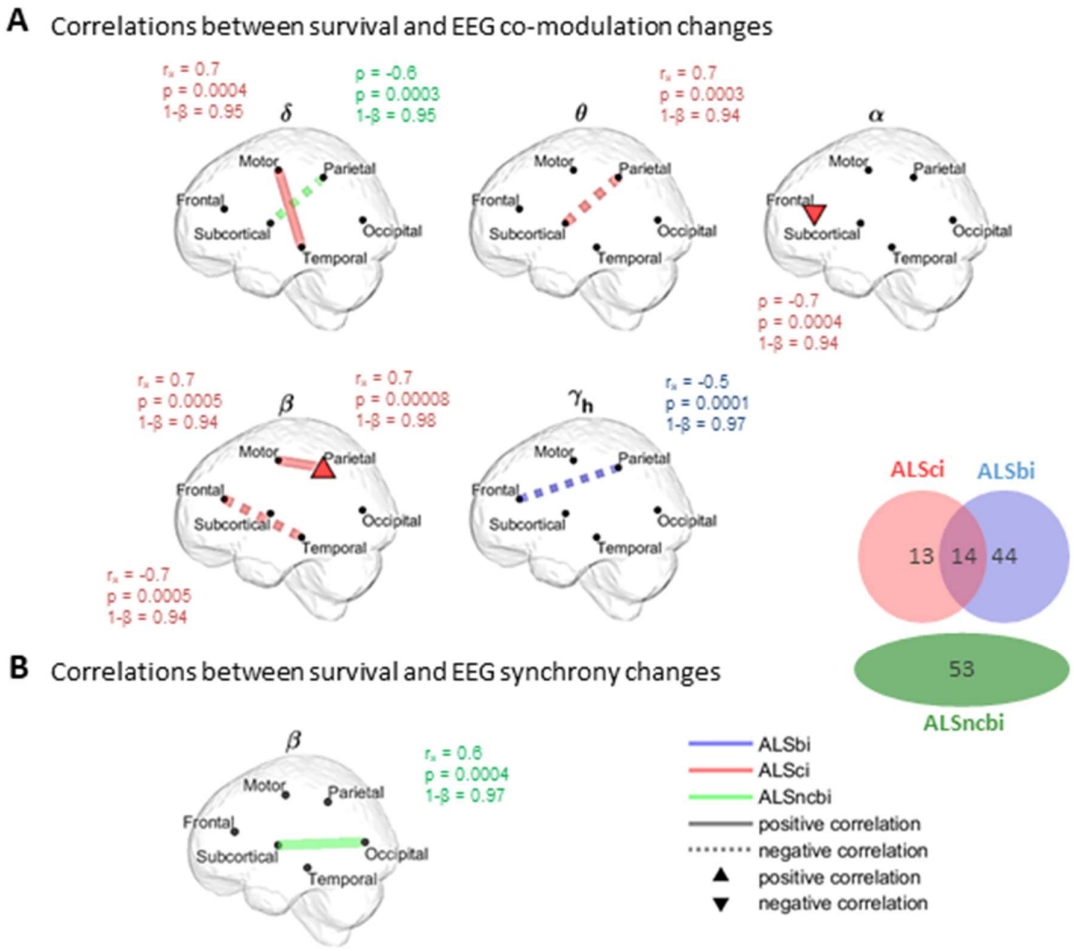

Figure 6: Survival and EEG functional connectivity in ALSci, ALSbi and ALSncbi subgroups. *Regions with significant correlations between survival and participant/ROI-specific connectivity (AEC and iCoh) progressions. Solid lines (or upper triangles) depict positive correlations, indicating that higher rates of functional connectivity change are associated with a better prognosis. In contrast, dashed lines (or lower triangles) represent negative correlations, signifying that higher rates of functional connectivity change are linked to a worse prognosis. In ALSci, ALSbi, and ALSncbi subgroups, the correlation coefficient, r_S, the p-value, p, and the statistical power,1-β, are given for each significant correlation. An adaptive FDR was applied to Spearman's correlations. ALSci: individuals with ALS and impaired cognition; ALSbi: individuals with ALS and impaired behaviour; ALSncbi: individuals with ALS with normal cognition and behaviour.*

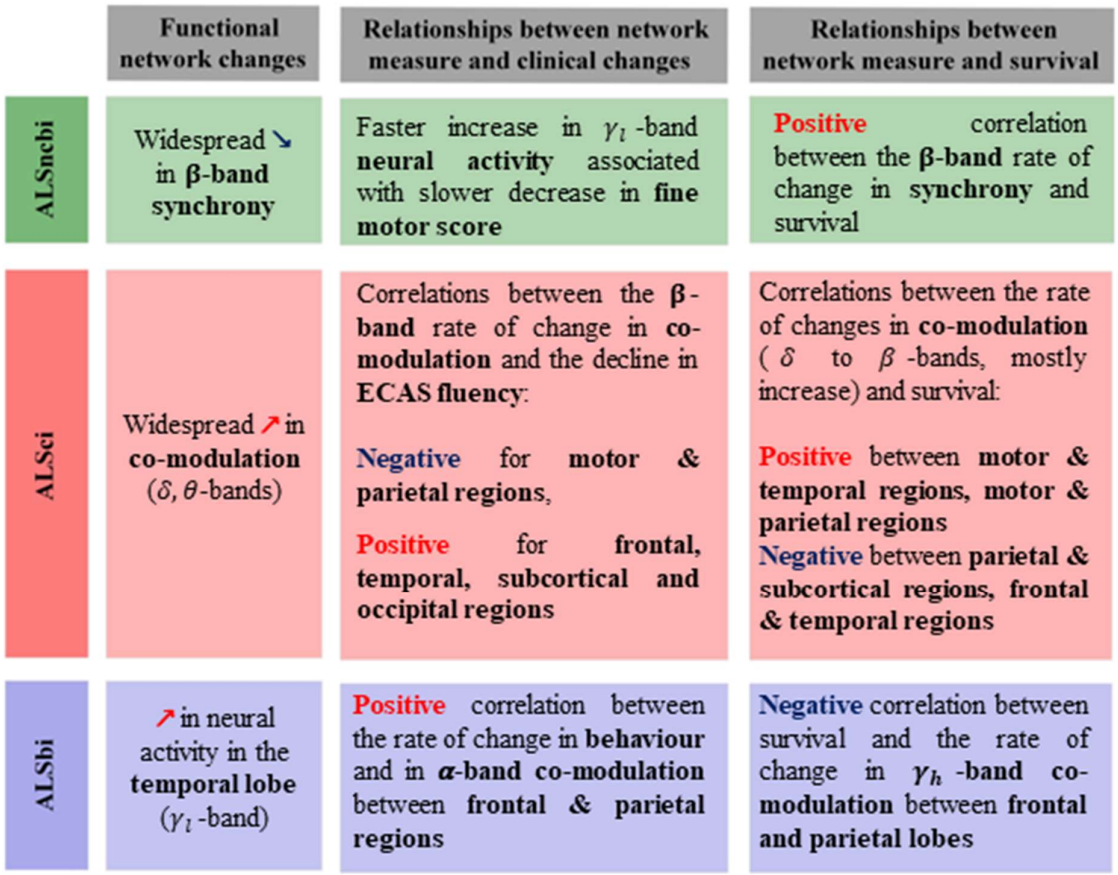

Figure 7: Summary of the main findings*. Distinct changes in functional networks characterise cognitive phenotypes in ALS and are clinically relevant. Positive correlations, indicates that higher rates of functional connectivity change are associated with a better prognosis/increased rate of change in cognition or behaviour. In contrast, negative correlations, signify that higher rates of functional connectivity change are linked to a worse prognosis/lower rate of change in cognition or behaviour.*

4. Discussion

This study identified significant longitudinal changes in neural activity within the fronto-temporal region in ALS regardless of their (cognitive) phenotype, which is characterized by a decrease in lower frequency bands and an increase in higher frequency bands. Further investigation of the potential link between the longitudinal frontotemporal changes and cognitive or behavioural impairments, showed that the ALS subgroups defined based on their cognitive and behavioural profiles present with very distinct longitudinal effects. In the ALSci subgroup, we observed a widespread increase in co-modulation, which strongly correlated with cognitive decline ($|r_s| > 0.5$, $1\text{-}\beta > 0.8$). Meanwhile, in the ALSbi subgroup, we found that higher rates of change in co-modulation between the frontal and parietal lobes were associated with increased rates of change in BBI impairment ($|r_s| = 0.4$, $1\text{-}\beta = 0.9$). Notably, ALSncbi displayed a widespread decrease in β-band synchrony over time. Furthermore, within the ALSncbi subgroup, motor decline was linked to neural activity changes ($|r_s| = 0.4$, $1\text{-}\beta > 0.8$).

In all subgroups, survival was strongly associated with the rates of change in functional connectivity between specific brain regions (correlation coefficients $|r_s| > 0.5$, statistical powers $1\text{-}\beta > 0.9$). The distinct neurophysiological (EEG) profiles in the three subgroups and the association of the EEG measures with the relevant clinical measures of progression, shows that the identified EEG measures do reflect the underlying network-level impairment in the cognitive, behavioural and non-cognitive-behavioural domains (**Figure 7**).

4.1. Frontotemporal longitudinal changes in neural activity

Functional networks in the frontotemporal lobe, a key region of atrophy in ALS, displayed significant changes over time. Decreased θ-band and increased γ-band spectral power was observed over time in the frontotemporal lobe. Lower θ-band spectral power has been previously observed, in the temporal area, in PwALS compared to controls(Dukic et al., 2019; Nasseroleslami et al., 2019) (see Table 2). Frontotemporal and frontal-subcortical circuitry are frequently highly impacted in dementias and neuropsychological diseases.(Bonelli & Cummings, 2007; Neary et al., 1998; Tekin & Cummings, 2002) Notably, post-mortem examinations have revealed synapse loss in the prefrontal cortex of PwALS, which correlated with cognitive decline.(Henstridge et al., 2018) As our observed frontotemporal network changes may have been driven by ALSbi or ALSci participants, we investigated longitudinal effects in ALSci, ALSbi and ALSncbi subgroups.

Table 2: Comparative table between the main cross-sectional and longitudinal results.

Spectral power – neural activity						
	δ	θ	α	β	γ_l	γ_h
Cross-sectional (ALS vs HC) (Dukic et al., 2019)	**↘ temporal and posterior regions**					
Longitudinal (all ALS)		**↘ frontal, temporal regions**			**↗ frontal and temporal regions**	
Co-modulation						
	δ	θ	α	β	γ_l	γ_h

Cross-sectional (ALS vs HC) (Dukic et al., 2019)	**↗ frontal, central, posterior regions**	**↗ central, posterior regions**			**↗ frontal, central, posterior regions**	
Longitudinal (all ALS)		**Widespread ↗**				
Longitudinal ALSci	**Widespread ↗**		**↗ frontal region**			
Longitudinal ALSncbi	**↗ posterior region**					

Synchrony						
	δ	θ	α	β	γ_l	γ_h
Cross-sectional results (ALS vs HC) (Dukic et al., 2019)	**↘ frontal, temporal regions**			**↘ sensorimotor network: central, temporal regions**		
Longitudinal ALSncbi				**Widespread ↘**		

4.2. Cognitive impairment and longitudinal increase in EEG co-modulation

We observed no significant longitudinal changes in neural activity (spectral power) in ALSci subgroup, despite previous cross-sectional studies reporting decreased spectral power in temporo-posterior region (all ALS group versus HC).

However, ALSci participants demonstrated widespread increases in δ-, θ- and β-bands co-modulation over time, which is consistent with previous cross-sectional findings of higher co-modulation in ALS group compared to controls in δ, θ and γ_l frequency bands (Dukic et al., 2019) (Table 2). Burgh et al. similarly observed longitudinal structural connectivity changes in participants with impaired cognition.(Burgh et al., 2020) This observed significant widespread increase in functional connectivity could appear antithetical to the findings of structural atrophy and metabolic reduction at rest in ALS.(Kew et al., 1993; Verstraete et al., 2010, 2014) However, approaches integrating structural and functional imaging showed increased functional connectivity within atrophied regions.(Douaud et al., 2011; Nasseroleslami et al., 2019; Proudfoot et al., 2018) This increasing connectivity could be explained by an increase in compensation to decreasing structural connectivity tracts along with a progressive loss of GABA-ergic inhibitory interneurons and disinhibition of remaining glutamatergic tracts.(Douaud et al., 2011; Lloyd et al., 2000) Such disinhibition and hyperexcitability is

evidenced by numerous histopathological, neurophysiological, neuroimaging and clinical studies.(Turner & Kiernan, 2012)

In ALSci, higher rate of connectivity changes in the frontotemporal, fronto-occipital, and subcortico-occipital areas (in the β-band) were associated with a more rapid decline in verbal fluency. Verbal fluency deficits are a well-documented cognitive impairment in ALS, frequently reported in previous studies.(Abrahams et al., 2000, 2014; Beeldman et al., 2016) These deficits are thought to be mediated by the frontotemporal areas.(Baldo et al., 2006) Furthermore, we found that higher rates of functional connectivity changes between most brain regions correlated with a more rapid decline in cognitive scores, both in terms of total scores and fluency scores on the ECAS. On the opposite, higher rates of connectivity changes involving motor or parietal regions (part of the sensorimotor network) were linked to a decreased rate of cognitive decline. This inverse relationship suggests a dissociation between connectivity changes involving sensorimotor regions and those involving other brain regions in individuals with ALS who experience cognitive impairment.

4.3. Temporal longitudinal changes in behaviourally impaired individuals with ALS

In ALSbi, an increase in γ-band power was observed in the temporal lobe. These findings are supported by structural observations of frontotemporal cerebral changes in behaviourally impaired PwALS,(Burgh et al., 2020; Lulé et al., 2018) but have not been reported before in RS-EEG. Furthermore, higher rate of change in co-modulation between the frontal and the parietal lobes were associated with increased rate of changes in BBI scores.

Furthermore, a higher rate of change in co-modulation between the frontal and parietal lobes was linked to an accelerated rate of changes in BBI scores. This suggests a meaningful connection between alterations in brain connectivity patterns and the progression of behavioral changes in ALS. In the combined ALSci/ASLbi group, the relationships observed between EEG functional connectivity and functional scores related to cognitive decline highlight the potential of EEG measures as a quantitative marker for disruptions in cognitive networks in ALS.

4.4. Motor and extra-motor functional changes in cognitively and behaviourally unaffected participants

In ALSncbi, we observed significant longitudinal changes in spectral power, specifically in the γ_l-band, localized to the frontal lobe. This suggests that cerebral changes extend beyond the primary motor cortex, a phenomenon previously linked to disease progression in the broader ALS population.(McMackin, Dukic, Costello, Pinto-Grau, McManus, et al., 2021; Menke et al., 2018) Evidence from diffusion tensor imaging has indicated a loss of structural connectivity spreading from motor regions to frontoparietal lobes(Verstraete et al., 2014), reinforcing the idea that ALS-related changes propagate from the primary motor cortex to other brain regions. In ALSncbi, we also noted an increase in connectivity (co-modulation) between the fronto-sensorimotor regions and other regions, particularly in the δ and θ frequency bands, aligning with the hypothesis of a progressive spread of ALS-related changes beyond the primary motor cortex.

Additionally, we observed a widespread decrease in β-band synchrony over time in ALSncbi, consistent with previous cross-sectional findings of reduced β-band synchrony in people with ALS (PwALS) (Table 2). This cross-sectional decrease in synchrony correlated with motor impairment and cortical atrophy, further highlighting its clinical relevance.

To confirm the clinical significance of our observations regarding fronto-temporo-parietal changes over time, we correlated them with changes in clinical scores. Associations between EEG data and clinical measures were detected at the whole-brain level, not limited to specific brain regions. The correlations between spectral power and fine motor scores suggest the potential development of a prognostic biomarker for motor decline in the ALSncbi group. Co-modulation between or within regions demonstrated links with neuropsychology, while synchrony showed association with motor function, as it was observed cross-sectionally.(Dukic et al., 2019)

4.5. Associations between functional connectivity and survival in ALS subgroups

In all ALS subgroups with distinct neuropsychological profiles (ALSci, ALSbi, ALSncbi), the rates of change in functional connectivity within specific brain regions showed robust associations with survival, as indicated by high correlation coefficients (r_s > 0.5) and strong statistical power (1-$\beta_{0.01}$ > 0.9).

Within the ALSncbi group, we observed that an increased rate of change in α-band synchrony between the subcortical and occipital areas was linked to extended survival. On the opposite, an increased rate of change in δ-band co-modulation between the subcortical and sensorimotor network was associated with shorter survival. This suggests that alterations in connectivity within non-motor regions (other than central and parietal regions), may reflect the role of cerebral compensation in slowing down the disease progression, highlighting enhanced plasticity as a potential target for future treatment research.

However, we also noted that increased rates of changes in frontotemporal and frontoparietal connectivity were associated with a less favorable prognosis, in participants with cognitive or behavioral impairments. In contrast, increased rate changes in connectivity within the sensorimotor network in ALSci were linked to longer survival.

These findings imply the coexistence of distinct mechanisms contributing to either a faster or slower progression of the disease. Moreover, these mechanisms appear to vary among ALS subgroups characterised by different neuropsychological profiles.

4.6. Limitations and considerations in longitudinal EEG studies for ALS

A limitation of this study is the attrition in repeated longitudinal recordings, with only 7 out of 124 participants attending the 5th session. Longitudinal changes can be more challenging to detect than cross-sectional differences due to the subtlety of measurements over time compared to the pronounced differences between the ALS and HC groups. While linear mixed-effects models can help account for missing data points, they do not eliminate potential bias. In this study, we assumed that missing recordings were missing at random, although they could be dependent on disease progression and therefore associated with EEG measures. In future research, obtaining longitudinal recordings from both PwALS and controls would allow for distinguishing between changes resulting from the disease and those associated with normal aging.

Additionally, the categorisation into ALSci, ALSbi, and ALSncbi is ideally based on a full neuropsychological assessment rather than just relying on ECAS and BBI scores. Furthermore, while ECAS fluency scores serve as a valid measure of verbal fluency, it is a screening task with reduced sensitivity and specificity compared to full-battery tasks when assessing cognitive impairment.(Pinto-Grau et al., 2017)

5. Conclusion

In conclusion, this study demonstrated significant longitudinal changes in neural activity within the fronto-temporal region in individuals with ALS. The investigation into distinct ALS subgroups, including ALSci, ALSbi, and ALSncbi, has provided valuable insights into the relationship between neural activity changes and cognitive or behavioral impairments. In the ALSci subgroup, a widespread increase in co-modulation was observed, strongly correlating with cognitive decline. Meanwhile, in the ALSbi subgroup, higher rates of change in co-modulation between frontal and parietal lobes were associated with increased rates of change in BBI impairment. ALSncbi displayed a widespread decrease in β-band synchrony over time, with motor decline linked to neural activity changes in this subgroup. Importantly, survival in all subgroups was strongly associated with the rates of change in functional connectivity between specific brain regions, highlighting the potential clinical relevance of these findings.

The study has provided evidence of the complex interplay between neural activity changes, cognitive and behavioral profiles, and disease progression in ALS. It suggests that different mechanisms may contribute to either a faster or slower progression of the disease, and these mechanisms vary among ALS subgroups characterised by different neuropsychological profiles.

Future research should continue exploring the intricate dynamics of neural activity changes in ALS, which may hold the key to more personalised approaches in clinical trials and treatments.

VI. Results: Data-driven classification of ALS patients based on resting-state EEG trajectories

The work described in this chapter is based on the previous chapter as well as on work from Mr Vlad Sirenko. Matlab code, that he developed for a parallel project, was adapted to the current analyses and further developed.

1. Introduction

The progression of ALS varies among individuals, resulting in differences in the rate of decline and the patterns of symptoms. This variability is evident not only in the rate of progression but also in the order in which symptoms appear, and the areas of the body affected. Such heterogeneity makes it challenging to predict the course of the disease (Bendotti et al., 2020).

In a previous study conducted by our team, we discovered stable network-based subphenotypes of ALS by clustering RS-EEG measures (Dukic et al., 2022). This finding provided valuable

insights into the nature of the disease. Building on this foundation, our current study focuses on data-driven analysis of the longitudinal trajectories of spectral EEG measures.

We applied clustering techniques on neural activity trajectories to identify significant and stable subgroups within the ALS population. By categorising the trajectories of resting-state spectral EEG measures over time, we aimed to uncover longitudinal patterns of network disruption that might remain hidden when analysing the entire ALS cohort as a whole. Furthermore, we sought to establish whether these identified subgroups align with specific clinical presentations, thereby enhancing our understanding of the clinical heterogeneity observed in individuals with ALS. The clinical profiles encompassed a range of factors, including motor function, respiratory health, cognitive decline, site of disease onset, and overall survival.

In the course of a precedent study (chapter V), we identified distinct changes in neural activity and functional connectivity (represented by the co-modulation and synchrony of EEG signals) over time among different ALS subgroups with different neuropsychological profiles. Additionally, distinct longitudinal progressions in white and grey matter changes were observed based on factors such as the site of disease onset, cognitive profile, or C9orf72 status (Burgh et al., 2020). It is worth exploring whether a data-driven classification of longitudinal trajectories of neural activity aligns with clinical profiles.

Our findings revealed distinct and statistically significant trajectories of neural activity progression in ALS subgroups. Moreover, the subgroups we identified exhibited significant differences in key clinical parameters, such as survival and decline in functional abilities (as indicated by longitudinal ALSFRS-R subscores).

2. Methods

2.1. Ethical approval

Ethical approval was obtained from the Tallaght University Hospital/St. James's Hospital Joint Research Ethics Committee in Dublin [reference: 2014 Chairman's Action 7 and 2019-05 List 17 (01)], as described in General material and methods (Chapter IV)

2.2. Participants

2.2.1. Recruitment – inclusion and exclusion criteria

Exclusion and inclusion criteria are described in Chapter IV, section 1.

2.2.2. Demographic profiles

An ALS cohort of 124 individuals (male: 69.3%; age [mean ± standard deviation]: 63.13 ± 15) was part of this study. Individuals participated in as many as four follow-up recording sessions. The time intervals between each session were approximately 5.4 ± 2.1 months. The total number of recordings conducted throughout the study amounted to 249, with 116 of them being baseline recordings and 60, 44, 22, and 7 being follow-up recordings for sessions 1-4 respectively. On average, patients attended two recording sessions, with a standard deviation of 1.2. *Table 3* provides a breakdown of the demographic information for each follow-up session.

Table 3: Demographic profiles. Numbers show mean ± standard deviation. The table details the gender proportions, the average ages at the time of recording and, when applicable, disease durations, delays between sessions, site of onset and the number of patients with FTD comorbidity.

Groups	N	Male (%)	Age (years)	Disease duration (months)	Follow-up intervals (months)	ALSFRS-R scores	Site of onset (N)			ALS-FTD diagnosis (N)
							Bulbar	*Spinal*	*Thoracic*	
Patients T1	116	74	62 ± 11	25 ± 18	/	36 ± 7	22	86	5	5
Patients T2	60	77	60 ± 11	32 ± 19	4.9 ± 1.2	35 ± 8	14	43	2	2
Patients T3	44	80	60 ± 12	37 ± 19	4.9 ± 1.3	33 ± 9	8	34	1	2
Patients T4	22	86	61 ± 11	42 ± 24	4.9 ± 1.1	33 ± 7	2	19	1	1
Patients T5	7	57	57 ± 13	52 ± 31	6.5 ± 2.4	33 ± 6	0	6	1	0

2.3. Experiment – EEG acquisition and Experimental paradigm

EEG data were collected at rest as described in Chapter IV, section 2.

2.4. Data analysis

2.4.1. Processing of EEG data

The EEG signals were preprocessed as described in Chapter IV, section 2.4.

2.4.2. Longitudinal models

Linear mixed-effects models were built to estimate the progressions of the EEG normalised spectral power. A detailed description of the models can be found in Chapter V. Subject-specific slopes were extracted from the 90 longitudinal models (one per brain region) to become the features of the unsupervised model.

2.4.3. Clustering of longitudinal trajectories

To follow up with our previous results (Chapter V) and cross-sectional observation of decreasing spectral power in lower frequency bands (θ to β-bands) (Dukic et al., 2019), we applied a clustering pipeline on each frequency band independently.

2.4.3.1. Feature selection

Feature selection was applied to identify the most relevant features when grouping participants into meaningful clusters. The inclusion of irrelevant measures that do not differentiate between clusters may lead to cluster structure being masked by noise. By selecting appropriate features, we can improve the quality and efficiency of the clustering process and potentially gain better insights from the data (Dy & Brodley, 2004). The features were normalised to ensure that they would all contribute equally to the clustering results. The Sparse Hierarchical Clustering (SPARCL) algorithm was applied to the normalised features (Witten & Tibshirani, 2010). Traditional data dimensionality reduction methods, such as principal component analysis and non-negativity matrix factorization, may not always yield optimal separability for clustering. This algorithm overcomes this limitation by incorporating weighted feature selection using L1 (lasso) and L2 penalties, guided by the gap statistic. By assigning weights to each feature (small gaps result in zero weights), the algorithm identifies and retains only the most relevant ones for clustering. Features with positive weights are considered meaningful and included in the subsequent clustering process. The possibility that all features were relevant was also considered.

2.4.3.2. Clustering computation

Participants' EEG longitudinal trajectories were analysed using a soft Gaussian mixture model, dividing them into two to seven subgroups. The trajectories are assumed to originate from a mixture of several Gaussian distributions, each having its set of unknown parameters. To define the parameters, a diagonal covariance matrix (shared between clusters) was fitted using the Expectation-Maximization algorithm, repeated five times. We chose a soft classification approach as it assigns probabilities of belonging to different classes, rather than a single definitive choice. This enables participants to potentially belong to multiple clusters simultaneously, which aligns well with the nature of the disease lying on a clinical spectrum that spans from ALS to frontotemporal dementia (FTD). This more nuanced approach has the potential to better capture the clinical manifestations along the spectrum.

2.4.3.3. Validation of the clustering results

Identifying clusters represents merely the visible part of the iceberg, validation steps play a key role in ensuring the accuracy, reliability, and interpretability of the clustering results.

Significance of the clusters – statistical analyses

The optimal number of clusters (or participants subgroups) was determined using the silhouette criterion, which estimates the similarity within versus between clusters. The statistical significance of the clusters was assessed through permutation-based significance testing. This involved generating an empirical null distribution, with the null hypothesis that the dataset contained only random cluster structures. To build the null distribution, we adopted a sampling approach based on a uniform distribution with bounds aligned to the principal components of the data, following a computational method similar to that employed by Tibshirani et al. for the gap statistic (Tibshirani et al., 2001). This sampling method is more likely to produce artificial clusters, resulting in a more conservative test. We calculated the silhouette criterion for each dataset generated from random sampling (a total of 1000 generated datasets). Subsequently, we determined the p-values by calculating the proportion of times the silhouette criterion from the null sampled datasets exceeded the criterion obtained from the original dataset. In brief, this methodology allowed us to obtain an optimal number of subgroups, while also statistically validating the significance of the identified clusters. We checked that the separation between clusters was not the result of chance or white noise. An adaptive FDR (Benjamini et al., 2006) ($q<.05$) was applied to account for the multiple feature selection methods (no selection versus SPARCL) and clustering algorithms (Soft GMM, hierarchical and spectral clustering).

Robustness of the clusters

To establish the robustness of the clusters, we iteratively left out 10% of the participants from the dataset. Subsequently, we performed feature selection and clustering again and checked whether the newly formed clusters were similar to the ones initially identified. The Adjusted Rand Index (ARI) was used to quantitatively measure the agreement between the original and perturbed clusters. The ARI had to be higher than 70% to deem the clusters as robust.

Consistency of the clusters

After defining the model based on 90% of the participants, we assessed its generalisability to the remaining 10% by employing a label propagation algorithm (Dukic et al., 2022). This additional step aimed to evaluate how well we could accurately classify the remaining participants. We again used the ARI to estimate the similarity with the results of the original

model, which ran on 100% of the participants. This validation step allowed us to validate the consistency of the identified clusters, ensuring that the results were not driven by specific subsets or biased towards particular participants.

Comparison with the results of other clustering algorithms

As a last validation step, we analysed the similarity with the results of other clustering algorithms: hierarchical and spectral clustering. The hierarchical clustering grouped data points sequentially based on their Euclidian distances. The data was organised in a tree-like structure by Ward's linkage, which minimises the within-cluster variance (Ward, 1963). This method is advantageous for exploratory purposes and relatively small datasets and was selected for its robustness to outliers (likely to form their own cluster). We additionally applied spectral clustering [Ng]. The Gaussian Similarity Kernel (GSK) was formed based on the Euclidian distance for all combinations of the number of 'nearest-neighbours' (2 to 7) and a scaling parameter σ among: {1.0, 1.25, 1.5, 1.75, 2.0}. An affinity matrix was obtained by averaging over all combinations, following the method described by Dukic et al. (Dukic et al., 2022). The eigenvectors of the normalised Laplacian of the affinity matrix were subsequently used to partition the data into clusters.

The Chi-square statistic (or the Fisher test in the case of 2 clusters) was applied to test the null hypothesis of independence of the proportions in each cluster between the clustering algorithms.

2.4.4. Longitudinal progression by cluster

After categorising participants based on the longitudinal progression of their EEG spectral power, we re-evaluated the progression and its significance within each subgroup, following the same methodology described in Chapter V but tailored to the characteristics of each subgroup instead of the overall ALS group. To simplify and prevent the problem of having too many parameters to estimate, we combined the measurements of 90 brain regions into broader groups such as frontal, temporal, motor, parietal, occipital, and subcortical areas. This grouping was initially based on the five lobes of the brain: frontal, temporal, centro-parietal, occipital, and subcortical. However, due to the significance of the motor cortex in ALS, we further divided the centro-parietal lobe into the parietal lobe and the motor network. Additional details can be found in Appendix – Chapter IV, Supplementary note 1: Brain Networks. To account for multiple comparisons, we applied an adaptive FDR correction (Benjamini et al., 2006).

2.4.5. Clinical profiles by cluster

Clinical profiles of the identified subgroups of participants were determined using the subscores of motor/respiratory (ALSFRS-R), cognitive (ECAS) and behavioural (BBI) decline (cross-sectional scores and longitudinal progressions) as well as the age, gender, medication (Riluzole), C9orf72 mutation, site of onset and survival. Significant clinical differences across the clusters were tested (for survival and for the ALSFRS-R, ECAS, BBI scores) using Kruskal–Wallis one-way ANOVA, or the Mann-Whitney U-test in the case of comparisons between only two clusters. The Chi-Square test of Independence was used to check for an association between the subgroups and categorical variables like the sites of onset. An adaptive FDR correction was applied ($q<.05$) to account for the multiple clinical measures.

3. Results

3.1. Stable clusters of longitudinal neural activity trajectories

Through an analysis of longitudinal neural activity trajectories, distinct clusters were identified, demonstrating the presence of stable trajectory patterns across different ALS subgroups (Figure 8). Notably, in the δ-band, we observed three stable clusters, while in the α-band, two clusters were identified. The β-band demonstrated five clusters and the γ_h-band exhibited three clusters. A 3D visualisation in principal components space of these clusters is presented in Figure 8. Frequency bands θ and γ_l did not show any significant stable clusters. However, the overall ALS group displayed significant longitudinal progressions in these two frequency bands (FDR, $q<.05$) (Figure 8).

Our clustering solutions achieved statistical significance, as well as high levels of robustness and consistency, suggesting reproducibility of our findings. Additionally, the results aligned significantly with those of other clustering algorithms, further validating the credibility of our analysis. Table 4 provides details on the performed validation results (corresponding methodology can be found in section 2.4.3.3).

δ	θ	α	β	γ_l	γ_h
2-4 Hz	4-7 Hz	7-13 Hz	13-30 Hz	30-47 Hz	53-97 Hz
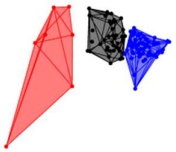	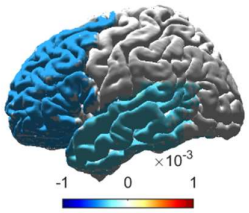	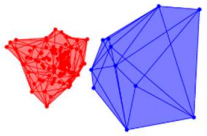	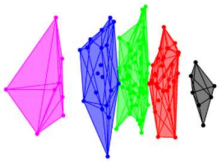	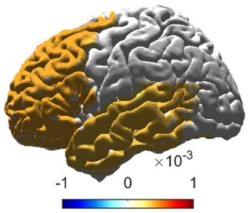	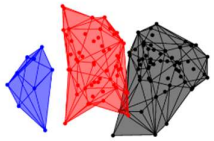

Figure 8: Summary of the clusters of longitudinal neural activity trajectories per frequency bands.Upper part of the table: Brainmaps are represented as a reminder of significant changes over time observed at group level. In θ- and γ_l-band, the overall ALS group displayed significant longitudinal progressions of neural activity in the frontotemporal area (FDR, q<.05). Lower part of the table: Schematic representations of the identified clusters per frequency band (if any) can be observed. In δ-, α-, β- and γ_h, no significant progression over time was found but stable clusters were identified. For each frequency band, the clusters are visualised in principal components space (3 dimensions). An adaptive FDR (q<.05) was applied to account for the multiple feature selection methods (no selection versus SPARCL) and clustering algorithms (Soft GMM, hierarchical and spectral clustering).

Table 4: Details of the validation analyses for the significant and stable clusters of longitudinal neural activity trajectories. For each frequency band in which stable clusters were observed, the feature selection method and clustering algorithm are indicated, as well as the results of statistical evaluations including: significance, robustness, consistency and comparison with other clustering algortihms. The feature selection methods included the Sparse Hierarchical Clustering (SPARCL) algorithm or the inclusion of all features. The significance of the clustering models was estimated using permutation-based testing. Significance was reached for clusters obtained using Soft Gaussian mixture modelling (GMM) (for δ, α, β-band) and using the hierarchical algorithm (γ_h-band). An adaptive FDR method (Benjamini et al., 2006) ($q<.05$) was applied to address the multiplicity arising from the various feature selection methods (no selection versus SPARCL) and clustering algorithms (Soft GMM, hierarchical, and spectral clustering). To ensure cluster robustness, 10% of participants were excluded, then feature selection and clustering were conducted again on the remaining participants to assess similarity with the initial clusters, measured using the adjusted rand index (ARI). Additionally, a label propagation algorithm was applied on the excluded 10% of participants and results were compared using ARI to validate cluster consistency. Comparison with another clustering algorithm (hierarchical or soft GMM, depending on the original algorithm, and spectral clustering) was evaluated using Chi-square statistic (or the Fisher test in the case of 2 clusters); the resulting p-values are shown in the last two columns of the table.

Freq	Feature selection method	Clustering algorithm	p-value	Robustness (ARI, %)	Consistency (ARI, %)	Comparison with hierarchical/GMM clustering	Comparison with spectral clustering
δ	-	Soft GMM	.001	91	86	$2 \cdot 10^{-4}$ (Chi^2 test)	0.01 (Chi^2 test)
α	SPARCL	Soft GMM	.001	94	84	$6 \cdot 10^{-16}$ (Fisher test)	$2 \cdot 10^{-24}$ (Chi^2 test)
β	SPARCL	Soft GMM	.002	82	70	$2 \cdot 10^{-71}$ (Chi^2 test)	$9 \cdot 10^{-60}$ (Chi^2 test)
γ_h	-	Hierarchical	.002	80	65	$4 \cdot 10^{-27}$ (Chi^2 test)	$2 \cdot 10^{-17}$ (Chi^2 test)

3.2. Distinct longitudinal progression of neural activity in ALS subgroups

The analysis of longitudinal trajectories of neural activity in the identified subgroups (or clusters) revealed evidence of distinct and statistically significant progression over time (q<.05). Significant progressions were observed within specific frequency bands, where no such progression was observed in the overall ALS group (Figure 9). In α-band, cluster 1 (depicted in red) exhibited a noticeable decrease in activity within the temporal region, while cluster 2 (shown in blue) demonstrated an increase in activity within the central/parietal regions. In β-band, one cluster (in blue) displayed a significant decrease over time in the temporal area. No significant progression over time was observed for the clusters identified in the δ- and γ_l-bands.

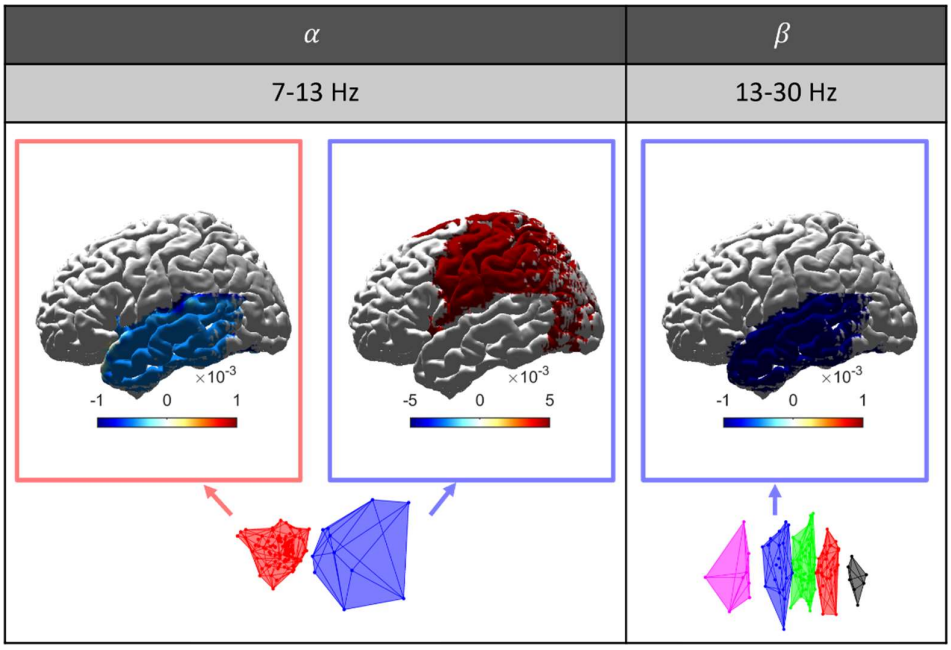

Figure 9: Significant longitudinal progression of neural activity in specific clusters. An adaptive FDR correction was applied to account for the multiple brain regions (q<.05).

3.3. Distinct prognostic and functional decline in ALS subgroups

The analysis of clinical profiles using clinical functional scores revealed distinct characteristics of specific ALS subgroups or clusters (Figure 10). In the clusters identified from the α-band neural activity trajectories, we observed significant differences in survival (Mann-Whitney U-test, p = 0.0002, r = -0.2, AUC = 0.6). Notably, Cluster 1 (n= 11, depicted in blue) exhibited the longest survival, with an average of 9.4 years, while Cluster 2 (n =113, represented in red) had the shortest survival, with an average of 3.4 years. Additionally, the two α-band clusters were associated with significant differences in the longitudinal decrease in ALSFRS-R

subscores, encompassing upper limbs, lower limbs, bulbar, and respiratory symptoms. Cluster 2 demonstrated a faster decline compared to Cluster 1 in all four functional subscores. The results for each subscore were as follows: upper limbs ($p = 0.0003$, $r = 0.6$, AUC = 0.8), lower limbs ($p = 0.0003$, $r = 0.5$, AUC = 0.8), bulbar ($p = 0.002$, $r = 0.5$, AUC = 0.7), and respiratory ($p = 0.0001$, $r = 0.6$, AUC = 0.8).

There were no significant differences between the clusters in terms of age, gender, medication, C9orf72 repeat expansion status, site of onset or cognitive scores ($q > .05$).

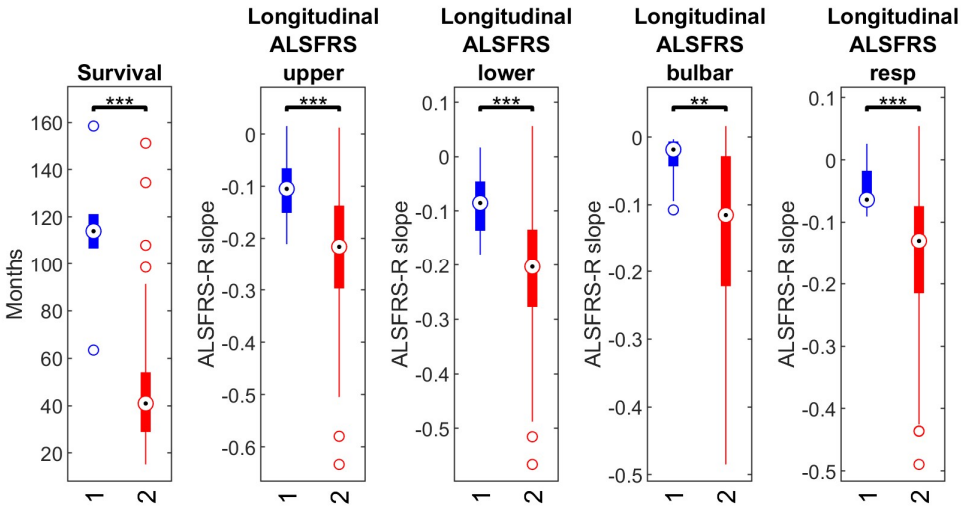

*Figure 10: Distinct clinical profiles of ALS subgroups derived from α-band neural activity trajectories over time. Cluster 1 (n= 11) is depicted in blue while cluster 2 (n = 113) is represented in red. * p<.05, ** p<.01, *** p<.001. An adaptive FDR correction was applied to account for the multiple clinical measures (q<.05).*

4. Discussion

We demonstrated that by analysing the longitudinal trajectories of neural activity through high-density quantitative EEG, it is possible to identify distinct ALS subgroups. These subgroups, identified via clustering, exhibited distinct patterns of brain activity progression in specific regions, that were undetectable when examining the group as a whole (see Chapter V for details). The longitudinal neural activity profiles showed robustness upon reassessment and consistency when extended to additional participants. Additionally, the identified ALS subgroups were associated with different prognostic outcomes.

4.1. ALS subgroups with distinct longitudinal progressions of brain activity

Our investigation of frequency-specific neural activity progressions over time showed stable and statistically significant ALS subgroups. Despite the variability among ALS patients, there are consistent patterns of neural activity changes over time that can be grouped into distinct clusters (or subgroups). In frequency bands where no progression of neural activity over time was observed in the whole ALS group, it was possible to detect subgroups with distinct longitudinal progressions of neural activity (Figure 8). By grouping patients based on their neural activity patterns, we were able to detect meaningful progression trends that were not apparent when considering the entire ALS population. The number of stable clusters varied across different frequency bands. For example, in the δ-band, three stable clusters were identified, while the α-band had two clusters, the β-band had five clusters, and the γ_h-band had three clusters. This suggests that different frequency bands might exhibit different levels of heterogeneity in neural activity patterns. For instance, individuals with ALS in a completely locked-in state (CLIS) exhibited a shift from higher (α_h to γ) toward lower frequency bands (δ to θ) (Maruyama et al., 2021). In earlier ALS stages, θ-band neural activity was observed to decrease longitudinal (Nasseroleslami et al., 2019).

The existence of such ALS subgroups, based on longitudinal EEG patterns, could be key to understanding ALS mechanisms. The clinical heterogeneity observed in ALS becomes critical in the context of drug development, as conventional clinical stratification parameters exhibit limited sensitivity as predictors of disease advancement and survival (Taga & Maragakis, 2018). The identification of these distinctive subgroups, with differing longitudinal neural activity patterns, may enhance our understanding of ALS progression and provide clues for more targeted therapeutic interventions.

4.2. Neural activity longitudinal patterns in α-band subgroups: implications for survival and functional decline

We observed disparities in both survival rates and the progression of functional decline between the two α-band subgroups. Cluster 2 within the α-band, represented in red, exhibited a faster decline across all four functional subscores: upper limbs, lower limbs, bulbar, and respiratory symptoms. These findings implicate that the neural activity patterns within the α-band clusters may serve as indicators of the rate of functional decline in distinct symptom domains. Individuals with longer survival (averaging 9.4 years) and a slower functional decline demonstrated increased α-band brain activity across central and parietal regions. Conversely, those with shorter survival (averaging 3.4 years) displayed reduce in α-band activity over time

localised in the temporal region (Figure 9, Figure 10). In β-band, a specific cluster (reported in blue) also exhibited a significant decrease in activity over time, particularly within the temporal area. While previous observations indicated a cross-sectional decrease in low-frequency bands (from delta to beta) within temporal and posterior regions (Dukic et al., 2019), our study identified a pronounced longitudinal increase in neural activity within a subgroup characterised by extended survival. This distinct progression within the α-band clusters might reflect different underlying mechanisms or responses to the disease.

While an extended disease duration could contribute to more degeneration time, the increase in α-band neural activity within a subgroup displaying longer survival might also be attributed to protective or compensatory mechanisms. Van der Burgh et al. noted significant cortical thinning in the primary motor and frontotemporal regions among individuals with shorter disease duration from onset to scan (less than 9-10 months, likely indicative of earlier stages) (Van Der Burgh, 2020). However, they did not observe further atrophy in follow-up examinations for individuals with longer disease durations at baseline (over 13 months). The longitudinal patterns of functional connectivity (fractional anisotropy, DTI) also exhibited divergence between the shorter and longer disease duration groups. It appears that substantial atrophy occurs at an early stage, with protective mechanisms possibly contributing to extended disease durations. Most neuroimaging studies typically occur later after onset (over 20-25 months after onset). These studies mainly revealed progressive atrophy in the primary motor and frontal regions (grey matter) (Bede & Hardiman, 2018; Menke et al., 2018). The progression of ALS has previously been interpreted either as a 'connectivity-based' spread (Christidi et al., 2019; Schmidt et al., 2016) or a contiguous spread (Braak et al., 2013), following the propagation of TDP-43 aggregates. However, Cardenas-Blanco et al. observed no longitudinal grey matter atrophy across three timepoints (spaced approximately 3 months apart) (Cardenas-Blanco et al., 2016). Similarly, Trojsi et al. did not observe any grey matter changes over time in a one-year study. Such inconsistencies may be attributed to heterogeneous mechanisms (Trojsi et al., 2020). The absence of longitudinal changes longer after onset could be attributed to more acute variations in neurodegenerative mechanisms, as suggested by our identification of subgroups based on patterns of longitudinal neural activity. While atrophy may progress in some individuals, it could decelerate in others, which would represent a crucial distinction.

4.3. Patterns of longitudinal neural activity and cognitive impairment

In the previous chapter (Chapter V), we presented our findings which demonstrated distinct progressions in EEG measures over time among individuals with different neuropsychological profiles. Despite these variations in spectral EEG measures over time, none of the identified subgroups based on the patterns of neural activity showed significant differences in terms of cognition or behaviour. However, by conducting further analyses to cluster functional connectivity trajectories over time, we may identify clusters associated with specific cognitive profiles. A recent MRI study established a connection between disruption in structural connectivity and motor impairment, as well as disruption in functional connectivity and cognitive/behavioural impairment (Basaia et al., 2020). When examining ALS participants from a cross-sectional perspective, those with impaired cognition and/or behaviour exhibited atrophy, particularly in the frontotemporal regions. Conversely, participants with normal cognition demonstrated atrophy primarily focused in the motor region (Agosta et al., 2016; Illán-Gala et al., 2020). This insight highlights the relationship between neural changes and cognitive/behavioural status.

Our own observation of a decline in neural activity over time within the temporal region for certain subgroups aligns with the progressive deterioration of the frontotemporal network observed by Trojsi et al (Trojsi et al., 2020). These changes in functional connectivity appeared to be distinct from changes in cognition, leading the authors to hypothesize that they may occur before the onset of cognitive or behavioural symptoms.

4.4. Limitations

The challenge of working with relatively small datasets introduced uncertainties in our clustering efforts. Other clustering solutions are likely to exist. To address this, we implemented validation analyses to mitigate a potential lack of reproducibility.

As outlined in Chapter V, our longitudinal models may suffer from non-random dropout. We additionally recognise the potential of using HC longitudinal data to disentangle the natural ageing processes and the progression of ALS, as discussed in Chapter V.

5. Conclusion

In conclusion, the results of this study highlight the importance of considering longitudinal trajectories of neural activity within distinct subgroups or clusters of ALS patients. The findings emphasise the heterogeneity of ALS and suggest that analysing neural activity longitudinal patterns can provide valuable insights into disease progression, survival outcomes,

and functional decline. This information could potentially contribute to a deeper understanding of the underlying mechanisms of ALS and guide more personalised approaches to diagnosis, treatment, and patient care.

VII. Results: Biomarkers of ALS based on dynamic resting-state episodes

The study described in this section is published in the peer-reviewed journal Human Brain Mapping:

Metzger M., Dukic S., et *al.*, Functional network dynamics revealed by EEG microstates reflect cognitive decline in Amyotrophic lateral sclerosis.

Figures, tables, results and discussion sections comes in full from this manuscript (combined main section and supplementary material). Introduction and methods sections from this manuscript have been abbreviated to avoid repetition of the contents of previous chapters.

1. Introduction

Whole-brain resting-state electroencephalographic (EEG) studies can provide robust evidence of motor and extra-motor degeneration in ALS. The most recent findings of frequency domain and source localisation analyses include increased co-modulation in the fronto-parietal area (θ, γ-band), and decreased synchrony in the fronto-temporal areas (δ, θ-band) (Dukic et al., 2019; Nasseroleslami et al., 2019). Although abnormal functional connectivity in both sensor and source-space has been shown, there is limited understanding of the temporal dynamics of brain networks in ALS.

Insights into the temporal dynamics of brain networks can be gained through the analysis of brain microstates, as described in Chapter II. Microstates are defined as transient, quasi-stable electric field configurations that repeat sequentially over time within an EEG recording. Microstate analysis involves identifying recurring topographical patterns of spontaneous neural activity across multiple time points and categorizing the EEG topography at each time point into one of these distinct microstate classes. Microstate transitions were originally attributed to changes in the coordination of synaptic activity (Lehmann et al., 1987). These distinct re-occurring topographies of the scalp electrical potential ('scalp maps') have a duration spanning from milliseconds to seconds. Four canonical classes (labelled A-D) of microstates have been repeatedly described and have been associated with well-established resting-state networks (RSNs) in fMRI, based on the estimated brain regions generating each microstate (Michel & Koenig, 2018). Analysing these microstates allows us to investigate changes in the temporal dynamics of brain networks instead of changes in functional connectivity between networks, which is more typically examined in EEG studies (Gschwind et al., 2016).

Changes in the properties of microstates have been previously associated with altered states of consciousness (Bai et al., 2021; Bréchet & Michel, 2022; Zanesco et al., 2021) and with neurological or neuropsychiatric conditions (Al Zoubi et al., 2019; Dierks et al., 1997; Faber et al., 2021; Gschwind et al., 2015; Koenig et al., 1999; Michel & Koenig, 2018; Nishida et al., 2013). Alterations in microstate characteristics are thought to represent alterations in the rhythm of neural processes. However, it is the microstates' temporal dependencies that can perhaps give us the greatest insight into how brain function is altered in neurodegenerative diseases like ALS. Neurological conditions seem to alter the brain's functional resting state transitions; forcing the brain to stay and/or change to specific functional networks. By examining the temporal dependencies between microstate sequences we can investigate how the transitions between functional brain networks are altered in disease. Temporal dependencies are modulated in mood or mental disorders, including FTD (Al Zoubi et al., 2019; Lehmann et al., 2005; Nishida et al., 2013). In Alzheimer's disease, in particular, transition patterns appear random while in healthy controls transitions between specific classes are preferred (Nishida et al., 2013).

These findings suggest that EEG microstates have strong potential as a tool for detecting and measuring neural abnormalities in individuals with ALS, particularly as a task-free assessment of cognitive and behavioural function. Microstate computation exploits the activity that pertains to specific brain regions (by clustering EEG topographies) and therefore microstate classes are hypothesised to reflect specific functional networks, as evidenced by studies examining the relationship between resting-state networks and microstates. By quantifying microstate properties, we gain the ability to investigate neural network activity.

The purpose of this study was to test whether microstate properties can differentiate ALS and HC groups, in standard characteristics (e.g., frequency of occurrence, duration) and temporal dependencies (e.g., transition probabilities and entropy in microstate sequences). This study also examined whether patients exhibit changes in microstate properties over time and whether microstate properties correlate with clinical presentation. To preface our results, RS EEG microstate analysis suggests that ALS affects both sensory and 'higher-order' networks, resulting in reduced dynamicity in brain state transitions. Microstate properties may be a useful ALS prognostic marker for cognitive decline and disease outcome.

2. Methods

2.1.Ethical approval

Ethical approval was obtained from the Tallaght University Hospital/St. James's Hospital Joint Research Ethics Committee in Dublin [reference: 2014 Chairman's Action 7 and 2019-05 List 17 (01)], as described in General material and methods (Chapter IV)

2.2.Participants

2.2.1. Recruitment – inclusion and exclusion criteria

Exclusion and inclusion criteria are described in Chapter IV, section 1.

2.2.2. Demographic profiles

EEG data recorded from 129 individuals with ALS (m: 77%; mean age: 60.89 +/- 11.4) and 78 age-matched healthy controls (m: 36%; mean age: 60 +/- 12) were analysed. Four follow-up sessions were conducted for patients, approximately 5.4 +/- 2.1 months apart. Patients attended an average of 2 +/- 1.2 recording sessions. Detailed information about the demographic of the dataset can be found in Table 5.

Table 5: Demographic profile for controls and patients. Up to five recording sessions were scheduled for the patients with in-between time delays representing delays between each session. The table details the gender proportions, the average ages at recording and, when applicable, disease durations, delays between sessions, site of onset and the number of patients with FTD comorbidity. Numbers show mean ± standard deviation.

Groups	N	Male (%)	Age (years)	Disease duration (months)	Follow-up intervals (months)	ALSFRS-R scores	Site of onset (N)			ALS-FTD diagnosis (N)
							Bulbar	*Spinal*	*Thoracic*	
Controls	78	36	60 ∓ 12	/	/	/	/	/	/	/
Patients T1	121	75	62 ∓ 11	25 ∓ 18	/	36 ∓ 7	22	86	5	5
Patients T2	60	77	60 ∓ 11	32 ∓ 19	4.9 ∓ 1.2	35 ∓ 8	14	43	2	2
Patients T3	45	80	61 ∓ 12	37 ∓ 19	5.3 ∓ 2.8	33 ∓ 9	8	34	1	2
Patients T4	22	86	61 ∓ 11	42 ∓ 24	4.9 ∓ 1.1	33 ∓ 7	2	19	1	1
Patients T5	7	57	57 ∓ 13	52 ∓ 31	6.5 ∓ 2.4	33 ∓ 6	0	6	1	0

2.3.Experiment – EEG acquisition and Experimental paradigm

EEG data were collected at rest as described in Chapter IV, section 2.

2.4.Data analysis

2.4.1. Preprocessing of EEG data

The EEG signals were preprocessed as described in Chapter IV, section 2.4.

2.4.2. Computation of the EEG microstates

To compute microstates, EEG data were low-pass filtered at 30Hz (zero-phase, Finite Impulse Response - 'Brickwall' filter, applied in dual pass form), as commonly recommended in microstate studies (Michel & Koenig, 2018). The computation steps following data pre-processing are represented in Figure 11. The global mean-field power (GFP; representing the

spatial standard deviation) was calculated for each participant with a Gaussian weighted moving average as a smoothing method (window of five timepoints or around 10ms) (Al Zoubi et al., 2019). Next, EEG topographies were extracted from the signals at 1000 randomly chosen instances of local maxima of the GFP curve (12 ∓ 2 % of the total number of peaks, calculated using a peak-finding algorithm). Only 1000, rather than all, peaks of GFP were used for each participant to facilitate computation with a relatively large dataset (Poulsen et al., 2018). These EEG topographies at GFP peaks were used to obtain the optimal signal-to-noise ratio, whereby peaks higher than 1.5 standard deviations from the mean were excluded from the selection. Very high GFP often represents non-neural activity and therefore needs to be rejected. Peaks with less than 10 ms delay in between were also excluded (Poulsen et al., 2018), as this minimum peak distance guarantees that all peaks are distinct. The selected EEG topographies were submitted to a modified K-means clustering algorithm, implemented in the Microstate EEGlab toolbox (Poulsen et al., 2018). The algorithm initially defines K microstate prototypes randomly selected from the EEG data. Each EEG sample is assigned to a cluster by minimising the Euclidean distance between the selected EEG maps and the associated prototype. New cluster prototypes are iteratively defined until convergence or a maximal number of repetitions (50 repetitions in our case) is reached. The algorithm models the signal strength and applies a constraint to only have one microstate active at a time.This differs from the original K-means algorithm by being polarity invariant (assigning opposite maps to the same cluster). The rationale for this approach is that the scalp potentials measured by EEG are generated by fluctuations in the synchronous firing of neurons; therefore an inverse polarity of the scalp potential field may happen while the same neuronal sources generate oscillations in the brain (Brodbeck et al., 2012; Michel & Koenig, 2018).

The K-means algorithm was chosen over the agglomerative hierarchical clustering (AAHC) as it has a shorter computational time and both algorithms have been shown to result in similar microstates (Murray et al., 2008). The optimal number of clusters (or microstate classes) was selected using a K=3 cross-validation approach on a subset of 3-11 maps. Microstate prototypes were identified from two-thirds of the concatenated GFP peaks and backfitted to the remaining data points (the remaining third of the GFP peaks was the test set), allowing for evaluation of the prototypes' performance on the test set using measures of fit like global explained variance and cross-validation criterion (Pascual-Marqui et al., 1995). The cross-validation method ensures the stability of the results, i.e. not getting microstate cluster representing noise. To derive sequences of microstates, the grand mean across groups prototypes were then back-fitted

to the original EEG recordings for both the HC and the ALS groups. Each EEG sample was associated with a prototype class using global map dissimilarity. Microstate time courses underwent temporal smoothing to minimize the influence of fast fluctuations, which may be caused by noise. Short microstate (<20ms) were modified to the next most probable microstate class (Poulsen et al., 2018). While temporal smoothing is beneficial for reducing noise-related artefacts, it is not suitable when investigating temporal dependencies within the microstate sequence. For this aspect of the study, temporal smoothing was intentionally omitted to preserve the inherent temporal structure of the microstate sequence, following the recommendation by von Wegner et al. (von Wegner et al., 2017).

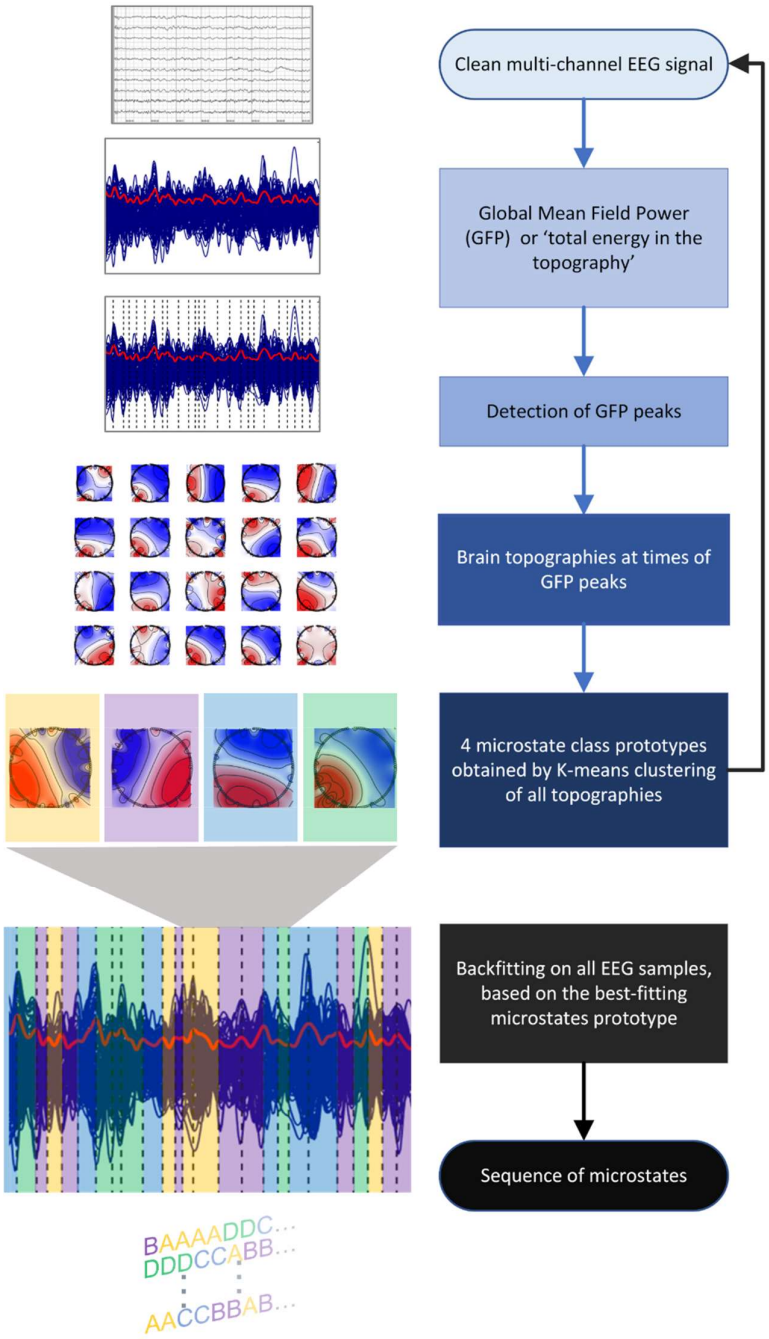

Figure 11: Microstate analysis pipeline. Description of the method used to compute microstates from EEG data. First, a low-pass filter was applied, and the global mean-field amplitude (GFP) was calculated for each participant. Next, EEG maps were extracted from the signals at 1000 randomly chosen local maxima of the GFP curve and a modified K-means clustering algorithm was used to cluster these maps into microstate classes. Finally, the microstate prototypes were back-fitted to the original EEG recordings to derive sequences of microstates for both the HC and the ALS groups.

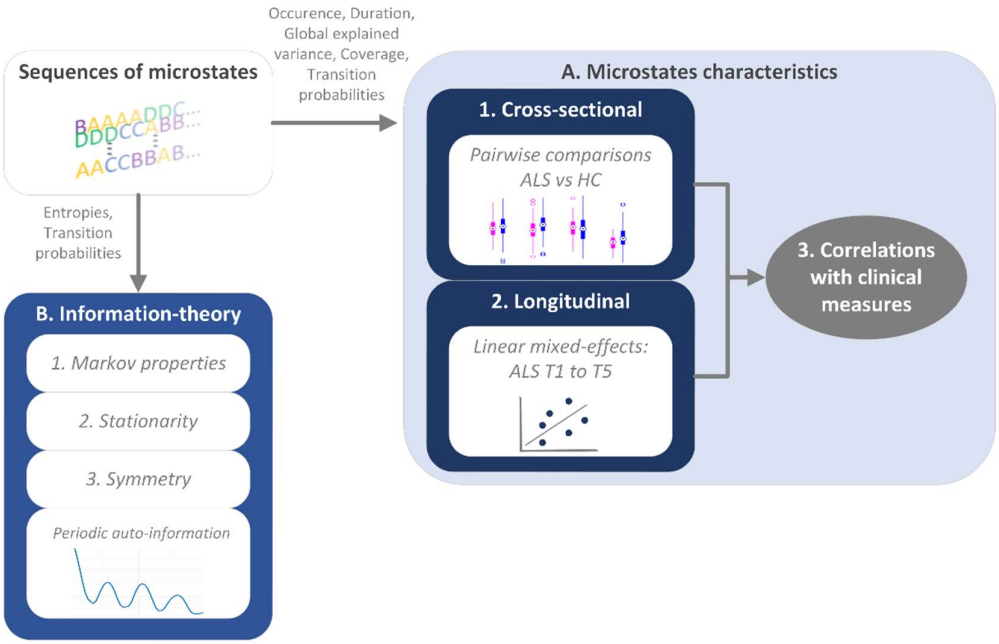

Figure 12: Microstates' stages of analysis. A. ALS and HC cohorts were compared cross-sectionally based on the microstate characteristics extracted from the sequence of microstates. The longitudinal changes of the extracted microstate characteristics were additionally examined. Both cross-sectional and longitudinal characteristics of the microstate sequences were analysed in association with clinical measures. B. The dynamics hidden inside the sequence of microstates were studied based on information theory.

2.4.3. EEG microstates analysis

After the microstate sequences were computed, two types of analysis were conducted. First, the standard microstate characteristics were extracted, including the global explained variance, occurrence, duration and transition probabilities. Three categories of statistical analyses were conducted on those properties: 1) pairwise comparisons between HC and ALS groups, 2) longitudinal analysis in individuals with ALS over the progression of the disease and 3) cross-sectional and longitudinal characteristics of the microstate sequences were analysed with respect to the clinical scores.

Secondly, the temporal dependencies between microstate classes were examined using Shannon entropy and transition probabilities to quantify the predictability and randomness of the microstate sequence (von Wegner et al., 2017). The sequences of microstates were tested for Markovianity of order 0 to 2. The time-lagged mutual information between microstates, as well as the stationarity and symmetry of the transition probability matrices were also assessed. These properties have the advantage of being independent of the method used to compute the microstates (von Wegner et al., 2018).

2.4.3.1. Standard properties of microstates

The global explained variance (GEV) measures how well each microstate class can explain the variance in the EEG signal. Basic temporal parameters were determined, including the average

duration (ms) of a microstate class, its frequency of occurrence (s^{-1}), and the fraction of time it is active during the recording (i.e. coverage). Transition probabilities were also derived from the sequences of microstates to quantify how often one class precedes another. The probabilities were not adjusted for class occurrences or durations, as we chose to report them both independently (Poulsen et al., 2018).

2.4.3.2. Statistical analysis

Cross-sectional pairwise comparisons

Mann-Whitney U tests were computed for each microstate parameter (coverage, occurrence, duration and transition probability) to compare the HC and ALS cohorts. A 10% adaptive False Discovery Rate (FDR) correction was used to account for the four microstate classes (or twelve transitions between classes), which was based on the Benjamini & Krieger method (Benjamini et al., 2006) as implemented in the Empirical Bayesian inference (EBI) toolbox (Nasseroleslami, 2018). The effect sizes were derived from the U-statistics using the rank-biserial correlation coefficient (Cureton, 1956): $r = \frac{2U}{n_1 \cdot n_2}$, as well as the Area Under the Receiver Operating Characteristic Curve (Hajian-Tilaki, 2013): $AUROC = \frac{U}{n_1 \cdot n_2}$. A post-hoc EBI-based estimation of the statistical power was then calculated (Nasseroleslami, 2018).

Microstate validation step

A K=5 cross-validation analysis was performed on the healthy-controls group. The microstate prototypes were extracted from a portion of the HC and then backfitted on another independent set of HC (test set). No significant difference could be found between cross-validation folds testing sets for any of the four measures of interest: occurrence, coverage, duration, GEV (Kruskal–Wallis one-way ANOVA, p = 0.88).

Longitudinal changes

In the ALS group, mixed-effects models were used to examine the changes in microstate parameters and clinical scores (from ALSFRS-R, ECAS and BBI tests) over time as the disease progressed. Mixed-effects models were implemented with an intercept and a time-related slope, reflecting the rate of change per month (from 5 to 113 months after onset). Subject-specific random-effects were included: a random intercept was chosen for the longitudinal model to allow for different baseline values across subjects and a random slope was chosen to allow for different rates of change over time. Age, gender and site of onset as random-effects did not improve the model fit (likelihood ratio test) and were therefore not included in the final model. Education as a random-effect was deemed relevant for the ECAS model only. A specific deviation from intercept and slope, representing the level of education, was added (as random-

effect) to the model of cognitive performance. The longitudinal model of cognition also contained an additional fixed-effect term to account for the three different versions of the ECAS questionnaire. The mixed-effects parameters were estimated using restricted maximum likelihood. The assumptions of normal distributions, independence, and constant variance of the residuals were checked (using the Kolmogorov–Smirnov test ($q<.05$); Ljung-Box Q-test ($q<.05$); Engle's ARCH test ($q<.05$) or diagnostic plots). A rank-based inverse normal transformation was applied in cases where the residuals did not follow a normal distribution (Beasley et al., 2009). To evaluate the linearity of the parameters' progressions over time, quadratic polynomial regression models were estimated per subject (when data from at least three recordings were available). The quadratic coefficients did not significantly differ from zero ($q<.05$), so only first-order models were kept for further analyses. All patients were included in the final models, regardless of the number of recording sessions they attended as mixed-effects models can adjust for missing data. To assess the repeatability of the models, the variances of the linear mixed-effects models were analyzed and decomposed to determine the proportion of variance attributed to various sources, including within-person and between-person measures (Rights & Sterba, 2021; Schielzeth & Nakagawa, 2022).

Correlations with clinical measures

Spearman rank correlations were computed between the microstate parameters and cross-sectional physical and cognitive clinical scores in the ALS group (survival, ALSFRS-R and ECAS scores at the first timepoint). The correlation between the variables that describe the microstate properties and clinical scores over time was also estimated. We evaluated correlations separately for those with cognitive impairment (ALSci; based on ECAS score), behavioural impairment (ALSbi; based on BBI scores) and those without cognitive or behavioural impairment, as people with ALS that have extramotor impairments exhibit different changes in functional connectivity (Burgh et al., 2020; Temp et al., 2021). An adaptive FDR correction was applied and the statistical power was estimated using EBI (Nasseroleslami, 2018) to account for the multiple clinical measures.

Gender, age and medication

To evaluate the effect of age, gender or medication on the observed EEG microstate properties, additional statistical tests were performed (Fisher's test, Kruskal-Wallis analysis of variance and linear regression). We applied linear modelling to verify if the pairwise differences between patients and controls were driven by the significant differences in gender. For each microstate class and parameter, we assessed the differences between HC and ALS patients (at T1), while controlling for gender. In Wilkinson notation, the model would be described as:

Parameter ~ Group + Gender. The rank-based inverse normal transformation was applied to ensure the normality of the observations. The previously observed group effects, by pairwise comparisons, were again significant while controlling for gender (FDR, q=0.05).

2.4.3.3. Information-theoretical properties to assess temporal dependencies

We performed an information-theoretical analysis of the temporal dependencies between microstate classes using Shannon entropy and by interrogating the transition probabilities (extracting their Markov properties, stationarity and symmetry), Figure 12, (von Wegner et al., 2017, 2018). Studying entropy-related properties is a way to determine the predictability of the next microstate class. A sequence with only one microstate class appearing (amongst the four classes labelled A, B, C and D) would represent maximum predictability and therefore minimum entropy (e.g. only B). We then derived the auto-information function (AIF) from the entropy values. AIF measures the time-lagged mutual information between microstates (it is an approximation of the auto-correlation function for nonmetric data). The AIF measures the time-lagged mutual information between microstates with time lag τ, which can be estimated as the difference between the marginal and conditional entropies: $I(\tau) = H(M_{t+\tau}) - H(M_{t+\tau}|M_t)$. The less 'uncertainty' about the time-lagged microstate $M_{t+\tau}$, when M_t is known, the more information is shared between the states and the higher the AIF is. The AIF was evaluated for all microstate classes as well as the contribution to AIF by each microstate class (the time-lagged mutual-information for each microstate class separately).

Then we examined the features of the transition probabilities. We first tested for Markovianity order 0 to 2, to check whether the transition probabilities rely on the current class, the previous class, or two previous classes of the sequence of microstates: with the null hypothesis of no memory effect. The stationarity of the transition probability matrix was then evaluated based on the homogeneity of non-overlapping blocks of varying lengths. Stationarity means that the frequency of any transition between two classes does not depend on time and would not be significantly different in different blocks (von Wegner et al., 2017, 2018). Finally, the symmetry of the transition matrix was assessed to check whether the probability to transition from a class M_i to another class M_j was equivalent to the probability of passing from M_j to M_i. Statistical significance for symmetry, stationarity and the Markovianity was estimated using G-tests (i.e. maximum-likelihood significance tests) and chi-squared distributions (Al Zoubi et al., 2019; von Wegner et al., 2017, 2018).

3. Results

3.1.Four microstate prototypes identified in HC and ALS cohorts

The topographies of the microstate prototypes and the optimal number of clusters identified in both HC and ALS groups (Figure 13) were similar to those conventionally reported in the literature (Michel & Koenig, 2018).

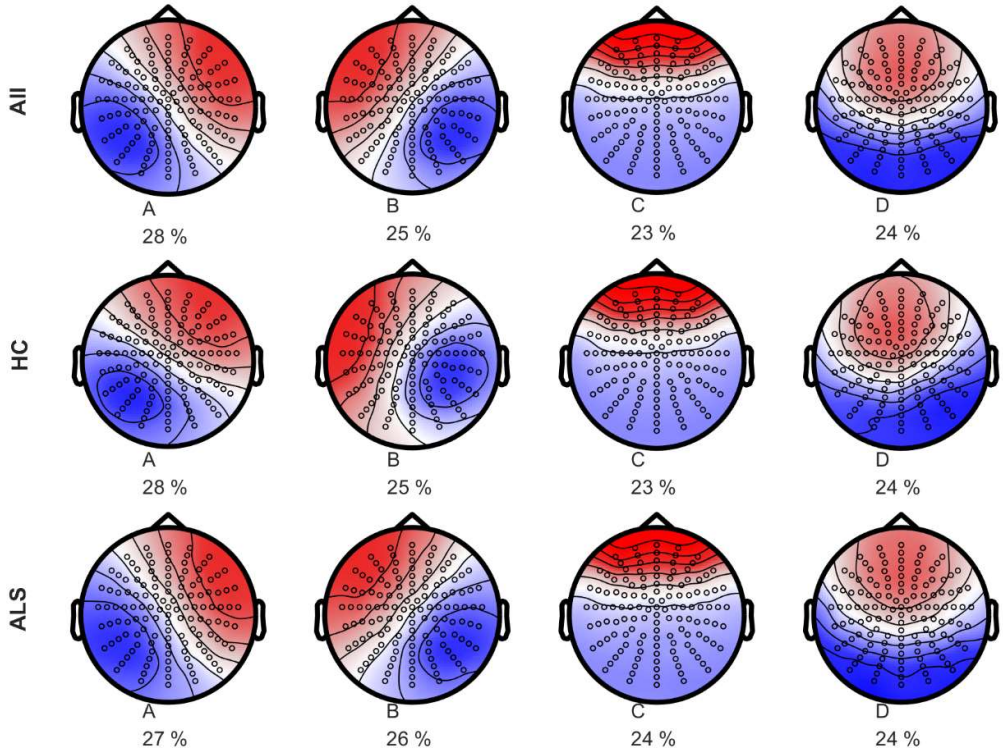

Figure 13: Spatial topographies of the four microstate classes labelled A-D for both the HC and the ALS groups. The polarity is not taken into account. The microstate maps were reordered, according to their topographies, to fit the literature. The contribution of each class to the sequence of microstates is indicated below (in percentage).

The portion of recordings explained by the four microstate prototypes (i.e., explained variance) was 58% for HC and 54% for the ALS group. The four topographies and the distributions of the explained variance did not differ between the two groups (t-test, $p>0.9$ and 2-sample Kolmogorov Smirnov test, $p = 0.7$, respectively).

3.2.Modulation of microstate properties by ALS disease

3.2.1. Distinct microstate properties between HC and ALS cohorts

There were no differences in the GEV distributions of the microstate classes between ALS (measured at the first timepoint) and control groups after FDR correction ($q<.1$). Microstate class B, in particular, seems to be most affected by ALS. The occurrences of both microstate classes A and B were higher in the ALS group (Figure 14, occurrence A: $p = 0.03$, $r= -0.2$, $1-\beta = 0.50$, AUC = 0.59; occurrence B: $p = 0.008$, $r = -0.2$, $1-\beta = 0.65$, AUC = 0.60). The coverages of classes A and B were also significantly higher in the ALS group (Figure 14,

duration A: p = 0.04, r = -0.2, 1-β = 0.41, AUC = 0.58; duration D: p = 0.02, r = 0.2, 1-β = 0.48, AUC = 0.60).

The transition probabilities were significantly different between groups for 7 out of 12 transitions (Figure 15). The largest difference between HC and ALS groups was observed for the transition of microstate C to microstate D ($p = 0.004, r = 0.3, 1 - \beta = 0.74, \text{AUC} = 0.63$). The transition C→D was more frequent in healthy controls.

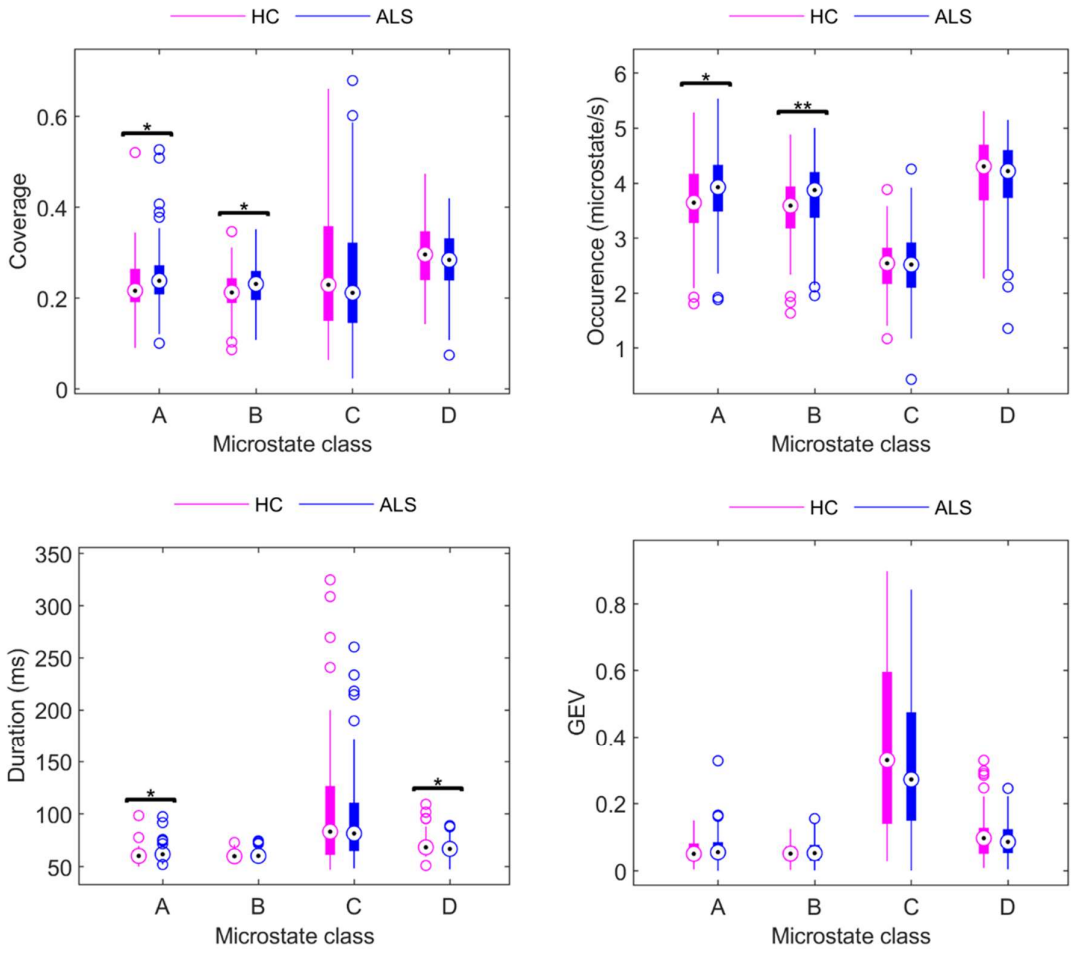

Figure 14: Distributions of specific characteristics for the microstate classes (A-D) for HC and ALS cohorts. Significant differences were observed for the coverage of classes A and B (coverage A: p = 0.02; coverage B: p = 0.03), the occurrence of classes A and B (occurrence A: p = 0.03; occurrence B: p = 0.008), and a significant difference was also observed for the duration of classes A and D microstate (duration A: p = 0.04, duration D: p = 0.02). No significant difference was observed for the GEV of the microstates. All effect sizes were moderate (|r| = 0.2). Benjamini & Krieger FDR, q <0. 1, was applied. $*p \leq .05$, $**p \leq .01$.

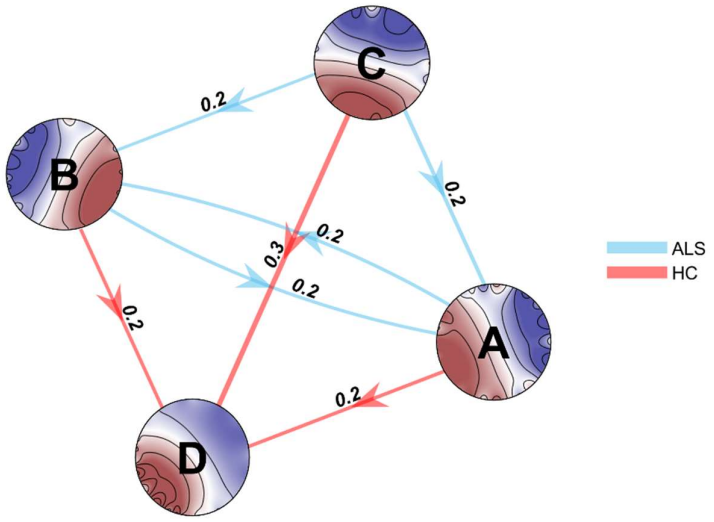

Figure 15: Significant differences in the transition probabilities for the microstates classes (A-D) between HC and ALS cohorts (7 out of 12 transitions). The blue arrows represent higher transition probabilities in ALS, while the red arrows represent higher transitions in controls. Effect size $|r|$ are represented above each arrow and the thickness of the arrows is equal to $10 \cdot |r|$. Benjamini & Krieger FDR, q <.1. Larger effect ($r = 0.3$) was observed for the transition from C to D.

3.2.2. Longitudinal changes of microstate properties in ALS

The longitudinal analysis of the microstate properties in the ALS group revealed a significant decrease in class B duration (5% increase) and GFP over time (2% increase) (Figure 16). The results emphasized the importance of taking into account different baseline values (using a random intercept model) between individuals and different rates of change over time (using a random slope model). This approach allows to effectively discern the sources of variability. In the longitudinal model of class B duration, the random slope variation accounts for approximately 1% of the total variance. In addition, roughly 60% of the outcome variance is attributable to person-specific differences at baseline. Similarly, for class B GFP, 4% of the total variance is attributed to random-time effects, while 70% is attributed to intercept variation. A summary of the linear mixed-effects models can be found in Table 6.

*Table 6: Model parameter estimates from longitudinal analyses of the microstates' properties. Fixed and random-effects of the models describing microstate occurrence, duration, coverage, global explained variance (GEV), and global field power (GFP) progressions over the time of the disease were computed. Only models with significant time effects (FDR correction, q=0.05) are shown. Standard errors were added in parenthesis for fixed-effects. The analysis included 129 patients and 1020 observations. *p < .05; **p < .01; ***p < .001.*

	CLASS B	
	Duration (ms)	**GFP**
Log-likelihood	-670	-370
Fixed-effects		
Intercept	59 (0.6) *ms* ***	4 (0.2) μV ***
Time	**0.05 (0.02) *ms/month* ***	**0.02 (0.005) μV/month ***
Random-effects		
Intercept variance	3 ms^2	2 μV^2
Time variance	0.02 $(ms/month)^2$	0.01 $(\mu V/\text{month})^2$
Residual	2 *ms*	0.6 μV

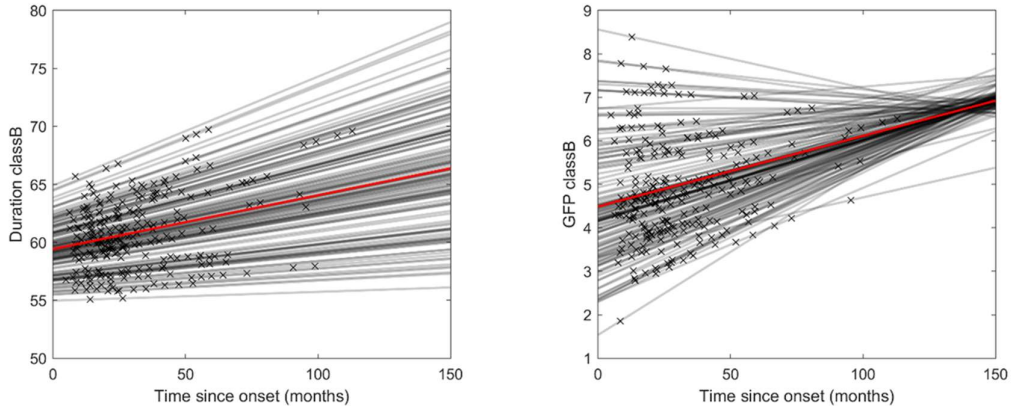

Figure 16: Directions of the significant (q <.05) longitudinal microstate changes per microstate class. Grey lines represent linear models of microstate property change per participant (based on random-effects), while red lines represent the overall linear changes (based on fixed-effects). Crosses represent recording times for each participant. Microstate duration is expressed in ms. Global field power (GFP) is expressed in µV.

3.2.3. Absence of gender, age or medication effect

Gender, age or medication did not have a significant effect on the observed cross-sectional differences in microstate properties between ALS and HC groups or longitudinal effects in the ALS group (Figure 17).

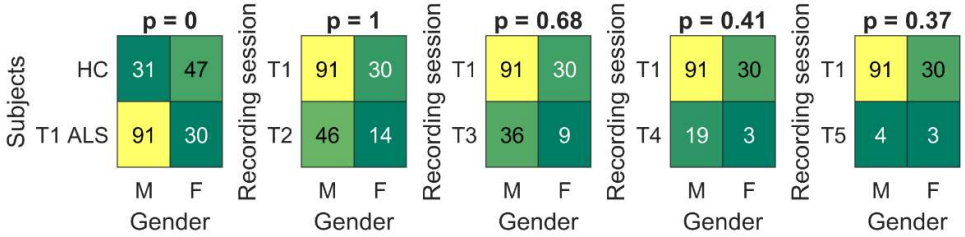

(a) Gender distributions in controls and in patients different recording sessions (T1-T5). Fisher's exact test (α=0.05, two-tailed) did not reveal any non-random association between gender and recording sessions for patients follow-ups.

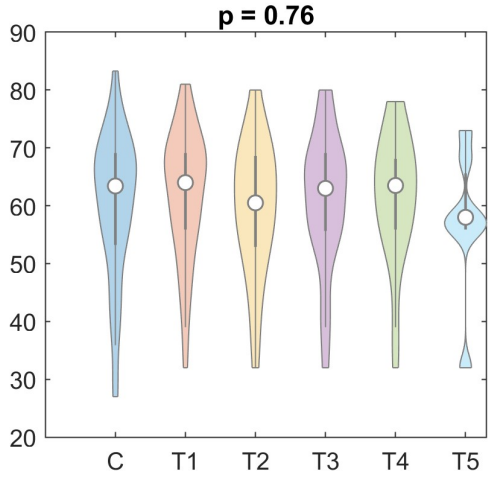

(b) Age distributions in the HC group and ALS group's different recording sessions (T1-T5). Kruskal-Wallis one-way analysis of variance revealed no statistical difference in age distribution between recording sessions.

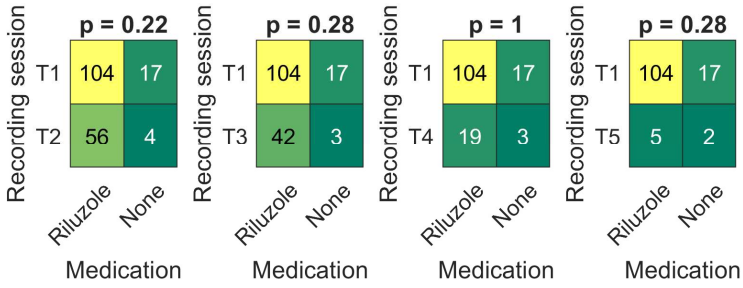

(c) Medication distributions in the ALS group's different recording sessions (T1-T5). Fisher's exact test (α=0.05, two-tailed) did not reveal any non-random association between medication and recording sessions.

Figure 17: Representations of the statistical tests to assess gender, age and medication effects.

3.2.4. Longitudinal changes of clinical measures in ALS

The clinical scores were also modelled using a linear mixed-effects model to investigate individual differences in progression (Appendix – Chapter VI, Supplementary material note 1). As expected, significant time effects were observed for each ALSFRS-R subscore ($p < .001$) (bulbar, lower limbs, upper limbs, respiratory), with a 0.1 to 0.2 points decline per month. The ECAS Total scores also significantly increased over time ($p = 0.02$, 0.2 points increase per month) but no increase was observed in the BBI scores ($p = 0.05$).

3.2.5. Changes in microstate properties are associated with cognitive decline and prognosis

We found that microstates episodes are not only affected by the disease but their characteristics are also associated with the level of cognitive decline. People with ALS who had shorter durations of microstate class B tended to have faster lower motor declines. Individuals with a faster increase in microstate C coverage had a slower decline in fine motor skills (Figure 18). Cognitively and behaviourally impaired participants (ALScbi, n=69) with lower transition probabilities in microstate C to B, A to D and C to D showed a slower increase in ECAS total scores. ECAS scores generally increase over time due to non-random dropout or practice effect. At subject level, if these participants showed less of a practice effect it can be interpreted as a sign of cognitive decline. A lower transition probability between microstates C and B was also associated with shorter survival (Figure 18).

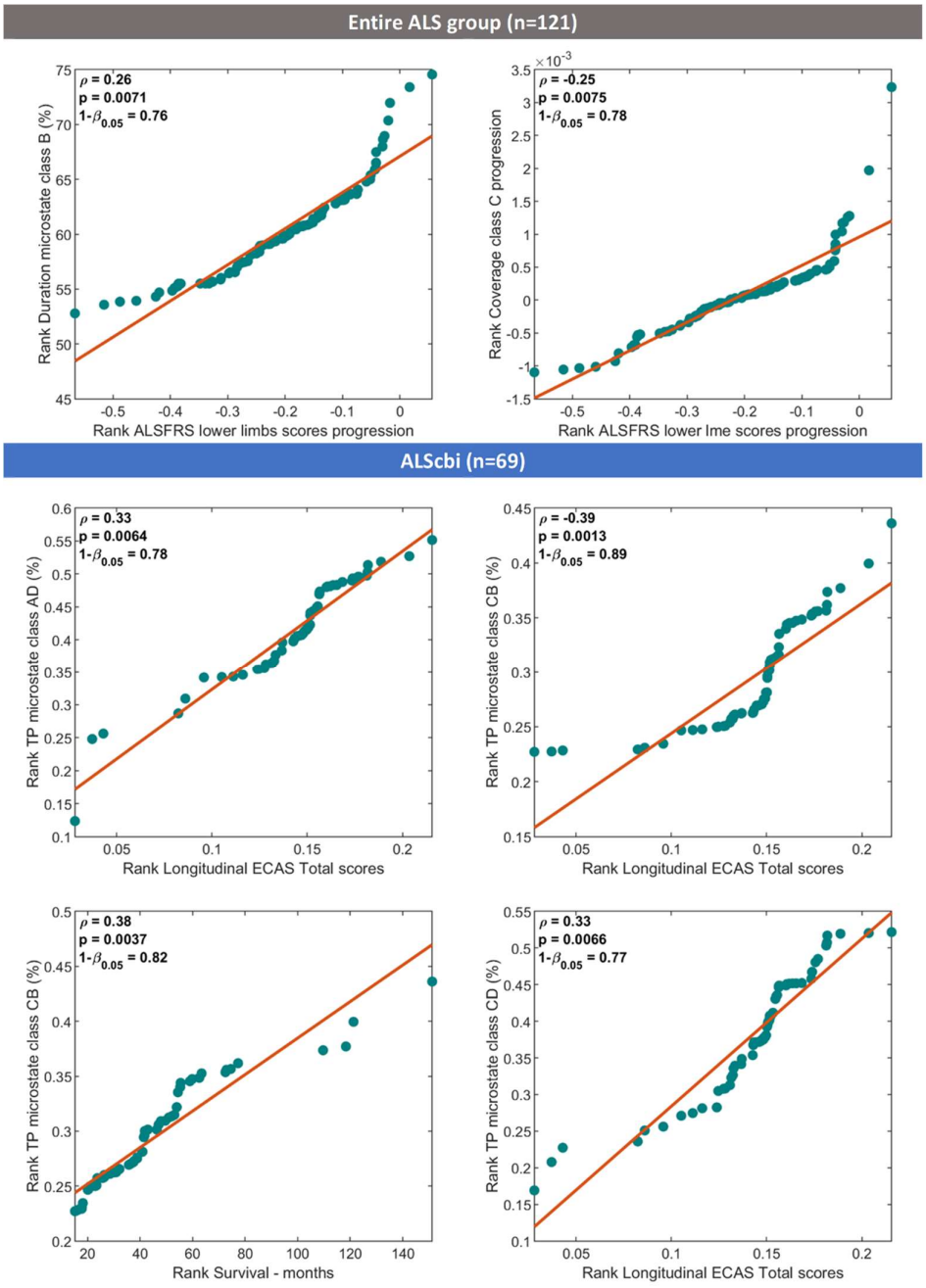

Figure 18: Significant Spearman's correlations between clinical scores progressions and properties of microstates classes for ALS cohort and subgroup of patients with distinct cognitive profiles (ALScbi). FDR correction at .05. TP: Transition Probability

3.3.Influence of ALS on temporal dependencies in microstate sequences

3.3.1. Memory effects in the sequences of microstates

For both HC and ALS groups, there were no long-range memory effects in the microstate sequences, as typically observed (Al Zoubi et al., 2019; von Wegner et al., 2017, 2018). This can be seen in the decay of the periodic peaks of the AIF for time lags larger than $1s$. The existence of a 'memory effect' in the microstate sequence was estimated based on the AIF, by

evaluating how much knowing the label at time t reduces uncertainty at time $t + \tau$. The subject-specific AIF revealed an oscillatory decay in function of the time lags (Figure 19, Control C47), with an average period of 35 +/- 5.5 ms for HC and 33 +/- 5.2 ms for ALS patients. For both HC and ALS groups, the AIF inspection showed that the temporal predictive information in previous time points dependence is less than 1‰ of that in the current time point (>1s lag) (Figure 20). In line with previous works on microstates' temporal dependencies (Al Zoubi et al., 2019; von Wegner et al., 2017, 2018), this suggests the absence of long-range memory in microstate sequences. Both ALS patients and HC groups showed similar overall AIF content but the contribution of microstate C to the AIF was higher in patients compared with controls (Figure 21).

The Markovianity tests were not significant for any order between zero and two, showing no Markov property (or 'memoryless' property, meaning the past is not important as long as the present is known) in the microstate sequences for ALS or HC groups (order 0: $p \sim 0$; order 1: $p < 3.6 \cdot 10^{-72}$; order 2: $p < 1.6 \cdot 10^{-26}$). Information from the current microstate is not enough to define the transition probability to the next microstate (Markov order 0). Information from the current and previous microstates is not enough to define the transition probability (Markov order 1). Information from the current and two previous microstates is still not enough to define the transition probability (Markov order 2). The rejection of the null hypotheses in the G-tests for low-order Markov property reveals memory effects stored at least two microstates in the past.

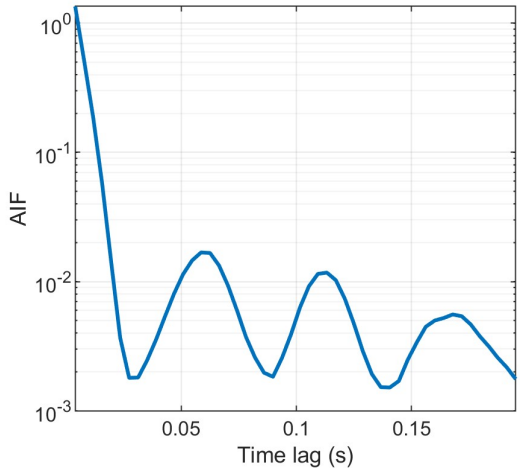

Figure 19: Auto-information or time-lagged mutual information of the microstate sequence for control C47. It shows a periodic oscillation, on a logarithmic y-scale.

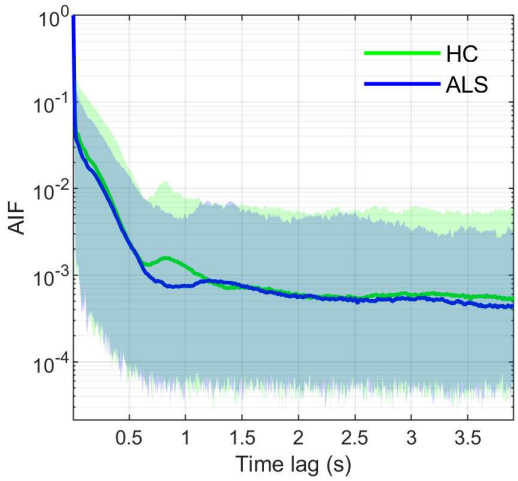

Figure 20: Averaged auto-information of the microstates sequences for HC (green) and ALS patients (blue), with 90% confidence intervals as shaded areas. Logarithmic y-scale.

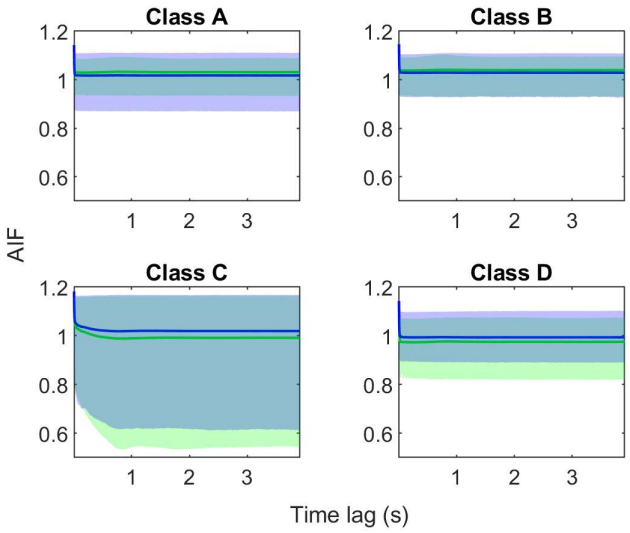

Figure 21: Individual microstate class contributions to the global auto-information function, with 90% confidence intervals as shaded areas, for HC (green) and ALS patients (blue).

3.3.2. Reduced dynamicity of microstate transitions in late-stage ALS

In controls and individuals with early-stage ALS, the percentage of people with predominantly non-stationary transition matrices decreased at a similar rate as the block length was increased (where block length is the time window over which the transition probabilities were studied) (Figure 22). Participants in the late stage of ALS (King's stage 4) were more likely to have stationary transition matrices. The frequency of a transition between two classes is staying the same in different blocks, thus becoming independent of time. In ~4s blocks, significantly more individuals with late-stage ALS (8%) have stationary transition matrices than individuals from earlier stages (1%) (Mann-Whitney U test, p=0.0032, FDR at 0.05). Higher stability in the

transitions between microstate classes has been interpreted as a reduction in the dynamicity of neuronal connectivity (Al Zoubi et al., 2019; von Wegner et al., 2017). No significant difference was observed between the King's stages <4 and the HC group.

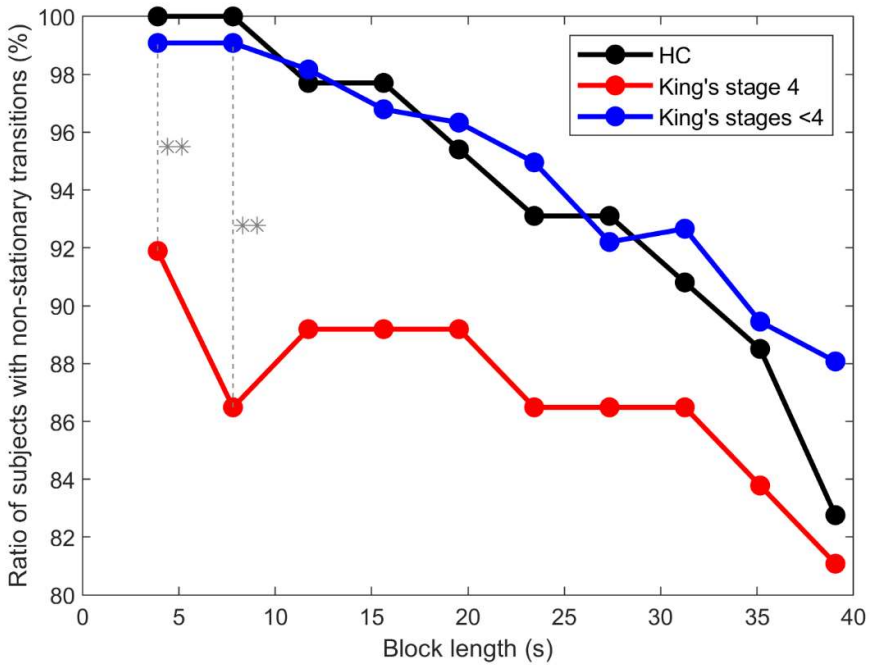

Figure 22: Ratio of subjects (HC, ALS patients in King's stage 4 and lower) with significantly (p<.01) non-stationary microstates transition matrices for different window lengths. For a ~4s window, significantly more people with King's stage 4 disease (8%) have stationary transition matrices than patients from earlier stages (1%) (Mann-Whitney U test, p=0.0047). Benjamini & Krieger FDR, q <0.05, was applied. $* p \leq .05$, $** p \leq .01$.

For 54% of the HC and 58% of the individuals with ALS, the likelihood of passing from microstate class M_i to class M_j was not statistically equivalent to the likelihood of transitioning from M_j to M_i. In most participants, the transition matrices were asymmetric. However, only 49% of individuals with late-stage ALS had asymmetric transition matrices.

4. Discussion

The results of this study demonstrate that the properties of EEG microstates can provide insight into ALS prognosis, particularly the degree of cognitive decline over time. The EEG microstates have been examined in a large cohort of people with ALS (n=129) and healthy controls (n=78), enabling a cross-sectional analysis. This analysis revealed that the standard properties of microstate classes A, B and D differ between ALS and control groups (Figure 14), which may indicate dysfunction in the somatosensory and attention networks. There were also significant differences in microstate transitions between ALS and control groups, Figure 15, suggesting that the normal fluctuations in neural activity are altered in ALS. We

also demonstrated that as ALS progresses, the neural dynamics undergo further changes. This is shown by longitudinal changes we observed in the standard properties of microstates (Table 6, Figure 16) and their temporal dependencies (Figure 22). Participants with late-stage disease showed more symmetry and stationarity in their transition matrices (Figure 22), which could reflect reduced neuronal flexibility (dynamicity in switching between brain microstates).

Finally, the correlations between microstate properties and ALS prognosis revealed that higher duration of class B and faster increase of class C coverage over time are associated with a slower decline in gross motor skills in ALS. For cognitively and behaviourally impaired patients, lower transition probabilities from A to D, C to B and C to D are specifically associated with cognitive decline. This suggests that the microstate parameters have particular potential for development as prognostic biomarkers for ALS.

4.1.Changes in microstate properties in ALS

We found that four cluster prototypes (Figure 13) explained ~60% of the variance and exhibited similar topographies in healthy controls and ALS groups (they were also similar to the maps described in the literature, see review (Michel & Koenig, 2018)). In studies including more topographies, the four maps initially found in 1999 (Koenig et al., 1999) are usually observed along other topographies, independently of ages, mental states or neurological conditions (Al Zoubi et al., 2019; Custo et al., 2014; Faber et al., 2021; Zanesco et al., 2020). The original A-D labels were kept based on topographical similarity to the initial maps. Consistent with previous studies (Michel & Koenig, 2018), we observed that four microstate prototypes explained at best the variance of topographical patterns in unrelated data. This cross-validation check of the optimal number of microstates ensured the microstate prototypes were not representing recording noise (Poulsen et al., 2018).

4.1.1. Distinct microstate properties between HC and ALS cohorts

The statistically significant increase in microstate class A duration and microstate class B coverage in the ALS group, when compared to healthy controls, is similar to what was observed in Parkinson's disease (C. Chu et al., 2020),-and in multiple sclerosis studies (Gschwind et al., 2016). The increase in class A and B coverage has also been demonstrated in Huntington's disease (Faber et al., 2021), and an increase in class A occurrence has been documented in both schizophrenia (Lehmann et al., 2005) and spastic diplegia (Gao et al., 2017).

The results of previous fMRI-EEG studies suggest that class A originates from the bilateral temporal gyri (Britz et al., 2010), occipital and posterior cingulate areas (Pascual-Marqui et al., 2014) or the sensorimotor cortex (Yuan et al., 2012). Diverse interpretations of microstate class

A's functional role have been reported; initially linked with the auditory network (Britz et al., 2010; Custo et al., 2017), a broader involvement including visual processing has been suggested, due to its increased coverage during visualization-oriented tasks compared to verbalization tasks (Milz et al., 2017). Both of these interpretations would situate the sources of class A microstate within the sensory network, which is known to be affected in ALS. A recent review analysis conducted by Tarailis et al. has further proposed a potential link between microstate class A and varying levels of brain arousal or alertness (Tarailis et al., 2023). Class B is thought to originate in the occipital lobe and is associated with visual function (Britz et al., 2010). Both microstates A and B appear to reflect the activation of sensory networks, as indicated by their modulations in multiple sclerosis (Gschwind et al., 2016) and movement disorders in general (ALS, Huntington's, Parkinson and spastic disorder).

Microstate class D occurrence was higher in the ALS cohort than in HC. A high contribution of fronto-parietal areas and anterior/posterior cingulate cortices (Britz et al., 2010; Pascual-Marqui et al., 2014) was observed during microstate class D, which altogether suggest an association of microstate D with the attention network. Microstates classes C and D have been associated with 'high-order functional networks' (as opposed to somatosensory or motor networks) (Michel & Koenig, 2018). The balance between such microstate classes was observed to be affected by neuropsychiatric conditions like schizophrenia or FTD (Nishida et al., 2013). While ALS is not primarily classified as a psychiatric disorder, the condition can often present with cognitive and behavioural symptoms.

Taken together the cross-sectional comparisons of microstate properties between ALS and HC cohorts echo the dual impairment of sensorimotor and cognitive functions in ALS.

4.1.2. Longitudinal changes of microstate properties in ALS

For individuals with ALS, the duration and the GFP of class B significantly increased by 0.05 and 0.02 points per month (Table 6). Neither of those properties was significantly different between the HC group and ALS group at the first recording session. The microstate properties showing significant differences between ALS and HC groups did not reveal any longitudinal change. This finding suggests the presence of important neuronal changes early in the disease, leading to distinct microstate properties in the ALS and HC groups. There may be slower or delayed continuous mechanisms causing changes in other microstate properties. Since early degeneration is usually compensated by remaining neuronal networks in neurodegeneration, such slower mechanisms may be compensatory. In ALS, symptoms only become apparent when a resilience threshold is crossed (Benatar et al., 2022; Keon et al., 2021).

4.2.Altered microstate dynamics in ALS

Previous literature has shown that there are differences in microstate transition probabilities in mood or mental disorders (Al Zoubi et al., 2019; Lehmann et al., 2005) and FTD (Nishida et al., 2013), and we hypothesised that the transition probabilities would also be altered in participants with ALS that exhibited cognitive and behavioural symptoms. As expected, we observed significant differences in microstate dynamics between ALS and HC groups in seven out of twelve of the transition probabilities ($q<0.1$, FDR correction) (Figure 15). More specifically, we observed that patients switch less frequently from microstate C to microstate D (Figure 15).

The results of previous studies on stroke, which reported no significant difference in transition probabilities compared to controls (Hao et al., 2022), suggest that the temporal dynamics of neural networks are not solely due to structural changes.

In this study, we employed the information-theoretical analysis proposed by von Wegner et al. to further investigate the dynamics of EEG microstates (von Wegner et al., 2017). Our findings align with their results indicating that the microstate sequence does not adhere to a low-order Markov property, suggesting that microstate labelling is influenced by not only the current state or the current and last two states, but also previous states. Furthermore, our analysis of the auto-information function revealed non-Markovian behaviour for time lags of up to 2 seconds, consistent with previous research (Al Zoubi et al., 2019; von Wegner et al., 2017), indicating the presence of extended short-range memory effects in the microstate sequences.

For the majority of the subjects (HC and ALS cohorts with King's stages <4), the transition matrices were asymmetric. This has been previously interpreted as a sign of 'non-equilibrium' of the neural networks (von Wegner et al., 2017). A lack of symmetry in transition matrices has been interpreted as a positive property, implying the existence of a "driving force" (if there were no "driving force", and the neural networks were at equilibrium, the transition from one state to a second state would be equal to the transition from the second state to the first one). It is not surprising therefore that the late-stage group (King's stages 4) tended to have more patients with symmetric and stationary transition matrices, Figure 22. The increased number of symmetric and stationary transition matrices observed in late-stage ALS may correspond to the dysfunction of this 'driving-force'. The thalamus, in particular, has been described as a key relay of energy, and could represent a hypothetic 'driving-force' (von Wegner et al., 2017) (thalamic involvement has been demonstrated in motor neuron diseases (Chipika, Christidi, et al., 2020; Chipika, Finegan, et al., 2020; Deymeer et al., 1989)).

The observed change in microstate transitions in late-stage disease could also be explained by the distress individuals with ALS may experience towards the end of their life. A higher ratio of symmetrical and stationary matrices in individuals with mood and anxiety disorders compared to healthy controls has been similarly shown by (Al Zoubi et al., 2019), which they interpreted as arising from "ruminative thoughts". Increased equilibrium could additionally arise due to a reduction in the flexibility of brain dynamics in ALS. A previous study has shown that the incidence of 'neuronal avalanches', a measure of brain dynamics determined by quantifying aperiodic bursts of neuronal activity diffusing across the brain, was reduced in ALS compared with healthy controls cohort and was associated with disease stage (Polverino et al., 2022).

4.3.Clinical relevance of EEG microstates

The main finding from the analysis of the correlation between microstate parameters and clinical measures was that lower duration of microstate class B and slower change in coverage of class C were significantly associated with faster functional decline in the lower limbs (Figure 18). These measures, therefore, have potential utility in prognostic prediction of motor function.

We evaluated correlations with clinical scores specifically for subgroups of ALS patients with distinct cognitive profiles as altered microstates characteristics have been specifically associated with impaired cognition and mental health (Al Zoubi et al., 2019; Dierks et al., 1997; Nishida et al., 2013; Tait et al., 2020). In cognitively and behaviourally impaired patients, the lower transition probabilities A to D, C to B and C to D are additionally associated with cognitive decline. This decline is suggested by the gradual improvement in cognitive performance (measured by ECAS Total scores), which is slower when compared to the average practice effect. Additionally, a lower transition rate from C to B was associated with shorter survival (Figure 18).

The transition probability C → B appear to be a key potential biomarker of ALS prognosis. Higher transition probabilities from C to B seem to represent signs of slower decline in ALS. This supports our hypothesis that changes in microstates dynamics could predict the progression of ALS, including cognitive decline.

4.4.Limitations and Future Directions

The EEG microstate analysis is based on a repeatedly observed phenomenon representing ongoing thought processes. However, there remains a lack of understanding of the neural mechanisms leading to the presence of microstates and their transitions. It remains unclear how microstates actually reflect conscious thoughts, despite new insights on microstates in various

states of consciousness (e.g., sleep, anaesthesia, wakefulness) (Bréchet & Michel, 2022) and rough estimations of the brain sources each microstate class originate from (Bréchet et al., 2020; Britz et al., 2010; Custo et al., 2017; Milz et al., 2017; Musso et al., 2010a; Pascual-Marqui et al., 2014). The interpretation of microstates' characteristics often relies heavily on estimated brain sources. Previous studies of the brain sources underlying different microstates have reported diverse findings, possibly as a result of differences in methodology and/or lack of temporal independence (difficulty of dissociating microstate sources as microstates are a continuous process). This complicates the interpretation of microstate changes (Britz et al., 2010; Mishra et al., 2020; Yuan et al., 2012). Microstates are fundamentally defined based on sensor space analysis. Therefore, for a precise association with brain sources, other methods can provide more information, such as examining patterns of activation directly in brain networks' functional connectivity. In this study, over-interpretation was carefully avoided by cross-examining microstates' hypothetic generators with paradigm-based studies.

One important consideration is the possible non-random dropout within the ALS cohort over time, wherein individuals with greater impairments are more likely to be lost to attrition. In the case of longitudinal ECAS scores, the observed increase may not solely be attributed to the practice effect but could also be influenced by artificial inflation of cognitive scores due to the dropout of more impaired participants. However, this potential bias is mitigated when examining correlations between EEG and clinical measures progressions at the subject level, as both are expected to be similarly affected by non-random dropout.

A limitation of the present study is the heterogeneity of onsets and cognitive/behavioural ALS profiles. In future studies, a more continuous collection of data should help to account for a greater number of clinical profiles and we envisage that a comparison of microstates in different ALS subphenotypes will be possible.

4.5.Conclusion

These RS EEG microstate results indicate that ALS impacts both sensory and higher-order networks. These findings are consistent with the range of motor, respiratory, and cognitive impairments observed in ALS clinical presentations. Temporal dynamics of resting state EEG enable us to further quantify the multidimensional impairments. Importantly, we found reduced dynamicity in brain state transitions, which may occur as a result of declining cognition, repetitive thoughts, anxiety, or neuronal loss. We have shown that changes in microstate properties are associated with cognitive decline and prognosis, making them a promising prognostic marker for ALS.

VIII. Results: Developing new measures of cognitive-behavioural impairment from spectral power and connectivity changes, using dynamic analysis of resting-state data

1. Introduction

Neural network disturbances in ALS have been associated not only with motor or respiratory impairments but also with cognitive and behavioural impairments, the latter occurring in a substantial proportion of cases. Research has revealed that specific dysfunctions within spectral power and functional connectivity are linked to ALS. For instance, disruptions in functional connectivity in regions spanning the frontal, frontoparietal, and fronto-temporal areas have been correlated with cognitive decline (Dukic et al., 2019).

As described in Chapter VII, EEG microstates, which are recurring topographies of scalp electrical potentials, revealed alterations in functional brain network dynamics in ALS. Specific microstate transition probabilities correlated with cognitive decline in individuals with cognitive impairments. Differences between ALS and HC in microstates associated with higher-order cognitive function were additionally observed.

Estimating precise and reliable brain sources for each microstate would deepen our understanding of microstates and their links with neural networks. Investigating brain sources underlying microstates led to varied outcomes due to methodological disparities and challenges in disentangling microstate sources given their continuous nature (Abreu et al., 2021; Custo et al., 2017; Musso et al., 2010b; Pascual-Marqui et al., 2014) (see Chapter VII for more information). Since microstates are primarily defined through sensor-space analysis, directly examining spectral patterns within brain networks would represent a promising alternative approach.

The aim of the current project was to identify spatially distinct patterns of brain states, reflecting functionally different brain networks, and examine whether abnormalities in brain states were associated with ALS. To achieve this, a hidden-Markov model (HMM) was applied in association with a multivariate autoregressive model (MAR) (Vidaurre et al., 2016; Vidaurre, Hunt, et al., 2018) on resting-state EEG data from 78 HC and 99 individuals with ALS. Twelve brain states were identified by identifying patterns of spectral measures (i.e. spectral power and coherence) from the source-reconstructed EEG timecourses in the 90 AAL brain regions described previously. The spectral properties of the identified states allow for

their association with known functional networks like the visual, sensorimotor or default mode networks. The exploration of recurring patterns in resting-state EEG data in source-space represents a compelling approach for understanding the dynamic intricacies of brain activity and their potential disruptions in ALS. Our preliminary results showed distinct temporal properties of the brain state associated with the posterior default mode network between the ALS and the HC groups.

This dynamic analysis has the potential to not only provide a deeper comprehension of the altered functional networks in ALS but also to offer valuable insights that could potentially pave the way for targeted therapeutic strategies.

2. Methods

2.1. Ethical approval

Ethical approval was obtained from the Tallaght University Hospital/St. James's Hospital Joint Research Ethics Committee in Dublin [reference: 2014 Chairman's Action 7 and 2019-05 List 17 (01)], as described in General material and methods (Chapter IV)

2.2. Participants

2.2.1. Recruitment – inclusion and exclusion criteria

Exclusion and inclusion criteria are described in Chapter IV, section 1.

2.2.2. Demographic profiles

EEG data recorded from 99 ALS patients (m: 73%; mean age: 60.89 ± 11.4) and 81 age-matched healthy controls (m: 43%; mean age: 60.93 ± 11.3) were analysed in this study. Detailed information about the demographic of the dataset can be found in *Table 3*.

Table 7: Demographic profiles. Numbers show mean ± standard deviation. The table details the gender proportions, the average ages at the time of recording and, when applicable, disease durations, delays between sessions, site of onset and the number of patients with FTD comorbidity.

Groups	N	Male (%)	Age (years)	Disease duration (months)	ALSFRS-R scores	Site of onset (N)			ALS-FTD diagnosis (N)
						Bulbar	*Spinal*	*Thoracic*	
HC	78	36	60 ∓ 12	/	/	/	/	/	/
ALS	99	73	61 ± 11	22 ± 17	37 ± 6.1	20	72	5	5

2.3. Experiment – EEG acquisition and Experimental paradigm

EEG data were collected at rest as described in Chapter IV, section 2.

2.4. Data analysis

2.4.1. Preprocessing of EEG data

The EEG signals were preprocessed as described in Chapter IV, section 2.4. Source-space timecourses were estimated in 90 brain regions from the AAL atlas (Tzourio-Mazoyer et al., 2002).

2.4.2. Source-space timecourse decomposition and spectral characterisation

We decomposed the source-space timecourses into transient, reoccurring brain states by applying a time-delay embedded Hidden Markov Model (TDE HMM). The model was trained to convert a source-reconstructed time course into a sequence of functional networks characterised by spectral power and signals coherence. The TDE HMM was inferred and state-specific spectral information extracted using the HMM-MAR toolbox (https://github.com/OHBA-analysis/HMM-MAR), which includes explanations about the model (Vidaurre, Hunt, et al., 2018). The TDE-HMM ran in parallel on a workstation with AMD Ryzen Threadripper PRO 5945WX processeur running at 4.1GHz to 4.5GHz, using 64Gb of RAM. The computation steps following data pre-processing are summarised in Figure 23.

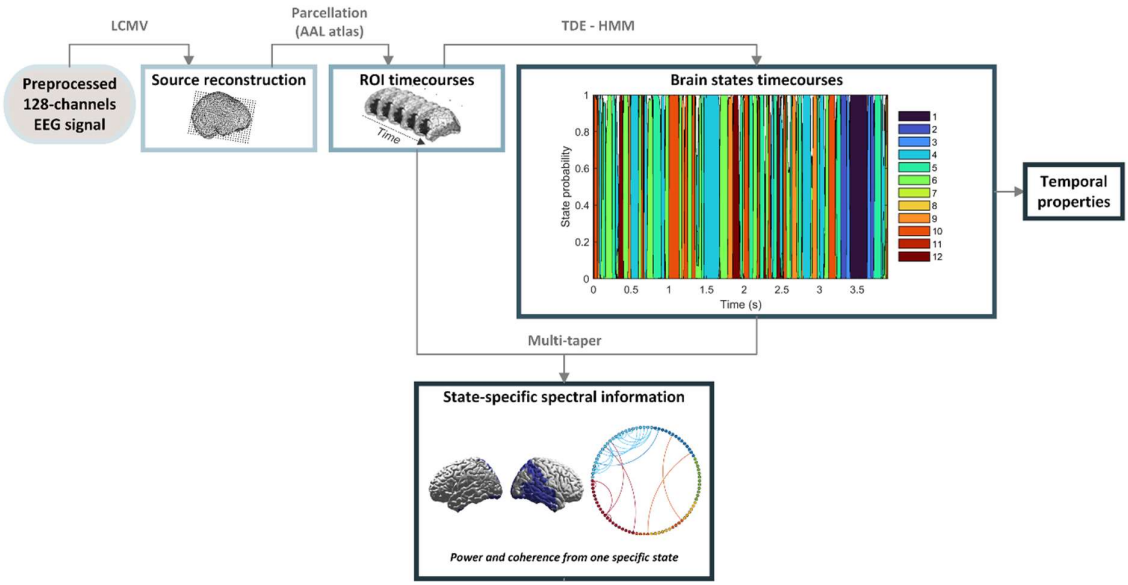

Figure 23: Brain states analysis pipeline. Description of the method used to compute brain state timecourses from EEG data. The process started with the application of a linear constraint minimum variance (LCMV) beamformer for source reconstruction. This allowed the estimation of the sources of brain activity within the raw EEG data. Subsequently, the estimation of timecourses within 90 distinct brain regions of interest (ROIs) was accomplished using the automated anatomical atlas (AAL). By employing the time-delay embedded hidden markov model (TDE-HMM), timecourses of recurring spectral patterns (which can be interpreted as brain states) were extracted from the combined data of both the ALS and HC groups. The temporal properties of the extracted timecourses were then calculated, providing insights into the occurence duration or transitions of these brain states. A multi-taper method was employed to obtain the distinct spectral signatures associated with each brain state. Finally, the spectral information was factorised per frequency band using non-negative matrix factorisation (NNMF). In summary, the brain state analysis pipeline inlcuded a series of interconnected steps, which allowed for the study of brain state dynamics using EEG data.

2.4.2.1. The Hidden Markov Model

A Hidden Markov Model (HMM) is a statistical approach, based on a set of hidden states and a set of observable outputs. The hidden states are unobserved variables that represent the underlying system dynamics, while the observable outputs are the measurements or observations we can directly observe. An EEG timeserie can therefore be modelled into a sequence of 'hidden' states, with one state for each timepoint. The model assumes that the system transitions between hidden states over time according to a probabilistic transition matrix. Each hidden state has associated probabilities for emitting different observable outputs, defined by an emission matrix. The probability of being at a specific state at each time point is influenced by the state at the preceding time point. A stochastic inference was carried to estimate the posterior probabilities despite the large size of our dataset (99 ALS and 81 HC participants, 256Hz, 6 min recordings) (Vidaurre, Abeysuriya, et al., 2018). Given a sequence of observable outputs, an HMM allowed us to infer the most likely sequence of hidden states that generated the observations. The Viterbi algorithm efficiently computed the maximum likelihood path through the model.

2.4.2.2. The time-delay embedded HMM (TDE-HMM)

The TDE-HMM was applied to infer brain states based on spectral power and signals coherence (or phase-locking as described by Vidaurre et al.). It has the advantages of being computationally efficient and avoiding overfitting when modelling whole-brain EEG data (90 brain regions in our case) (Vidaurre, Hunt, et al., 2018). The spectral activity was examined over a time window using a Gaussian distribution: the multivariate autocovariance was computed. This 'embedding' allowed us to efficiently identify patterns in the timecourses (transient and recurring brain states). Additionally a principal component analysis (PCA) decomposition was applied to simplify computation and avoid overfitting.

2.4.2.3. TDE-HMM parameters

Before applying the TDE-HMM, the polarity of the source-reconstructed signals was harmonised to ensure uniformity across all participants. To optimise sign alignment among all participants, the lagged partial correlation between pairs of regions was computed (Vidaurre, Hunt, et al., 2018). The TDE-HMM was then applied on the concatenated timecourses from both the ALS and HC groups. For the time-delay embedding, a window of 15 time points (equivalent to 58.6 ms) was used. Stochastic inference was performed with 10 participants per batch. The inference was run iteratively until a minimum decrease in free energy (tolerance 10^{-6}) or a maximal number of 500 cycles was reached. The TDE-HMM analysis was

conducted on the principal components decomposition of the windowed space, for K = 12 states. The number of principal components used was twice the count of brain regions (2x90 ROIs).

2.4.2.4. Spectral decomposition of the model

After obtaining the sequence of brain states from the TDE-HMM, we extracted spectral information (power and coherence) for each state using the multivariance covariance matrix. A multi-taper method was applied to extract for each state, the spectral power and coherence per frequency bin between 1 and 45Hz.

2.4.3. Statistical analysis

2.4.3.1. Pairwise comparisons of brain states' temporal properties

From the sequences of brain states, temporal properties were computed for each participant to determine how often they reoccur, how long they last and how they transition. We computed the transition probabilities between each pair of states, while also calculing metrics like the fractional occupancy of each state, the rate of transitions between states (or switching rate), the state lifetime (indicating the number of time points per state occurrence), and the state interval time (representing the number of time points between each state's occurrences).

We performed Mann-Whitney U tests on all state sequence parameters to compare between the HC and ALS groups. To address potential false positives, a 10% adaptive FDR correction was applied, to account for the twelve brain states. This correction followed the approach of Benjamini & Krieger (Benjamini et al., 2006) as implemented in the Empirical Bayesian inference (EBI) toolbox (Nasseroleslami, 2018). Effect sizes were computed from U-statistics using the rank-biserial correlation coefficient (Cureton, 1956): $r = \frac{2U}{n_1 \cdot n_2}$, along with the Area Under the Receiver Operating Characteristic Curve (AUROC) (Hajian-Tilaki, 2013): $AUROC = \frac{U}{n_1 \cdot n_2}$. Additionally, a post-hoc estimation of statistical power using EBI toolbox was calculated (Nasseroleslami, 2018).

2.4.3.2. Significance of the spectral measures in each state

To study the spectral measures characterising the identified brain state, a permutation test was performed (Vidaurre, Hunt, et al., 2018). The spectral power and functional connectivity in each state were computed for each participant. Null distributions of the relative spectral measures within-state (in relation to the average in the state), were obtained, by shuffling the

relative spectral measures 5000 times. Significantly higher neural activations and functional connectivities, across participants, were extracted for each state. Multiple comparisons correction was applied to account for the number of brain regions (FDR, q<.01) (Benjamini & Hochberg, 1995).

3. Results

3.1. Recurring brain states in ALS and HC, identified using TDE-HMM

Twelve brain states with distinct patterns of spectral power and coherence were identified for the combined ALS and HC group, using the TDE-HMM method. Additionally, for each participant, a timecourse of the probabilities of activation of each brain state was obtained. The portion of variance in the timecourses explained by the twelve brain states (i.e., explained variance) was ~70%.

3.2. Contrasting temporal dynamics of brain states between ALS and HC Groups

Analysis of the timecourses of brain state occurrences enabled an examination of the temporal properties of these states, including factors such as lifetimes of each state occurence, intervals between occurrences, fractional occupancy, and switching rates. In average across states, the brain states last 98. 6 ms for HC and 98.8ms for individuals with ALS. Figure 24 shows the distributions of the properties for each state in the ALS and the HC groups. Notably, individuals with ALS exhibited significantly longer durations of brain state 10 in contrast to the HC group ($p = 0.004$, $r = 0.3$, AUC = 0.64, $1 - \beta_{0.05} = 0.79$). Those with ALS, additionally, displayed shorter intervals, indicating a lower number of timepoints between occurrences of state 10 ($p = 0.0005$, $r = -0.3$, AUC = 0.64, $1 - \beta_{0.05} = 0.92$). No statistically significant differences were observed in switching rates or fractional occupancy between the ALS and HC groups.

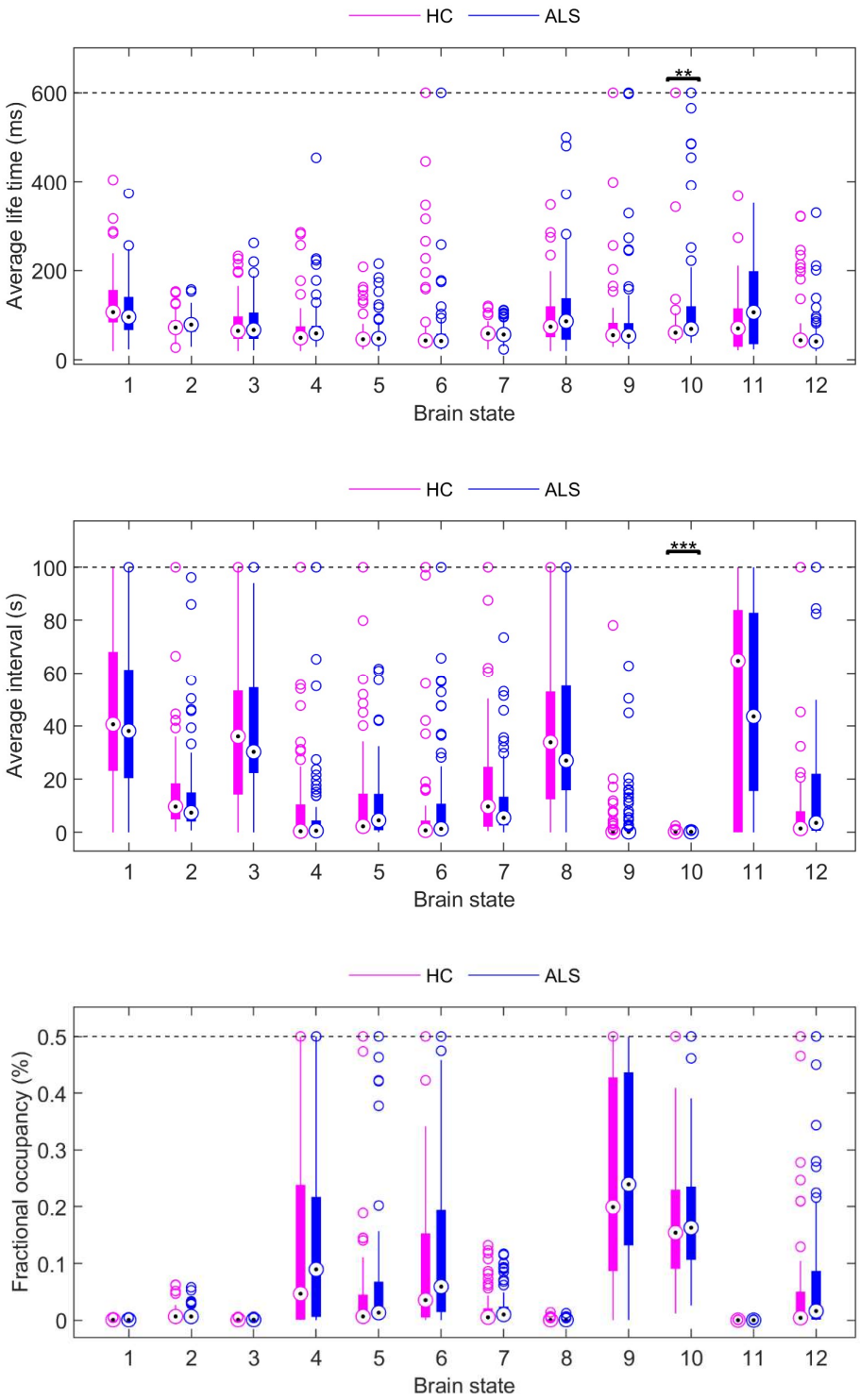

Figure 24: Distinct temporal dynamics of brain states between the ALS and HC groups. Distribution of life times, intervals and fractional occupancy for each brain state. Effect sizes were moderate. A dotted line was added in case some outliers lied outside the scope to facilitate visualisation. Benjamini & Krieger FDR, q <0.1, was applied. $* p \leq .05$, $** p \leq .01$, $*** p \leq .001$.

3.3. Wideband distinct spectral measures across brain states

The neural activity and functional connectivity of the identified brain states exhibit distinct patterns. This is illustrated in Figure 25, where spectral measures (power and coherence), spanned across a wide frequency range (1-45Hz), are displayed for each state, relative to the average within-state. To enhance clarity, a mask highlighting values significantly higher or lower than the average within-state across participants has been applied.

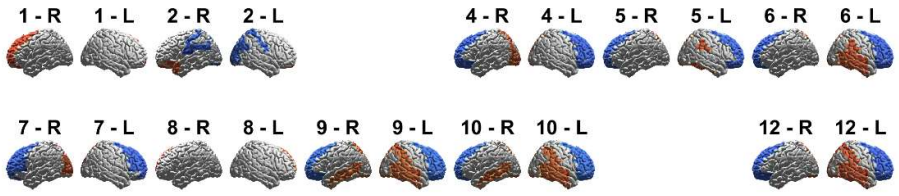

Figure 25: Spectral power in the twelve states resulting from the TDE-HMM model in the overall group (HC and ALS groups combined). The coloured areas correspond to areas of significant neural activation: red for higher and blue for lower than the average within-state. The TDE-HMM model captures distinct neural activation patterns in most of the states within the overall group. The lack of significant neural activity in states 3 and 11 may indicate that these states rely more on the functional connectivity between different brain regions than localised activation. Benjamini & Hochberg FDR was applied (q<.01).

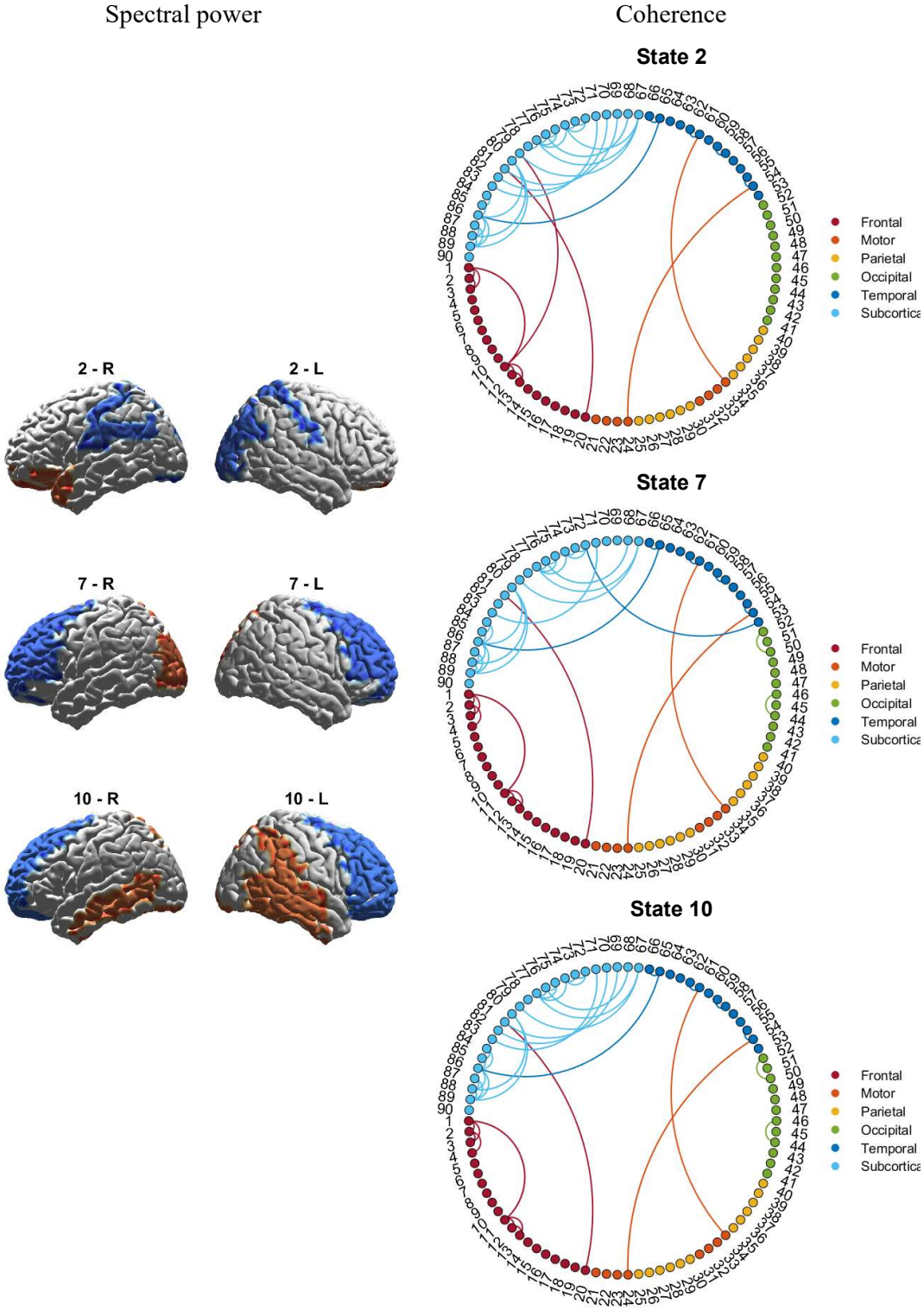

Figure 26: Significant spectral power and functional connectivity for states 2, 7 and 10. In terms of spectral power, the color scheme differentiates higher values in red from lower ones in blue, both relative to the within-state average. Concerning functional connectivity, we focus on connections that are not only significantly above the within-state average, but also limit the display to the top 1% of these

to facilitate visualisation. Benjamini & Hochberg FDR was applied (q<.01).

Examining states 2, 7, and 10, Figure 26 visualises neural activity that significantly deviates from the average within-state activity. In this figure, higher activity is denoted in red, while lower activity is indicated in blue.

State 2 exhibits activation within the inferior frontal region, possibly indicating a connection with the ventral attention network. In State 7, significant activation is mainly observed in the occipital area, implying activation of the visual network. State 10 demonstrates activation in regions corresponding to the posterior default mode network, including the bilateral posterior cingulate cortex and precuneus (Table 8).

Table 8: Summary of the brain regions showing significant neural activity (spectral power) in each state of interest in the combined healthy controls and ALS group. Each state is characterised by distinct significant higher neural activity in some brain regions relatively to the average neural activity within-state (non-parametric statistical testing, q<.01). The brain regions listed, suggest association of brain states 2, 7 and 10, respectively with the ventral attention network, the visual network and the posterior default mode network.

State 2 Ventral attention network	**State 7** Visual network	**State 10** Posterior default mode network
Rectus L/R	*Precuneus R*	*Precuneus L/R*
Frontal Sup Orb L	*Occipital Sup L*	*Parietal Inf R*
Frontal Inf Orb L	*Occipital Mid L*	*SupraMarginal R*
Temporal Pole Sup L	*Cuneus L*	*Occipital Inf L*
Temporal Pole Mid L		*Calcarine L/R*
Olfactory L/R		*Lingual L/R*
		Fusiform L/R
		Temporal Mid L/R
		Heschl R
		Temporal Sup R
		Temporal Inf R
		Cingulum Mid L
		Cingulum Post L/R

Regarding functional connectivity, the patterns are remarkably consistent across the three states of interest (as depicted in Figure 26). In each instance, there is a tendency of high functional connectivity within subcortical areas. In addition to this, our observations revealed that state 10 had lower spectral power and total coherence when compared to state 2 (ventral attention network) and 7 (visual network) (Figure 27). Overall, the spectral power demonstrated largest differences between states than the coherence.

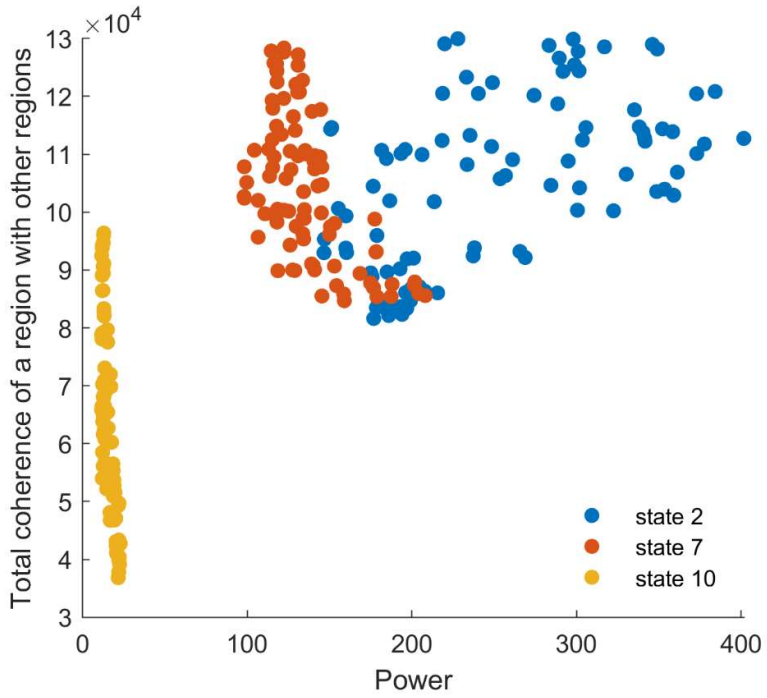

Figure 27: Separability of states 2,7 and 10 in relation to power and coherence. The total coherence of a given region with all the others regions in relation to power is observed, across three states of interest. Within the broad frequency range of 1-45 Hz, it is within the spectral power domain that the most pronounced differences emerge among states 2, 7, and 10.

4. Discussion

The study examined dynamical patterns of brain states in individuals with ALS compared to healthy controls. Through the application of a data-driven TDE-HMM method combined with a multiple autoregression, twelve distinct transient and recurring brain states were identified in the combined ALS and HC group, which were characterized by unique patterns of spectral power and coherence. Brain state activation probabilities over time were obtained for each participant.

The average duration of brain states was 98.7 ms, which is in the same magnitude as the average duration of the transient and recurring states observed at sensor level (see Chapter VII for more details). The observations of brain state dynamic on a milliseconds timescale are consistent with those of EEG microstate and fMRI resting-state networks (Damoiseaux et al., 2006; Khanna et al., 2015). Collectively, they endorse an emerging understanding of brain function based on a limited set of networks being activated in sequence to coordinate brain activity.

While these recurring brain patterns have been majoritively observed during periods of rest, they have also been reported during task-based MEG (Vidaurre, Abeysuriya, et al., 2018).

The fractional occurrence observed per states (Figure 24) raises the question of whether the actual number of states is fewer than 12, given that approximately four states demonstrated low fractional occurrence. This consideration highlights the need for further analyses evaluating the stability and generalisability of the identified states, possibly suggesting that the true number of distinct states might be lower than initially presumed.

A key finding arised when comparing the temporal dynamics of these brain states between the ALS and HC groups. Analysis of the timecourses provided various temporal properties, including the duration of state occurrences, intervals between occurrences, fractional occupancy, and switching rates. Figure 24 represents the distributions of these properties for each state within the two groups. ALS patients showed considerably extended durations of brain state 10 compared to the HC group. Furthermore, individuals with ALS demonstrated reduced gaps between occurrences of state 10, as shown by the shorter time intervals between the occurrences of state 10. No significant differences were observed in switching rates or fractional occupancy between the ALS and HC groups. While the temporal properties of brain state 10 differ between the two groups, other aspects of state dynamics remain similar.

Moving on to the analysis of wideband distinct spectral measures across brain states, the study revealed that these identified brain states exhibited unique neural activity and functional connectivity patterns. Figure 25 visually presents significant neural activity, across a broad frequency range (1-45Hz), for each state, relative to the average within-state. A closer examination of states 2, 7, and 10 is depicted in Figure 26. This visualization shows neural activity and functional connectivity that significantly differs from the average within-state measure. State 2 was linked to the ventral attention network. In contrast, State 7 displays significant occipital lobe activation, suggesting an association with the visual network. State 10, which showed significantly different temporal properties between ALS and HC groups, exhibits activation in areas aligning with the posterior default mode network.

The distinct patterns in neural activity across the identified states suggest a connection with specific functional neural networks. By decomposing EEG source-reconstructed timecourses, recurring functional networks can be identified, that align with fMRI resting-state networks, including the visual or default mode networks. These preliminary findings show potential to link ALS domains of impairment with the disruptions of these specialised functional networks, similar to what has been accomplished for neuropathic pain or major depression (Fauchon et al., 2022; Zhang et al., 2022). These associations would enhance our comprehension of the

fundamental neural processes impacted by ALS, and might offer potential targets for therapeutic interventions.

In terms of functional connectivity, a consistent pattern emerged across the three states of interest (as seen in Figure 26), characterized by high connectivity within subcortical areas. The eventual lack of reliability of subcortical signals reconstruction may represent a limitation to the present study. This area is susceptible to higher uncertainties (Barzegaran & Knyazeva, 2017), which calls for careful consideration when interpreting its role within the identified states. Although the current study did not utilize any of the following methods – higher-density electrodes (256-channels), participant-specific MRI headmodel, or Finite Element Model reconstruction – which could potentially enhance the accuracy of deep source localization (Piastra et al., n.d.; Seeber et al., 2019; Van Den Broek et al., 1998), their implementation could result in improved outcomes. The observed prevalence of subcortical functional connectivity in our brain states (Figure 26) could be attributed to an excessive assignement of neighboring regions' sources to subcortical areas. Exploring model variations when excluding the subcortical region, as applied by precedent studies (Fauchon et al., 2022; Vidaurre, Hunt, et al., 2018), could provide a clearer perspective on its contribution.

Additionally, differences among the states of interest were more pronounced in spectral power compared to coherence, as evident from Figure 27. This distinction emphasizes the importance of spectral power in delineating the brain states. Furthermore, the relationship between changes in coherence and changes in power warrants attention. Since power dynamics could influence changes in coherence to some extent (Guevara & Corsi-Cabrera, 1996), modelling the data based solely on changes in power may represent an interesting complementary option.

Further analyses are required to confirm the reproducibility of the identified states. Additionally, the potential coexistence of multiple networks, which would only be distinguishable at slower time scales, prompts caution against oversimplification. Alternative representations of the data could exist.

5. Conclusion

In conclusion, the examination of the identified brain states offers valuable insights into their temporal differences in ALS and HC groups, and the distinct neural networks they reflect. This study demonstrates altered properties of functional networks in ALS. Acknowledging the limitations of reproducibility, subcortical involvement, and potential alternative data representations, this study paves the way for a deeper understanding of ALS-related disruptions

in neural networks and their implications for clinical applications, by investigating the relationship between alterations in EEG signals and specific functional domains in ALS.

IX. Discussion

This chapter provides a comprehensive overview and interpretation of the findings, discusses how these results are relevant for understanding and quantifying cognitive impairment in ALS, acknowledges the limitations of the project, and outlines future research directions.
Section 1 offers a condensed summary of the results. Section 2 elaborates on the benefits of using resting-state EEG measures to monitor dysfunction in cognitive networks among ALS patients. In section 3, we explore the potential implications and clinical applications of this research. The limitations of this study are outlined in section 4, and section 5 outlines prospective work that can extend the impact of this project. Finally, section 6 provides a concise conclusion regarding the entire thesis.

1. Summary of the result chapters

1.1. Longitudinal neural activity and functional connectivity results

In this project, up to five recordings of resting-state high-density EEG signals were conducted from individuals diagnosed with ALS. Prior to this study, our research team had already characterised altered functional connectivity in ALS patients at the sensor level, which persisted longitudinally (Nasseroleslami et al., 2019). The team had also identified cross-sectional alterations in spectral measures at source level (Dukic et al., 2019). Building upon this foundation, the current project started with a longitudinal analysis of the resting-state signals after source reconstruction.

1.1.1. Longitudinal neural activity changes in subgroups with distinct neuropsychological profiles

This study revealed significant longitudinal alterations in neural activity within the fronto-temporal region. These changes manifest as a decline in lower frequency (θ-band) and an increase in higher frequency (γ-band) spectral power. To delve deeper into the potential relationship between these longitudinal frontotemporal changes and cognitive or behavioural impairments, I investigated distinct categories of individuals with ALS, each characterised by specific cognitive and behavioural profiles.

In the ALSci subgroup, referring to individuals with ALS and cognitive impairment, we observed a widespread increase in co-modulation of brain activity over time. This increase showed a strong correlation with cognitive decline (correlation coefficient $|\rho| > 0.5$, statistical power $1\text{-}\beta > 0.8$). Within the ALSbi subgroup, which represents individuals with ALS and behavioural impairment, we found that higher rates of change in fronto-parietal co-modulation of brain activity were associated with increased rates of change in behaviour as reported by BBI scores (correlation coefficient $|\rho| = 0.4$, statistical power $1\text{-}\beta = 0.9$).

In the ALSncbi subgroup, which comprises individuals with ALS but without cognitive or behavioural impairment, there was a widespread decrease in β-band synchrony over time and we also observed a correlation between motor decline and changes in neural activity (correlation coefficient $|\rho| = 0.4$, statistical power $1\text{-}\beta > 0.8$).

In all subgroups, survival was strongly associated with the rate of changes in functional connectivity between specific brain regions (correlation coefficients $|\rho| > 0.5$, statistical power $1\text{-}\beta > 0.9$).

These longitudinal findings within various ALS subgroups provide valuable insights into the heterogeneity of ALS progressions.

1.1.2. Longitudinal neural activity patterns in ALS: a data-driven analysis

Cognitive phenotypes in ALS were characterised by distinct longitudinal changes of functional network disruptions. I further explored whether a data-driven classification of these longitudinal neural activity trajectories corresponds to the clinical profiles. The clustering results showed statistical significance and exhibited high levels of robustness and consistency, suggesting that our findings can be reproduced.

While examining longitudinal neural activity patterns, distinct clusters were identified, indicating consistent trajectory patterns across various subgroups of ALS patients. Specifically, three stable clusters were observed in the δ-band, two in the α-band, five in the β-band, and three in the γ_h-band.

Additionally, distinct patterns of significant neural activity progression were observed among the different ALS subgroups identified. In the β-band, one cluster displayed a significant temporal activity decrease over time. In the α-band, one cluster, labelled cluster 1, exhibited a

notable decrease in temporal activity, while another, labelled cluster 2, demonstrated an increase in central/parietal activity.

Except for α-band cluster 2, most subgroups exhibited a decreasing spectral power in lower frequency bands and an increasing spectral power in higher frequencies, specifically in the γ-band. As explained in section 1.1.1, I observed a longitudinal decrease in θ-band spectral power and an increase in γ-band spectral power within the overall ALS group.

The analysis of clinical profiles using functional scores revealed additional distinct characteristics of α-band Cluster 2 compared to the other α-band cluster. Notably, significant differences in survival were observed, with Cluster 1 having the longest average survival of 9.4 years and Cluster 2 the shortest at 3.4 years. Additionally, these two clusters showed significant differences in the longitudinal decline of subscores. Furthermore, Cluster 2 exhibited a faster decline in all four ALSFRS-R functional subscores (related to upper limbs, lower limbs, bulbar, and respiratory symptoms) when compared to Cluster 1.

These results highlight the heterogeneity within ALS and the importance of examining the long-term patterns of neural activity in specific subgroups of ALS patients. Longitudinal neural activity patterns can offer valuable insights into how the disease advances, affects survival and leads to functional deterioration.

1.2. Decomposition of EEG signals into recurring, transient brain states

Despite demonstrating abnormal spectral measures in both sensor and source space, which persisted longitudinally, there remains a limited understanding of the temporal dynamics of brain networks in ALS.

i. Sensor-space patterns

Analysing brain microstates, as discussed in Chapter II, offered us insights into the temporal dynamics of brain networks by identifying transient, recurring and quasi-stable electric field configurations known as microstates within EEG recordings. Our results indicated that the properties of EEG microstates can offer valuable insights into the prognosis of ALS, particularly in terms of the extent of cognitive deterioration over time.

Differences in the standard properties (coverage, occurrence and duration) of microstate classes A, B, and D were observed between the ALS and control groups. Based on paradigm-based

and source localisation studies, alterations of the properties of those specific microstates potentially indicate dysfunction within the somatosensory and attention networks.

There were also notable differences in microstate transitions between the ALS and control groups, suggesting alterations in the usual fluctuations of neural activity in ALS. Furthermore, our study showed that as ALS progresses, there are further changes in neural dynamics, evident in the longitudinal alterations in the standard properties of microstates and their temporal dependencies. Participants in the late stages of the disease displayed greater symmetry and stability in their transition matrices, which could signify reduced neuronal adaptability, indicating less dynamic switching between brain microstates.

Lastly, our examination of the correlations between microstate properties and ALS clinical measures (ALSFRS-R, ECAS, BBI) revealed that a longer duration of class B and a faster increase in class C coverage over time are linked to a slower decline in gross motor skills in ALS (correlation coefficients $|\rho| = 0.3$, statistical powers $1-\beta = 0.8$). In patients with cognitive and behavioural impairments, lower transition probabilities from A to D, C to B, and C to D are specifically associated with cognitive decline (correlation coefficients $|\rho| > 0.3$, statistical powers $1-\beta > 0.75$).

These findings suggest that microstate properties have substantial potential as prognosis biomarkers for ALS and in particular for cognitive impairment in ALS.

ii. Source-space patterns

EEG microstates, revealed changes, with potential prognosis value, in functional brain network dynamics in ALS, at sensor level. Investigating the precise brain sources from which these microstates originate could deepen our understanding of the neurophysiological mechanisms behind them which are disrupted in ALS. However, exploring the brain regions generating these microstates presented challenges, widely discussed in the literature, notably due to a possible continuous nature of the microstate.

We, therefore, opted for an alternative approach, which consisted of a direct examination of spectral patterns within brain networks, based on a combined HMM and multivariate autoregression approach.

Dynamic brain state patterns were examined in a combined ALS and HC group, identifying twelve distinct transient and recurring brain states with unique spectral power and coherence patterns. These states had an average duration of 98.7 ms, consistent with previous findings in EEG microstate and fMRI resting-state networks. ALS patients showed extended durations and reduced intervals for brain state 10, while other state dynamics remained similar. Spectral measures across states revealed unique neural activity and functional connectivity patterns, linking specific states to functional neural networks, potentially shedding light on ALS domains of impairment. In particular, state 10, characterised by differences in its temporal characteristics between the ALS and HC groups, demonstrated activation in regions corresponding to the posterior part of the default mode network.

Although additional analyses are necessary, this particular project serves as a proof of concept, demonstrating the importance of dynamic analyses in investigating disruptions within neural networks linked to ALS. These findings could hold clinical significance by revealing how alterations in EEG signals are connected to specific functional aspects of ALS.

2. Advantages of the new resting-state EEG measures to track cognitive networks dysfunction in ALS?

Detecting cognitive or behavioural impairments in individuals with ALS can pose significant challenges, primarily because they frequently rely on input from caregivers for identification. Nevertheless, these changes can be observed and measured, albeit with some limitations. Cognitive assessments are influenced not only by an individual's educational background but also by the degree of fatigue they may experience, which can be exacerbated due to other ALS symptoms. On the other hand, evaluating behavioural changes can be somewhat subjective, which in the past led to the dismissal of their significance in the context of ALS (C. Crockford et al., 2018; Pender et al., 2020). Recognizing these issues, there is a growing recognition of the need for more comprehensive assessments aimed at quantifying cognitive and behavioural impairments in ALS cases.

2.1. Progressions of resting-state EEG measures over time

EEG can be recorded using resting-state EEG or event-locked EEG. In this study, we exclusively concentrate on whole-brain resting-state EEG, which monitors brain activity when

a participant is awake without involvement in a particular task or response to stimuli. The benefits of using resting-state EEG were elaborated upon in Chapter II, Section 1.2.

In the ALS group, neural activity was observed to decrease over time in the lower frequency band (θ-band), while it increased in higher frequency bands (γ-band). These findings were consistent with the reduced spectral power observed in individuals with ALS compared to healthy controls in lower frequency bands ranging from θ to β (Dukic et al., 2019). When looking at the data from a cross-sectional perspective, a trend toward increased γ-band power, which falls into the higher frequency range, was also noted.

In the ALSci subgroup, characterized by cognitive impairment, the observed increase in brain activity co-modulation over time was not only widespread but also strongly correlated with cognitive decline (correlation coefficients: $0.5 \leq |\rho| \leq 0.7$). Similarly, in the ALSbi subgroup, which comprises individuals with behavioural impairment, the study found a notable association between changes in fronto-parietal co-modulation of brain activity and alterations in behaviour, as measured by BBI scores (correlation coefficient: $|\rho| = 0.4$). These findings reinforce the link between EEG spectral measures and the cognitive and behavioural symptoms in individuals with ALS. In conclusion, this study sheds light on the heterogeneity of ALS progressions by revealing distinct neural activity patterns and their associations with cognitive and behavioural impairments within different subgroups of ALS patients.

2.2. Dynamical analyses: sensor versus source space

2.2.1. Sensor-space: association of microstate properties with cognitive decline

While functional connectivity has shown promise as a biomarker for ALS, with supporting evidence from both sensor and source-space analyses as well as longitudinal studies (Dukic et al., 2019; Nasseroleslami et al., 2019), our understanding of the temporal dynamics of brain networks in ALS remains limited. To gain deeper insights into the alterations in temporal dynamics caused by ALS, we have examined brain microstates, as detailed in Chapter VIII. These microstates are transient configurations of the electric field, detected at the sensor level, which exhibit repetitive patterns.

Alterations in the properties of specific microstate classes may be indicative of dysfunction within somatosensory and attention networks in ALS patients. This is a significant finding, as it links EEG microstate changes to specific neural networks that are known to be affected in

ALS. Among other processes, the attention network plays a pivotal role in sustaining attention over time. In individuals with ALS, alterations in the brain regions responsible for sustaining attention were observed. Notably, changes in the activity of the inferior parietal lobule and insular regions showed strong discriminatory power (AUC > 0.75) in distinguishing between individuals with ALS and HC (McMackin et al., 2020).

Additionally, the associations between specific microstate transition probabilities and cognitive decline in individuals with ALS and cognitive-behavioural impairments (correlation coefficients $|\rho| > 0.3$) underscore the potential utility of EEG microstates in predicting cognitive outcomes in this population.

2.2.2. Source-space: alterations in the temporal dynamics of functional brain networks

EEG microstates offer a method to decompose intricate and constantly shifting EEG signals into distinct and understandable patterns. These patterns are based on stable electric field configurations that persist for a very short period, typically around 80-100 milliseconds.

Similar rapid fluctuations in patterns of neural activity and functional connectivity in source space have been observed (Tewarie et al., 2019; Vidaurre et al., 2016). While functional networks have been extensively studied using fMRI, the lower temporal resolution of fMRI signals may obscure the detection of neuronal interactions occurring at faster timescales. To address this limitation, dynamical analyses conducted in source space provide a promising avenue for exploring the impact of ALS on various functional networks (Vidaurre, Hunt, et al., 2018). These networks encompass areas relevant to cognition, sensorimotor processing, visual processing, and the default mode network. Although direct connections between specific brain states and cognitive functioning in ALS have not been definitively identified, the application of dynamic analyses represents a valuable approach for evaluating disruptions within these networks. Cognition is hypothesised to depend more on the dynamic changes of synchrony between signals than the synchrony itself (Breakspear et al., 2004). By further examining the dynamic interactions, we could uncover subtle changes that may underlie cognitive impairments and other neurological symptoms associated with ALS.

2.3. Machine learning for the assessment of prognostic biomarkers and the stratification of the ALS group into subcategories

Machine learning (ML) and nationwide databases provide unique opportunities to evaluate potential biomarkers, especially in the context of diseases like ALS, where ML can help identify meaningful EEG patterns that may serve as biomarkers for diagnosis, prognosis, monitoring, or prediction (Bede, 2017; Grollemund et al., 2019). In a recent systematic analysis conducted by Fernandes et al. (Fernandes et al., 2021), they examined 18 articles that assessed the efficacy of ML algorithms applied to biomedical signals (EMG, EEG, gait rhythm and MRI) for tasks such as ALS diagnosis/classification (72%), survival prediction (6%), and communication intermediation (22%). The study revealed consistent improvements in various models, achieving high accuracy rates, ranging from 71% to 100%, and, when reported, high levels of specificity and sensitivity (>90%). These results underscore the potential of machine learning to address critical inquiries in ALS. All the studies included in this review employed supervised machine learning methods, which involve training a model based on labelled data, as opposed to unsupervised methods which seek to uncover patterns or structures without specific target labels.

2.3.1. Supervised vs. unsupervised learning

Supervised learning includes classification, where models categorize features into predefined groups, and regression, where models predict continuous outcomes by establishing mathematical relationships between predictors and target variables (Hosseini et al., 2021). For instance, neuroimaging measures have been classified into ALS or other disease categories (Bede et al., 2021). In contrast, regression models, such as those used in ALS prognosis, utilize longitudinal EEG spectral data to forecast changes and link them to clinical observations (Chapter VI).

On the other hand, unsupervised learning holds promise in the context of ALS, addressing the disease's heterogeneity not fully captured by clinical assessments. It can aid in patient stratification by revealing novel data patterns, providing researchers with novel insights. Unsupervised learning can also reduce the reliance on large, well-labeled datasets. For example, clustering algorithms can be applied to study longitudinal EEG spectral patterns (Chapter VI) or temporal dynamics in EEG signals (at sensor or source levels) (Chapter VIII,

Chapter IX). However, further development is required to demonstrate the generalisability and performance of unsupervised methods.

2.3.2. Overfitting

In machine learning, a common challenge is overfitting, which occurs when a model becomes too focused on the training data, capturing even the noise and random fluctuations instead of just the underlying patterns. This results in a model that excels on the training data but performs poorly on new, unseen data. To detect overfitting, it is crucial to evaluate the model on data that has not been seen before, such as through cross-validation. While underfitting is a concern because it inadequately represents the data, overfitting poses a significant problem. An overfit model may seem like a perfect fit for the training data but fails to generalise effectively. The key to addressing this challenge lies in finding the right balance between model complexity, which reduces bias and prevents underfitting, and the model's ability to perform well on new, unseen data, which reduces variance and prevents overfitting (Grollemund et al., 2019). To mitigate overfitting, various techniques are employed, including regularisation and dimensionality reduction. Additionally, increasing the amount of training data available can also reduce the risk of overfitting. Dataset size is a critical factor that can significantly impact the performance and effectiveness of a model. In general, larger datasets tend to yield better model performance, as they provide more information for the model to learn from.

Obtaining a sufficiently large number of EEG recordings from individuals with ALS for ML modelling is challenging due to potential participant discomfort and time constraints. Despite promising results seen in EEG modelling studies, notably in the field of epilepsy (Abbasi & Goldenholz, 2019), sample size remains a common limitation.

3. Impact on treatment development and disease understanding

3.1. Unraveling the Complexity of ALS: Insights from longitudinal cortical activity and altered temporal dynamics

3.1.1. Progression of ALS: Insights from longitudinal changes in cortical activity

The longitudinal studies, described in this thesis, revealed neural activity progressions in the fronto-temporal areas in individuals with ALS, highlighting the importance of recognising changes in non-motor regions. This observation aligns with the notion that ALS does not solely impact motor pathways, but involves a broader neural involvement (De Marchi et al., 2021;

Dukic et al., 2019; Nasseroleslami et al., 2019). Fronto-temporal brain regions are particularly relevant in conditions like frontotemporal dementia (FTD), where degeneration in these areas leads to progressive cognitive and behavioural decline. The left frontal and temporal lobes (Broca's and Wernicke's areas), particularly, are integral to language comprehension and production. Damage to these regions may explain why fluency deficits are the most common form of cognitive impairment observed in ALS (Abrahams et al., 2000). A Japanese research group specifically associated decreased functional connectivity in the lingual/fusiform gyrus and increased connectivity in the left temporal gyrus with semantic deficits (Ogura et al., 2019).

Furthermore, within ALS subgroups, distinct progressions emerge, particularly in individuals with cognitive-behavioural impairments, emphasizing the relevance of considering neuropsychological factors when assessing cortical activity changes.

Interestingly, variations in neural activity patterns extend beyond neuropsychological characteristics, suggesting a multifaceted nature of ALS progression, as reported in Chapter VI and previously by Burgh et al. (Burgh et al., 2020). Specific groupings (or clusters) were observed that pointed to consistent trajectory patterns among different subsets of individuals with ALS. Notably, while most lower frequency band neural activities exhibited a decline, consistent with cross-sectional findings compared to healthy controls (Dukic et al., 2019), a noteworthy exception was observed in one α-band cluster, where activity in sensorimotor networks displayed an increase. These distinct findings highlight the complexity of ALS and the need for further investigation into the neurobiology of its heterogeneous presentation.

3.1.2. Altered temporal dynamics

The findings regarding differences in microstate transitions between individuals with ALS and control groups represent a step forward in understanding the neurobiology of ALS. These results suggest that ALS disrupts not only cortical activity and functional connectivity but also the typical patterns of neural activity fluctuations, which are hypothesised to be crucial to the organisation and adaptability of the functional networks of the brain (Van der Ville, 2010). The association of altered microstate classes with both sensory and higher-order cognitive networks reflects the complex clinical presentation of ALS. Furthermore, individuals in the late stages of ALS displayed greater symmetry and stability in their transition matrices. This finding suggests that as the disease advances, the brain becomes less capable of dynamically switching between different transient microstates.

Moreover, the study presented in Chapter IX brought to light the dynamic changes occurring in the posterior Default Mode Network (DMN), a functional network typically associated with resting state activity. The observation of temporal alterations within the DMN dynamic adds a dimension to our understanding of ALS. While resting state activity in this network is a common finding, the documented changes further demonstrate the broader impact of ALS on functional networks, extending beyond the sensorimotor domains. These findings emphasize that ALS has far-reaching consequences on brain network dynamics.

3.2. Treatment development: Potential prognosis biomarkers

Several key requirements must be met to obtain reliable biomarkers, while balancing these considerations with the practical aspect of clinical trial accessibility, particularly in terms of ease of use. Firstly, accuracy is paramount, demanding precision and dependability in measurement. Secondly, sensitivity and specificity, often interlinked, must be rigorously evaluated. Sensitivity reflects the ability of a biomarker to correctly identify true positive cases, while specificity gauges its capacity to accurately rule out true negatives. Striking the right balance between these two attributes is crucial to prevent false positives or negatives. Additionally, validation procedures should be conducted to assess reproducibility (Benatar et al., 2016).

3.2.1. Validation of resting-state EEG spectral measures as potential prognostic biomarkers

Previous research had identified increased co-modulation and decreased synchrony in both motor and non-motor networks as potential biomarkers due to their strong performance with an AUC greater than 0.7 (Dukic et al., 2019). However, it was crucial to further validate these findings. In Chapter V, we delve into the alignment between cross-sectional observations and the longitudinal progression of EEG spectral measures in individuals with ALS. Notably, we found that the decrease in spectral power in lower frequency bands and the concurrent increase in higher frequency band power were consistently observed over time. Similarly, the widespread increase in co-modulation, particularly in the β-band, persisted longitudinally. However, the decrease in synchrony observed in the cross-sectional analysis was only consistently observed longitudinally in the ALS subgroup without cognitive or behavioural impairment.

3.2.2. Stratification of individuals with ALS based on resting-state EEG measures

Differential progression of spectral EEG measures among ALS subgroups with distinct neuropsychological profiles was demonstrated (Chapter V). This divergence in the progression of EEG measures strongly implies the presence of underlying neurophysiological factors contributing to the heterogeneity of symptom progression seen in ALS. Furthermore, the association between functional connectivity, particularly the co-modulation of source-reconstructed EEG signals, and clinical measures of cognitive impairment highlights the potential of EEG-based biomarkers to capture cognitive network dysfunction in ALS (correlation coefficients: $0.5 \leq |\rho| \leq 0.7$). The ALSncbi subgroup, consisting of ALS patients without cognitive or behavioural impairment, displayed a distinct pattern of decreasing β-band synchrony over time. This subgroup exhibited a correlation between motor decline and neural activity changes (correlation coefficient $|\rho| = 0.4$), emphasizing the relevance of motor-related neural alterations in the absence of cognitive or behavioural symptoms. One overarching finding across all subgroups was also the strong association between survival and the rate of changes in functional connectivity between specific brain regions (correlation coefficients $|\rho| > 0.5$). This underscores the critical role of neural network dynamics in influencing disease progression and prognosis.

Prior research similarly demonstrated that cross-sectional EEG spectral measures can be used to classify individuals with ALS in subgroups, likely to represent subphenotypes of the disease (Dukic et al., 2022). The stable and robust classification of EEG spectral power progressions over time, as discussed in Chapter VI, allowed us to identify ALS subgroups that exhibited distinct survival and motor decline patterns. This suggests that EEG-based biomarkers can be valuable for stratifying patients and predicting their disease trajectories. A similar data-driven analysis of EEG co-modulation (which showed the strongest association with cognitive decline) may lead to the identification of ALS subgroups that align with clinically established neuropsychological profiles. This potential alignment between neuroelectrophysiological and neuropsychological characteristics could offer a more comprehensive understanding of the disease and further enhance the utility of EEG-based biomarkers in monitoring cognitive and behavioural symptoms in ALS.

Collectively, these findings indicate that resting-state EEG spectral measures hold promise as valuable prognostic biomarkers of cognitive and behavioural impairment in ALS. They may

enable clinicians to anticipate the progression of ALS and adjust treatment plans accordingly, ultimately improving patient care and resource allocation in clinical practice. Integrating EEG data into clinical trial protocols may provide valuable insights to assess their potential as predictive and monitoring biomarkers.

3.2.3. New biomarker of cognitive-behavioural impairment candidates based on dynamic analysis of resting-state data

Based on dynamic analysis, several novel biomarker candidates have been identified which display excellent discrimination of individuals with ALS from controls and were specifically associated with cognitive-behavioural impairment. Notably, based on the four canonical categories of microstates, which are labelled A to D. Microstate classes C and D have been linked to higher cognitive networks rather than somatosensory networks. Specifically, class C is associated with self-reflection or 'self-referential internal mentation' (Tarailis et al., 2023), while class D is associated with the attention network. In our study, we observed a reduction in the duration of class D microstates, with an area under the curve (AUC) of 0.6, in individuals with ALS in comparison to HC.

Moreover, in patients who exhibited cognitive and behavioural impairments, we found that lower transition probabilities from class C to class D (TP CD) were associated with cognitive decline (correlation coefficient $\rho = 0.4$). Similarly, lower TP CD values were also detected in individuals with ALS compared to HC, with an AUC greater than 0.7. This suggests the potential utility of TP CD as a novel biomarker for identifying cognitive impairment in ALS.

4. Limitations

4.1. Potential non-random attrition

The attrition rate is a concern in ALS research, particularly in longitudinal studies, as it can introduce bias. Individuals who discontinue their participation in the study may not accurately represent the original study group, resulting in a non-random loss of participants. Rapidly progressing disease symptoms can contribute to participant attrition. When examining cognitive and behavioural impairments, impairment such as apathy, may also lead to dropouts. The potential impact of this bias was discussed in the context of our longitudinal findings, specifically in Chapters V and VI.

4.2. Potential limitations in cognitive and behavioral assessments

In studies focused on cognitive and behavioural impairment in ALS, it is crucial to consider the impact of practice effects and measurement bias. The ALS group participating in EEG recordings largely does not exhibit cognitive impairment (~80%). Consequently, their performance reflects an average response to practice effects, but incorporating normative data from healthy controls would enhance precision.

Additionally, ALS patients often experience symptoms like fatigue and motor or respiratory issues that can mimic cognitive impairment. To obtain a more accurate assessment of cognitive and behavioural impairment, a comprehensive neuropsychological battery is necessary, as screening tests like ECAS or BBI are designed for quick assessments. However, currently, this comprehensive battery is exclusively administered when suspicions arise regarding cognitive or behavioural issues. The selective use of these extensive data for some participants alone has the potential to introduce outcome measurement bias. Therefore, we opted to use consistent measures for all participants to minimise the risk of bias.

4.3. Data sparsity

EEG data from 121 individuals with ALS and 81 HC represent enough data for statistical comparison analyses and even sufficient sample size for most ML models. However, ALS subphenotypes such as ALS-FTD or ALS with thoracic onset are not well represented in our dataset. Multicenter protocols and international collaborations could solve this issue, while also demonstrating replicability between centers.

Moreover, the curse of dimensionality implies that the complexity and challenges of working with high-dimensional data spaces become increasingly problematic as the number of dimensions (features or variables) grows. As the dimensionality increases, the amount of data required to adequately represent the space also increases exponentially, which can lead to data sparsity and difficulties in finding meaningful patterns. This curse makes tasks like clustering, classification, and regression more computationally intensive, often requiring larger datasets to maintain model accuracy and interpretability (Grollemund et al., 2019). In our case, when considering functional connectivity, for instance, the number of connections can be up to 90x90 in 6 frequency bands, which makes the number of features higher than the number of samples.

Dimensionality reduction techniques help to address this issue and extract relevant information from high-dimensional data. The computational power required remains high.

4.4. Computational power

The requirement for substantial computational power resulted in delays during the project based on the time-delayed embedded hidden Markov model (Chapter VIII). Recognizing that this model could not efficiently run on a standard workstation, I drafted a proposal to secure access to the high-performance computing resources at the Irish Centre for High-End Computing (ICheck). The later access to a high-performance workstation addressed the computational requirements, alleviating the delays.

5. Future work

5.1. Further longitudinal resting-state EEG data collection

As discussed in section 2.3, the sample size plays a pivotal role in machine learning analyses and remains a primary obstacle to establishing robust and validated biomarkers (Grollemund et al., 2019). The collection of longitudinal resting-state EEG data from individuals with ALS has been an ongoing effort both before and throughout this project, and it will be pursued. This continuous data collection is particularly crucial, given that ALS, and especially its subphenotypes like ALS-FTD, are relatively rare conditions.

Moreover, the acquisition of longitudinal RS EEG data from healthy controls is planned to ensure that any observed changes in the ALS population are not solely attributed to normal ageing. This additional data from HC subjects will serve as an additional means of validation, confirming the specificity of our findings in relation to ALS-related changes.

5.2. Clustering of the longitudinal progressions of functional connectivity

Our previous research has highlighted that the longitudinal increase in the co-modulation of EEG signals in individuals with ALS and cognitive impairment shows the most significant correlation with cognitive decline. Building on this insight, I plan to employ data-driven clustering analyses focused on co-modulation, akin to what we have previously done with spectral power. This approach holds the potential to uncover distinct subgroups within the ALS population, each associated with specific neuropsychological profiles. I intend to conduct an

in-depth examination of clusters formed by the longitudinal changes in co-modulation. This analysis aims to validate the belief that there are subgroups within the ALS population that exhibit unique patterns of co-modulation changes over time. By doing so, I hope to gain a deeper understanding of the relationship between EEG signal co-modulation, cognitive function, and the heterogeneity that exists within the ALS population.

5.3. Further analyses of dynamical patterns in ALS and other MND variants

In Chapter IX, we conducted a dynamic analysis of patterns in spectral power and functional connectivity, revealing timecourses of both transient and recurring functional networks. These networks exhibit striking similarities to well-established fMRI resting-state networks (Damoiseaux et al., 2006; Vidaurre et al., 2016; Vidaurre, Hunt, et al., 2018). Extending this analysis to other motor neuron disease variants, like primary lateral sclerosis characterized by dominant upper motor neuron impairment, or other neurological conditions affecting motor function such as multiple sclerosis or post-polio syndrome, could yield valuable insights. My plan involves leveraging existing databases collected by colleagues working on separate projects to investigate whether individuals with various MND variants or different neurological disorders display distinct temporal dynamics within their functional networks. This exploration will study nuanced differences in the spectral, temporal and spatial EEG patterns of these conditions.

6. Overall conclusion

In the context of ALS research, the identification of cognitive and behavioural impairments poses significant challenges, often relying on qualitative input. Recognizing the need for more comprehensive evaluations, this thesis focused on EEG measures to reveal neural activity patterns linked to cognitive-behavioural impairment in ALS.

The research demonstrated distinct longitudinal patterns of neural activity and functional connectivity within ALS subgroups exhibiting diverse neuropsychological profiles. Specifically, strong associations were established between cognitive-behavioural impairments in ALS and unique neural activity longitudinal patterns.

Additional patterns were observed at both the sensor and source levels, capturing temporal dynamics in EEG signals. These comprehensive approaches have not only deepened our understanding of ALS but have also revealed novel potential biomarker candidates.

I will further look into the clustering of functional connectivity patterns and extend my dynamic analyses to encompass other MND variants. By doing so, I aim to gain a more profound understanding of the alterations within the temporal dynamics of functional networks experienced by individuals affected by neurological conditions such as ALS, Primary Lateral Sclerosis (PLS), or others. Broadening the analysis beyond ALS to include other MND variants presents an opportunity to advance our understanding of the spectrum of motor neuron diseases, offering insights that are not only specific to each variant but also revealing commonalities that may inform clinical practice and therapeutic development.

In sum, these findings not only contribute significantly to our comprehension of ALS but also hold promise as prognostic biomarker candidates for cognitive and behavioural impairment. This advancement has the potential to greatly enhance patient care and facilitate progress in treatment development by providing reliable stratification of individuals with ALS.

X. Bibliography

Abbasi, B., & Goldenholz, D. M. (2019). Machine learning applications in epilepsy. *Epilepsia*, *60*(10), 2037–2047. https://doi.org/10.1111/epi.16333

Abrahams, S., Leigh, P. N., Harvey, A., Vythelingum, G. N., Grisé, D., & Goldstein, L. H. (2000). Verbal fluency and executive dysfunction in amyotrophic lateral sclerosis (ALS). *Neuropsychologia*, *38*(6), 734–747. https://doi.org/10.1016/S0028-3932(99)00146-3

Abrahams, S., Leigh, P. N., Kew, J. J. M., Goldstein, L. H., Lloyd, C. M. L., & Brooks, D. J. (1995). A positron emission tomography study of frontal lobe function (verbal fluency) in amyotrophic lateral sclerosis. *Journal of the Neurological Sciences*, *129*, 44–46. https://doi.org/10.1016/0022-510X(95)00060-F

Abrahams, S., Newton, J., Niven, E., Foley, J., & Bak, T. H. (2014). Screening for cognition and behaviour changes in ALS. *Amyotrophic Lateral Sclerosis and Frontotemporal Degeneration*, *15*(1–2), 9–14. https://doi.org/10.3109/21678421.2013.805784

Abreu, R., Jorge, J., Leal, A., Koenig, T., & Figueiredo, P. (2021). EEG Microstates Predict Concurrent fMRI Dynamic Functional Connectivity States. *Brain Topography*, *34*(1), 41–55. https://doi.org/10.1007/s10548-020-00805-1

Agarwal, S., Highton-Williamson, E., Caga, J., Howells, J., Dharmadasa, T., Matamala, J. M., Ma, Y., Shibuya, K., Hodges, J. R., Ahmed, R. M., Vucic, S., & Kiernan, M. C. (2021). Motor cortical excitability predicts cognitive phenotypes in amyotrophic lateral sclerosis. *Scientific Reports*, *11*(1), 2172. https://doi.org/10.1038/s41598-021-81612-x

Agarwal, S., Highton-Williamson, E., Caga, J., Matamala, J. M., Dharmadasa, T., Howells, J., Zoing, M. C., Shibuya, K., Geevasinga, N., Vucic, S., Hodges, J. R., Ahmed, R. M., & Kiernan, M. C. (2018). Primary lateral sclerosis and the amyotrophic lateral sclerosis–frontotemporal dementia spectrum. *Journal of Neurology*, *265*(8), 1819–1828. https://doi.org/10.1007/s00415-018-8917-5

Agosta, F., Ferraro, P. M., Riva, N., Spinelli, E. G., Chiò, A., Canu, E., Valsasina, P., Lunetta, C., Iannaccone, S., Copetti, M., Prudente, E., Comi, G., Falini, A., & Filippi, M. (2016). Structural brain correlates of cognitive and behavioral impairment in MND. *Human Brain Mapping*, *37*(4), 1614–1626. https://doi.org/10.1002/hbm.23124

Al Zoubi, O., Mayeli, A., Tsuchiyagaito, A., Misaki, M., Zotev, V., Refai, H., Paulus, M., Bodurka, J., Investigators, the T. 1000, Aupperle, R. L., Khalsa, S. S., Feinstein, J. S., Savitz, J., Cha, Y.-H., Kuplicki, R., & Victor, T. A. (2019). EEG Microstates Temporal Dynamics Differentiate Individuals with Mood and Anxiety Disorders

From Healthy Subjects. *Frontiers in Human Neuroscience*, *13*. https://doi.org/10.3389/fnhum.2019.00056

Al-Chalabi, A., & Hardiman, O. (2013). The epidemiology of ALS: A conspiracy of genes, environment and time. *Nature Reviews Neurology*, *9*(11), 617–628. https://doi.org/10.1038/nrneurol.2013.203

Al-Chalabi, A., Hardiman, O., Kiernan, M. C., Chiò, A., Rix-Brooks, B., & van den Berg, L. H. (2016). Amyotrophic lateral sclerosis: Moving towards a new classification system. *The Lancet Neurology*, *15*(11), 1182–1194. https://doi.org/10.1016/S1474-4422(16)30199-5

Bagdasarov, A., Roberts, K., Bréchet, L., Brunet, D., Michel, C. M., & Gaffrey, M. S. (2022). Spatiotemporal dynamics of EEG microstates in four- to eight-year-old children: Age- and sex-related effects. *Developmental Cognitive Neuroscience*, *57*, 101134. https://doi.org/10.1016/j.dcn.2022.101134

Bai, Y., He, J., Xia, X., Wang, Y., Yang, Y., Di, H., Li, X., & Ziemann, U. (2021). Spontaneous transient brain states in EEG source space in disorders of consciousness. *NeuroImage*, *240*, 118407. https://doi.org/10.1016/j.neuroimage.2021.118407

Baillet, S. (2017). Magnetoencephalography for brain electrophysiology and imaging. *Nature Neuroscience*, *20*(3), 327–339. https://doi.org/10.1038/nn.4504

Baldo, J. V., Schwartz, S., Wilkins, D., & Dronkers, N. F. (2006). Role of frontal versus temporal cortex in verbal fluency as revealed by voxel-based lesion symptom mapping. *Journal of the International Neuropsychological Society*, *12*(06). https://doi.org/10.1017/S1355617706061078

Balendra, R., Jones, A., Jivraj, N., Knights, C., Ellis, C. M., Burman, R., Turner, M. R., Leigh, P. N., Shaw, C. E., & Al-Chalabi, A. (2014). Estimating clinical stage of amyotrophic lateral sclerosis from the ALS Functional Rating Scale. *Amyotrophic*

Lateral Sclerosis & Frontotemporal Degeneration, *15*(3/4), 279–284. https://doi.org/10.3109/21678421.2014.897357

Barzegaran, E., & Knyazeva, M. G. (2017). Functional connectivity analysis in EEG source space: The choice of method. *PLOS ONE*, *12*(7), e0181105. https://doi.org/10.1371/journal.pone.0181105

Basaia, S., Agosta, F., Cividini, C., Trojsi, F., Riva, N., Spinelli, E. G., Moglia, C., Femiano, C., Castelnovo, V., Canu, E., Falzone, Y., Monsurrò, M. R., Falini, A., Chiò, A., Tedeschi, G., & Filippi, M. (2020). Structural and functional brain connectome in motor neuron diseases: A multicenter MRI study. *Neurology*, *95*(18), e2552–e2564. https://doi.org/10.1212/WNL.0000000000010731

Beasley, T. M., Erickson, S., & Allison, D. B. (2009). Rank-Based Inverse Normal Transformations are Increasingly Used, But are They Merited? *Behavior Genetics*, *39*(5), 580–595. https://doi.org/10.1007/s10519-009-9281-0

Bechtold, B. (2022). *Violin Plots for Matlab* [MATLAB]. https://github.com/bastibe/Violinplot-Matlab (Original work published 2016)

Bede, P. (2017). From qualitative radiological cues to machine learning: MRI-based diagnosis in neurodegeneration. *Future Neurology*, *12*(1), 5–8. https://doi.org/10.2217/fnl-2016-0029

Bede, P., & Hardiman, O. (2018). Longitudinal structural changes in ALS: A three time-point imaging study of white and gray matter degeneration. *Amyotrophic Lateral Sclerosis and Frontotemporal Degeneration*, *19*(3–4), 232–241. https://doi.org/10.1080/21678421.2017.1407795

Bede, P., Murad, A., & Hardiman, O. (2021). Pathological neural networks and artificial neural networks in ALS: Diagnostic classification based on pathognomonic

neuroimaging features. *Journal of Neurology*. https://doi.org/10.1007/s00415-021-10801-5

Beeldman, E., Raaphorst, J., Twennaar, M. K., Visser, M. de, Schmand, B. A., & Haan, R. J. de. (2016). The cognitive profile of ALS: A systematic review and meta-analysis update. *Journal of Neurology, Neurosurgery & Psychiatry*, *87*(6), 611–619. https://doi.org/10.1136/jnnp-2015-310734

Benatar, M., Boylan, K., Jeromin, A., Rutkove, S. B., Berry, J., Atassi, N., & Bruijn, L. (2016). ALS biomarkers for therapy development: State of the field and future directions. *Muscle & Nerve*, *53*(2), 169–182. https://doi.org/10.1002/mus.24979

Benatar, M., Wuu, J., McHutchison, C., Postuma, R. B., Boeve, B. F., Petersen, R., Ross, C. A., Rosen, H., Arias, J. J., Fradette, S., McDermott, M. P., Shefner, J., Stanislaw, C., Abrahams, S., Cosentino, S., Andersen, P. M., Finkel, R. S., Granit, V., Grignon, A.-L., … First International Pre-Symptomatic ALS Workshop. (2022). Preventing amyotrophic lateral sclerosis: Insights from pre-symptomatic neurodegenerative diseases. *Brain*, *145*(1), 27–44. https://doi.org/10.1093/brain/awab404

Bendotti, C., Bonetto, V., Pupillo, E., Logroscino, G., Al-Chalabi, A., Lunetta, C., Riva, N., Mora, G., Lauria, G., Weishaupt, J. H., Agosta, F., Malaspina, A., Basso, M., Greensmith, L., Van Den Bosch, L., Ratti, A., Corbo, M., Hardiman, O., Chiò, A., & Silani, V. (2020). Focus on the heterogeneity of amyotrophic lateral sclerosis. *Amyotrophic Lateral Sclerosis & Frontotemporal Degeneration*, *21*(7/8), 485–495. https://doi.org/10.1080/21678421.2020.1779298

Benjamini, Y., & Hochberg, Y. (1995). Controlling the False Discovery Rate: A Practical and Powerful Approach to Multiple Testing. *Journal of the Royal Statistical Society: Series B (Methodological)*, *57*(1), 289–300. https://doi.org/10.1111/j.2517-6161.1995.tb02031.x

Benjamini, Y., Krieger, A. M., & Yekutieli, D. (2006). Adaptive linear step-up procedures that control the false discovery rate. *Biometrika*, *93*(3), 491–507. https://doi.org/10.1093/biomet/93.3.491

Bersano, E., Sarnelli, M. F., Solara, V., Iazzolino, B., Peotta, L., De Marchi, F., Facchin, A., Moglia, C., Canosa, A., Calvo, A., Chiò, A., & Mazzini, L. (2020). Decline of cognitive and behavioral functions in amyotrophic lateral sclerosis: A longitudinal study. *Amyotrophic Lateral Sclerosis and Frontotemporal Degeneration*, *21*(5–6), 373–379. https://doi.org/10.1080/21678421.2020.1771732

Bonelli, R. M., & Cummings, J. L. (2007). Frontal-subcortical circuitry and behavior. *Dialogues in Clinical Neuroscience*, *9*(2), 141–151.

Bonferroni, C. (1936). Teoria statistica delle classi e calcolo delle probabilita. *Pubblicazioni Del R Istituto Superiore Di Scienze Economiche e Commericiali Di Firenze*, *8*, 3–62.

Bowser, R., Turner, M. R., & Shefner, J. (2011). Biomarkers in amyotrophic lateral sclerosis: Opportunities and limitations. *Nature Reviews Neurology*, *7*(11), Article 11. https://doi.org/10.1038/nrneurol.2011.151

Braak, H., Brettschneider, J., Ludolph, A. C., Lee, V. M., Trojanowski, J. Q., & Tredici, K. D. (2013). Amyotrophic lateral sclerosis—A model of corticofugal axonal spread. *Nature Reviews Neurology*, *9*(12), 708–715. https://doi.org/10.1038/nrneurol.2013.221

Breakspear, M., Williams, L. M., & Stam, C. J. (2004). A Novel Method for the Topographic Analysis of Neural Activity Reveals Formation and Dissolution of 'Dynamic Cell Assemblies.' *Journal of Computational Neuroscience*, *16*(1), 49–68. https://doi.org/10.1023/B:JCNS.0000004841.66897.7d

Bréchet, L., Brunet, D., Birot, G., Gruetter, R., Michel, C. M., & Jorge, J. (2019). Capturing the spatiotemporal dynamics of self-generated, task-initiated thoughts with EEG and fMRI. *NeuroImage*, *194*, 82–92. https://doi.org/10.1016/j.neuroimage.2019.03.029

Bréchet, L., Brunet, D., Perogamvros, L., Tononi, G., & Michel, C. M. (2020). EEG microstates of dreams. *Scientific Reports*, *10*(1), Article 1. https://doi.org/10.1038/s41598-020-74075-z

Bréchet, L., & Michel, C. M. (2022). EEG Microstates in Altered States of Consciousness. *Frontiers in Psychology*, *13*. https://www.frontiersin.org/article/10.3389/fpsyg.2022.856697

Bressler, S. L., & Menon, V. (2010). Large-scale brain networks in cognition: Emerging methods and principles. *Trends in Cognitive Sciences*, *14*(6), 277–290. https://doi.org/10.1016/j.tics.2010.04.004

Britz, J., Van De Ville, D., & Michel, C. M. (2010). BOLD correlates of EEG topography reveal rapid resting-state network dynamics. *NeuroImage*, *52*(4), 1162–1170. https://doi.org/10.1016/j.neuroimage.2010.02.052

Brodbeck, V., Kuhn, A., von Wegner, F., Morzelewski, A., Tagliazucchi, E., Borisov, S., Michel, C. M., & Laufs, H. (2012). EEG microstates of wakefulness and NREM sleep. *NeuroImage*, *62*(3), 2129–2139. https://doi.org/10.1016/j.neuroimage.2012.05.060

Brookes, M. J., Woolrich, M., Luckhoo, H., Price, D., Hale, J. R., Stephenson, M. C., Barnes, G. R., Smith, S. M., & Morris, P. G. (2011). Investigating the electrophysiological basis of resting state networks using magnetoencephalography. *Proceedings of the National Academy of Sciences*, *108*(40), 16783–16788. https://doi.org/10.1073/pnas.1112685108

Burgh, H. K. van der, Westeneng, H.-J., Walhout, R., Veenhuijzen, K. van, Tan, H. H. G., Meier, J. M., Bakker, L. A., Hendrikse, J., Es, M. A. van, Veldink, J. H., Heuvel, M. P. van den, & Berg, L. H. van den. (2020). Multimodal longitudinal study of structural brain involvement in amyotrophic lateral sclerosis. *Neurology*, *94*(24), e2592–e2604. https://doi.org/10.1212/WNL.0000000000009498

Burke, T., Pinto-Grau, M., Lonergan, K., Bede, P., O'Sullivan, M., Heverin, M., Vajda, A., McLaughlin, R. L., Pender, N., & Hardiman, O. (2017). A Cross-sectional population-based investigation into behavioral change in amyotrophic lateral sclerosis: Subphenotypes, staging, cognitive predictors, and survival. *Annals of Clinical and Translational Neurology*, *4*(5), 305–317. https://doi.org/10.1002/acn3.407

Burkhardt, C., Neuwirth, C., & Weber, M. (2017). Longitudinal assessment of the Edinburgh Cognitive and Behavioural Amyotrophic Lateral Sclerosis Screen (ECAS): Lack of practice effect in ALS patients? *Amyotrophic Lateral Sclerosis and Frontotemporal Degeneration*, *18*(3–4), 202–209. https://doi.org/10.1080/21678421.2017.1283418

Byrne, S., Heverin, M., Elamin, M., Bede, P., Lynch, C., Kenna, K., MacLaughlin, R., Walsh, C., Al Chalabi, A., & Hardiman, O. (2013). Aggregation of neurologic and neuropsychiatric disease in amyotrophic lateral sclerosis kindreds: A population-based case–control cohort study of familial and sporadic amyotrophic lateral sclerosis. *Annals of Neurology*, *74*(5), 699–708. https://doi.org/10.1002/ana.23969

Byrne, S., Jordan, I., Elamin, M., & Hardiman, O. (2013). Age at onset of amyotrophic lateral sclerosis is proportional to life expectancy. *Amyotrophic Lateral Sclerosis and Frontotemporal Degeneration*, *14*(7–8), 604–607. https://doi.org/10.3109/21678421.2013.809122

Cardenas-Blanco, A., Machts, J., Acosta-Cabronero, J., Kaufmann, J., Abdulla, S., Kollewe, K., Petri, S., Schreiber, S., Heinze, H.-J., Dengler, R., Vielhaber, S., & Nestor, P. J. (2016). Structural and diffusion imaging versus clinical assessment to monitor amyotrophic lateral sclerosis. *NeuroImage: Clinical*, *11*, 408–414. https://doi.org/10.1016/j.nicl.2016.03.011

Castelnovo, V., Canu, E., Calderaro, D., Riva, N., Poletti, B., Basaia, S., Solca, F., Silani, V., Filippi, M., & Agosta, F. (2020). Progression of brain functional connectivity and frontal cognitive dysfunction in ALS. *NeuroImage: Clinical*, *28*, 102509. https://doi.org/10.1016/j.nicl.2020.102509

Cedarbaum, J. M., Stambler, N., Malta, E., Fuller, C., Hilt, D., Thurmond, B., & Nakanishi, A. (1999). The ALSFRS-R: A revised ALS functional rating scale that incorporates assessments of respiratory function. BDNF ALS Study Group (Phase III). *Journal of the Neurological Sciences*, *169*(1–2), 13–21. https://doi.org/10.1016/s0022-510x(99)00210-5

Charcot, J. (1874). De la sclérose latérale amyotrophique. Leçons recueillies par Bourneville. *Prog Med*, *24*, 29–31.

Chen, T., Su, H., Zhong, N., Tan, H., Li, X., Meng, Y., Duan, C., Zhang, C., Bao, J., Xu, D., Song, W., Zou, J., Liu, T., Zhan, Q., Jiang, H., & Zhao, M. (2020). Disrupted brain network dynamics and cognitive functions in methamphetamine use disorder: Insights from EEG microstates. *BMC Psychiatry*, *20*(1), 334. https://doi.org/10.1186/s12888-020-02743-5

Chipika, R. H., Christidi, F., Finegan, E., Li Hi Shing, S., McKenna, M. C., Chang, K. M., Karavasilis, E., Doherty, M. A., Hengeveld, J. C., Vajda, A., Pender, N., Hutchinson, S., Donaghy, C., McLaughlin, R. L., Hardiman, O., & Bede, P. (2020). Amygdala

pathology in amyotrophic lateral sclerosis and primary lateral sclerosis. *Journal of the Neurological Sciences*, *417*, 117039. https://doi.org/10.1016/j.jns.2020.117039

Chipika, R. H., Finegan, E., Li Hi Shing, S., McKenna, M. C., Christidi, F., Chang, K. M., Doherty, M. A., Hengeveld, J. C., Vajda, A., Pender, N., Hutchinson, S., Donaghy, C., McLaughlin, R. L., Hardiman, O., & Bede, P. (2020). "Switchboard" malfunction in motor neuron diseases: Selective pathology of thalamic nuclei in amyotrophic lateral sclerosis and primary lateral sclerosis. *NeuroImage: Clinical*, *27*, 102300. https://doi.org/10.1016/j.nicl.2020.102300

Christidi, F., Karavasilis, E., Rentzos, M., Velonakis, G., Zouvelou, V., Xirou, S., Argyropoulos, G., Papatriantafyllou, I., Pantolewn, V., Ferentinos, P., Kelekis, N., Seimenis, I., Evdokimidis, I., & Bede, P. (2019). Hippocampal pathology in amyotrophic lateral sclerosis: Selective vulnerability of subfields and their associated projections. *Neurobiology of Aging*, *84*, 178–188. https://doi.org/10.1016/j.neurobiolaging.2019.07.019

Chu, C. J., Kramer, M. A., Pathmanathan, J., Bianchi, M. T., Westover, M. B., Wizon, L., & Cash, S. S. (2012). Emergence of Stable Functional Networks in Long-Term Human Electroencephalography. *Journal of Neuroscience*, *32*(8), 2703–2713. https://doi.org/10.1523/JNEUROSCI.5669-11.2012

Chu, C., Wang, X., Cai, L., Zhang, L., Wang, J., Liu, C., & Zhu, X. (2020). Spatiotemporal EEG microstate analysis in drug-free patients with Parkinson's disease. *NeuroImage: Clinical*, *25*, 102132. https://doi.org/10.1016/j.nicl.2019.102132

Cohen, I. van de V., Michael X. (2019). Electrophysiological Phase Synchrony in Distributed Brain Networks as a Promising Tool in the Study of Cognition. In *New Methods in Cognitive Psychology*. Routledge.

Costello, E., Lonergan, K., Madden, C., O'Sullivan, M., Mays, I., Heverin, M., Pinto-Grau, M., Hardiman, O., & Pender, N. (2020). Equivalency and practice effects of alternative versions of the Edinburgh Cognitive and Behavioral ALS Screen (ECAS). *Amyotrophic Lateral Sclerosis and Frontotemporal Degeneration*, *21*(1–2), 86–91. https://doi.org/10.1080/21678421.2019.1701681

Costello, E., Rooney, J., Pinto-Grau, M., Burke, T., Elamin, M., Bede, P., McMackin, R., Dukic, S., Vajda, A., Heverin, M., Hardiman, O., & Pender, N. (2021). Cognitive reserve in amyotrophic lateral sclerosis (ALS): A population-based longitudinal study. *Journal of Neurology, Neurosurgery & Psychiatry*, *92*(5), 460–465. https://doi.org/10.1136/jnnp-2020-324992

Crockford, C. J., Kleynhans, M., Wilton, E., Radakovic, R., Newton, J., Niven, E. H., Al-Chalabi, A., Hardiman, O., Bak, T. H., & Abrahams, S. (2018). ECAS A-B-C: Alternate forms of the Edinburgh Cognitive and Behavioural ALS Screen. *Amyotrophic Lateral Sclerosis and Frontotemporal Degeneration*, *19*(1–2), 57–64. https://doi.org/10.1080/21678421.2017.1407793

Crockford, C., Newton, J., Lonergan, K., Madden, C., Mays, I., O'Sullivan, M., Costello, E., Pinto-Grau, M., Vajda, A., Heverin, M., Pender, N., Al-Chalabi, A., Hardiman, O., & Abrahams, S. (2018). Measuring reliable change in cognition using the Edinburgh Cognitive and Behavioural ALS Screen (ECAS). *Amyotrophic Lateral Sclerosis and Frontotemporal Degeneration*, *19*(1–2), 65–73. https://doi.org/10.1080/21678421.2017.1407794

Cureton, E. E. (1956). Rank-biserial correlation. *Psychometrika*, *21*(3), 287–290. https://doi.org/10.1007/BF02289138

Custo, A., Van De Ville, D., Wells, W. M., Tomescu, M. I., Brunet, D., & Michel, C. M. (2017). Electroencephalographic Resting-State Networks: Source Localization of Microstates. *Brain Connectivity*, *7*(10), 671–682.

Custo, A., Vulliemoz, S., Grouiller, F., Van De Ville, D., & Michel, C. (2014). EEG source imaging of brain states using spatiotemporal regression. *NeuroImage*, *96*, 106–116. https://doi.org/10.1016/j.neuroimage.2014.04.002

Damborská, A., Piguet, C., Aubry, J.-M., Dayer, A. G., Michel, C. M., & Berchio, C. (2019). Altered Electroencephalographic Resting-State Large-Scale Brain Network Dynamics in Euthymic Bipolar Disorder Patients. *Frontiers in Psychiatry*, *10*. https://www.frontiersin.org/articles/10.3389/fpsyt.2019.00826

Damoiseaux, J. S., Rombouts, S. A. R. B., Barkhof, F., Scheltens, P., Stam, C. J., Smith, S. M., & Beckmann, C. F. (2006). Consistent resting-state networks across healthy subjects. *Proceedings of the National Academy of Sciences*, *103*(37), 13848–13853. https://doi.org/10.1073/pnas.0601417103

De Marchi, F., Carrarini, C., De Martino, A., Diamanti, L., Fasano, A., Lupica, A., Russo, M., Salemme, S., Spinelli, E. G., Bombaci, A., & on behalf of SIgN. (2021). Cognitive dysfunction in amyotrophic lateral sclerosis: Can we predict it? *Neurological Sciences*, *42*(6), 2211–2222. https://doi.org/10.1007/s10072-021-05188-0

DellaBadia Jr, J., Bell, W. L., Keyes Jr, J. W., Mathews, V. P., & Glazier, S. S. (2002). Assessment and cost comparison of sleep-deprived EEG, MRI and PET in the prediction of surgical treatment for epilepsy. *Seizure*, *11*(5), 303–309. https://doi.org/10.1053/seiz.2001.0648

Delorme, A., & Makeig, S. (2004). EEGLAB: An open source toolbox for analysis of single-trial EEG dynamics including independent component analysis. *Journal of Neuroscience Methods*, *134*(1), 9–21. https://doi.org/10.1016/j.jneumeth.2003.10.009

Deymeer, F., Smith, T. W., DeGirolami, U., & Drachman, D. A. (1989). Thalamic dementia and motor neuron disease. *Neurology*, *39*(1), 58–58. https://doi.org/10.1212/WNL.39.1.58

Dierks, T., Jelic, V., Julin, P., Maurer, K., Wahlund, L. O., Almkvist, O., Strik, W. K., & Winblad, B. (1997). EEG-microstates in mild memory impairment and Alzheimer's disease: Possible association with disturbed information processing. *Journal of Neural Transmission*, *104*(4), 483–495. https://doi.org/10.1007/BF01277666

Douaud, G., Filippini, N., Knight, S., Talbot, K., & Turner, M. R. (2011). Integration of structural and functional magnetic resonance imaging in amyotrophic lateral sclerosis. *Brain*, *134*(12), 3470–3479. https://doi.org/10.1093/brain/awr279

Dukic, S., Iyer, P. M., Mohr, K., Hardiman, O., Lalor, E. C., & Nasseroleslami, B. (2017). Estimation of coherence using the median is robust against EEG artefacts. *2017 39th Annual International Conference of the IEEE Engineering in Medicine and Biology Society (EMBC)*, 3949–3952. https://doi.org/10.1109/EMBC.2017.8037720

Dukic, S., McMackin, R., Buxo, T., Fasano, A., Chipika, R., Pinto-Grau, M., Costello, E., Schuster, C., Hammond, M., Heverin, M., Coffey, A., Broderick, M., Iyer, P. M., Mohr, K., Gavin, B., Pender, N., Bede, P., Muthuraman, M., Lalor, E. C., … Nasseroleslami, B. (2019). Patterned functional network disruption in amyotrophic lateral sclerosis. *Human Brain Mapping*, *0*(0). https://doi.org/10.1002/hbm.24740

Dukic, S., McMackin, R., Costello, E., Metzger, M., Buxo, T., Fasano, A., Chipika, R., Pinto-Grau, M., Schuster, C., Hammond, M., Heverin, M., Coffey, A., Broderick, M., Iyer, P. M., Mohr, K., Gavin, B., McLaughlin, R., Pender, N., Bede, P., … Nasseroleslami,

B. (2022). Resting-state EEG reveals four subphenotypes of amyotrophic lateral sclerosis. *Brain*, *145*(2), 621–631. https://doi.org/10.1093/brain/awab322

Dy, J. G., & Brodley, C. E. (2004). Feature Selection for Unsupervised Learning. *Journal of Machine Learning*.

Elamin, M., Bede, P., Byrne, S., Jordan, N., Gallagher, L., Wynne, B., O'Brien, C., Phukan, J., Lynch, C., Pender, N., & Hardiman, O. (2013). Cognitive changes predict functional decline in ALS: A population-based longitudinal study. *Neurology*, *80*(17), 1590–1597. https://doi.org/10.1212/WNL.0b013e31828f18ac

Elamin, M., Pinto-Grau, M., Burke, T., Bede, P., Rooney, J., O'Sullivan, M., Lonergan, K., Kirby, E., Quinlan, E., Breen, N., Vajda, A., Heverin, M., Pender, N., & Hardiman, O. (2017). Identifying behavioural changes in ALS: Validation of the Beaumont Behavioural Inventory (BBI). *Amyotrophic Lateral Sclerosis and Frontotemporal Degeneration*, *18*(1–2), 68–73. https://doi.org/10.1080/21678421.2016.1248976

Faber, P. L., Milz, P., Reininghaus, E. Z., Mörkl, S., Holl, A. K., Kapfhammer, H.-P., Pascual-Marqui, R. D., Kochi, K., Achermann, P., & Painold, A. (2021). Fundamentally altered global- and microstate EEG characteristics in Huntington's disease. *Clinical Neurophysiology*, *132*(1), 13–22. https://doi.org/10.1016/j.clinph.2020.10.006

Faber, P. L., Travis, F., Milz, P., & Parim, N. (2017). EEG microstates during different phases of Transcendental Meditation practice. *Cognitive Processing*, *18*(3), 307–314. https://doi.org/10.1007/s10339-017-0812-y

Falzone, Y. M., Domi, T., Mandelli, A., Pozzi, L., Schito, P., Russo, T., Barbieri, A., Fazio, R., Volontè, M. A., Magnani, G., Del Carro, U., Carrera, P., Malaspina, A., Agosta, F., Quattrini, A., Furlan, R., Filippi, M., & Riva, N. (2022). Integrated evaluation of a panel of neurochemical biomarkers to optimize diagnosis and prognosis in

amyotrophic lateral sclerosis. *European Journal of Neurology*, *29*(7), 1930–1939. https://doi.org/10.1111/ene.15321

Fauchon, C., Kim, J. A., El-Sayed, R., Osborne, N. R., Rogachov, A., Cheng, J. C., Hemington, K. S., Bosma, R. L., Dunkley, B. T., Oh, J., Bhatia, A., Inman, R. D., & Davis, K. D. (2022). A Hidden Markov Model reveals magnetoencephalography spectral frequency-specific abnormalities of brain state power and phase-coupling in neuropathic pain. *Communications Biology*, *5*(1), Article 1. https://doi.org/10.1038/s42003-022-03967-9

Feldman, E. L., Goutman, S. A., Petri, S., Mazzini, L., Savelieff, M. G., Shaw, P. J., & Sobue, G. (2022). Amyotrophic lateral sclerosis. *The Lancet*. https://doi.org/10.1016/S0140-6736(22)01272-7

Femiano, C., Trojsi, F., Caiazzo, G., Siciliano, M., Passaniti, C., Russo, A., Bisecco, A., Cirillo, M., Monsurrò, M. R., Esposito, F., Tedeschi, G., & Santangelo, G. (2018). Apathy Is Correlated with Widespread Diffusion Tensor Imaging (DTI) Impairment in Amyotrophic Lateral Sclerosis. *Behavioural Neurology*, *2018*, 2635202. https://doi.org/10.1155/2018/2635202

Fernandes, F., Barbalho, I., Barros, D., Valentim, R., Teixeira, C., Henriques, J., Gil, P., & Dourado Júnior, M. (2021). Biomedical signals and machine learning in amyotrophic lateral sclerosis: A systematic review. *BioMedical Engineering OnLine*, *20*(1), Article 1. https://doi.org/10.1186/s12938-021-00896-2

Finegan, E., Chipika, R. H., Li Hi Shing, S., Hardiman, O., & Bede, P. (2019). Pathological Crying and Laughing in Motor Neuron Disease: Pathobiology, Screening, Intervention. *Frontiers in Neurology*, *10*. https://www.frontiersin.org/articles/10.3389/fneur.2019.00260

Finger, E. C. (2016). Frontotemporal Dementias. *Continuum : Lifelong Learning in Neurology*, *22*(2 Dementia), 464–489. https://doi.org/10.1212/CON.0000000000000300

Finsel, J., Uttner, I., Vázquez Medrano, C. R., Ludolph, A. C., & Lulé, D. (2022). Cognition in the course of ALS—a meta-analysis. *Amyotrophic Lateral Sclerosis and Frontotemporal Degeneration*, *0*(0), 1–12. https://doi.org/10.1080/21678421.2022.2101379

Fonov, V., Evans, A., McKinstry, R., Almli, C., & Collins, D. (2009). Unbiased nonlinear average age-appropriate brain templates from birth to adulthood. *NeuroImage*, *47*, S102. https://doi.org/10.1016/S1053-8119(09)70884-5

Forgrave, L. M., Ma, M., Best, J. R., & DeMarco, M. L. (2019). The diagnostic performance of neurofilament light chain in CSF and blood for Alzheimer's disease, frontotemporal dementia, and amyotrophic lateral sclerosis: A systematic review and meta-analysis. *Alzheimer's & Dementia: Diagnosis, Assessment & Disease Monitoring*, *11*, 730–743. https://doi.org/10.1016/j.dadm.2019.08.009

Fraschini, M., Lai, M., Demuru, M., Puligheddu, M., Floris, G., Borghero, G., & Marrosu, F. (2018). Functional brain connectivity analysis in amyotrophic lateral sclerosis: An EEG source-space study. *Biomedical Physics & Engineering Express*, *4*(3), 037004. https://doi.org/10.1088/2057-1976/aa9c64

Gao, F., Jia, H., Wu, X., Yu, D., & Feng, Y. (2017). Altered Resting-State EEG Microstate Parameters and Enhanced Spatial Complexity in Male Adolescent Patients with Mild Spastic Diplegia. *Brain Topography*, *30*(2), 233–244. https://doi.org/10.1007/s10548-016-0520-4

Garn, H., Coronel, C., Waser, M., Caravias, G., & Ransmayr, G. (2017). Differential diagnosis between patients with probable Alzheimer's disease, Parkinson's disease

dementia, or dementia with Lewy bodies and frontotemporal dementia, behavioral variant, using quantitative electroencephalographic features. *Journal of Neural Transmission*, *124*(5), 569–581. https://doi.org/10.1007/s00702-017-1699-6

Gil, R., Neau, J.-P., Dary-Auriol, M., Agbo, C., Tantot, A. M., & Ingrand, P. (1995). Event-Related Auditory Evoked Potentials and Amyotrophic Lateral Sclerosis. *Archives of Neurology*, *52*(9), 890–896. https://doi.org/10.1001/archneur.1995.00540330068017

Glover, G. H. (2011). Overview of Functional Magnetic Resonance Imaging. *Neurosurgery Clinics of North America*, *22*(2), 133–139. https://doi.org/10.1016/j.nec.2010.11.001

Gordon, P. H., Cheng, B., Salachas, F., Pradat, P.-F., Bruneteau, G., Corcia, P., Lacomblez, L., & Meininger, V. (2010). Progression in ALS is not linear but is curvilinear. *Journal of Neurology*, *257*(10), 1713–1717. https://doi.org/10.1007/s00415-010-5609-1

Goutman, S. A., Hardiman, O., Al-Chalabi, A., Chió, A., Savelieff, M. G., Kiernan, M. C., & Feldman, E. L. (2022). Emerging insights into the complex genetics and pathophysiology of amyotrophic lateral sclerosis. *The Lancet Neurology*. https://doi.org/10.1016/S1474-4422(21)00414-2

Gregory, J. M., McDade, K., Bak, T. H., Pal, S., Chandran, S., Smith, C., & Abrahams, S. (2020). Executive, language and fluency dysfunction are markers of localised TDP-43 cerebral pathology in non-demented ALS. *Journal of Neurology, Neurosurgery & Psychiatry*, *91*(2), 149–157. https://doi.org/10.1136/jnnp-2019-320807

Grollemund, V., Pradat, P.-F., Querin, G., Delbot, F., Le Chat, G., Pradat-Peyre, J.-F., & Bede, P. (2019). Machine Learning in Amyotrophic Lateral Sclerosis: Achievements, Pitfalls, and Future Directions. *Frontiers in Neuroscience*, *13*, 438192. https://doi.org/10.3389/fnins.2019.00135

Gschwind, M., Hardmeier, M., Van De Ville, D., Tomescu, M. I., Penner, I.-K., Naegelin, Y., Fuhr, P., Michel, C. M., & Seeck, M. (2016). Fluctuations of spontaneous EEG topographies predict disease state in relapsing-remitting multiple sclerosis. *NeuroImage: Clinical*, *12*, 466–477. https://doi.org/10.1016/j.nicl.2016.08.008

Gschwind, M., Michel, C. M., & Van De Ville, D. (2015). Long-range dependencies make the difference—Comment on "A stochastic model for EEG microstate sequence analysis." *NeuroImage*, *117*, 449–455. https://doi.org/10.1016/j.neuroimage.2015.05.062

Guevara, M. A., & Corsi-Cabrera, M. (1996). *EEG coherence or EEG correlation?*

Hajian-Tilaki, K. (2013). Receiver Operating Characteristic (ROC) Curve Analysis for Medical Diagnostic Test Evaluation. *Caspian Journal of Internal Medicine*, *4*(2), 627–635.

Hanagasi, H. A., Gurvit, I. H., Ermutlu, N., Kaptanoglu, G., Karamursel, S., Idrisoglu, H. A., Emre, M., & Demiralp, T. (2002). Cognitive impairment in amyotrophic lateral sclerosis: Evidence from neuropsychological investigation and event-related potentials. *Cognitive Brain Research*, *14*(2), 234–244. https://doi.org/10.1016/S0926-6410(02)00110-6

Hanoglu, L., Toplutas, E., Saricaoglu, M., Velioglu, H. A., Yildiz, S., & Yulug, B. (2022). Therapeutic Role of Repetitive Transcranial Magnetic Stimulation in Alzheimer's and Parkinson's Disease: Electroencephalography Microstate Correlates. *Frontiers in Neuroscience*, *16*. https://www.frontiersin.org/articles/10.3389/fnins.2022.798558

Hao, Z., Zhai, X., Cheng, D., Pan, Y., & Dou, W. (2022). EEG Microstate-Specific Functional Connectivity and Stroke-Related Alterations in Brain Dynamics. *Frontiers in Neuroscience*, *16*. https://www.frontiersin.org/articles/10.3389/fnins.2022.848737

Hardiman, O., Al-Chalabi, A., Brayne, C., Beghi, E., van den Berg, L. H., Chio, A., Martin, S., Logroscino, G., & Rooney, J. (2017). The changing picture of amyotrophic lateral sclerosis: Lessons from European registers. *Journal of Neurology, Neurosurgery & Psychiatry*, *88*(7), 557–563. https://doi.org/10.1136/jnnp-2016-314495

Hardiman, O., Al-Chalabi, A., Chio, A., Corr, E. M., Logroscino, G., Robberecht, W., Shaw, P. J., Simmons, Z., & van den Berg, L. H. (2017). Amyotrophic lateral sclerosis. *Nature Reviews Disease Primers*, *3*(1), 17071. https://doi.org/10.1038/nrdp.2017.71

Hardiman, O., van den Berg, L. H., & Kiernan, M. C. (2011). Clinical diagnosis and management of amyotrophic lateral sclerosis. *Nature Reviews Neurology*, *7*(11), 639–649. https://doi.org/10.1038/nrneurol.2011.153

Henstridge, C. M., Sideris, D. I., Carroll, E., Rotariu, S., Salomonsson, S., Tzioras, M., McKenzie, C.-A., Smith, C., von Arnim, C. A. F., Ludolph, A. C., Lulé, D., Leighton, D., Warner, J., Cleary, E., Newton, J., Swingler, R., Chandran, S., Gillingwater, T. H., Abrahams, S., & Spires-Jones, T. L. (2018). Synapse loss in the prefrontal cortex is associated with cognitive decline in amyotrophic lateral sclerosis. *Acta Neuropathologica*, *135*(2), 213–226. https://doi.org/10.1007/s00401-017-1797-4

Higashihara, M., Pavey, N., Bos, M. van den, Menon, P., Kiernan, M. C., & Vucic, S. (2021). Association of Cortical Hyperexcitability and Cognitive Impairment in Patients With Amyotrophic Lateral Sclerosis. *Neurology*, *96*(16), e2090–e2097. https://doi.org/10.1212/WNL.0000000000011798

Hinault, T., Kraut, M., Bakker, A., Dagher, A., & Courtney, S. M. (2020). Disrupted Neural Synchrony Mediates the Relationship between White Matter Integrity and Cognitive Performance in Older Adults. *Cerebral Cortex*, *30*(10), 5570–5582. https://doi.org/10.1093/cercor/bhaa141

Honsbeek, R., Kuiper, T., & Metting Van Ruij, C. (1998). *ActiveTwo System* [Computer software]. Biosemi.

Hosseini, M.-P., Hosseini, A., & Ahi, K. (2021). A Review on Machine Learning for EEG Signal Processing in Bioengineering. *IEEE Reviews in Biomedical Engineering*, *14*, 204–218. https://doi.org/10.1109/RBME.2020.2969915

Hu, T., Hou, Y., Wei, Q., Yang, J., Luo, C., Chen, Y., Gong, Q., & Shang, H. (2020). Patterns of brain regional functional coherence in cognitive impaired ALS. *International Journal of Neuroscience*, *130*(8), 751–758. https://doi.org/10.1080/00207454.2019.1705806

Hunyadi, B., Woolrich, M. W., Quinn, A. J., Vidaurre, D., & De Vos, M. (2019). A dynamic system of brain networks revealed by fast transient EEG fluctuations and their fMRI correlates. *NeuroImage*, *185*, 72–82. https://doi.org/10.1016/j.neuroimage.2018.09.082

Hutchison, R. M., Womelsdorf, T., Allen, E. A., Bandettini, P. A., Calhoun, V. D., Corbetta, M., Della Penna, S., Duyn, J. H., Glover, G. H., Gonzalez-Castillo, J., Handwerker, D. A., Keilholz, S., Kiviniemi, V., Leopold, D. A., de Pasquale, F., Sporns, O., Walter, M., & Chang, C. (2013). Dynamic functional connectivity: Promise, issues, and interpretations. *NeuroImage*, *80*, 360–378. https://doi.org/10.1016/j.neuroimage.2013.05.079

Illán-Gala, I., Montal, V., Pegueroles, J., Vilaplana, E., Alcolea, D., Dols-Icardo, O., de Luna, N., Turón-Sans, J., Cortés-Vicente, E., Martinez-Roman, L., Sánchez-Saudinós, M. B., Subirana, A., Videla, L., Sala, I., Barroeta, I., Valldeneu, S., Blesa, R., Clarimón, J., Lleó, A., … Rojas-García, R. (2020). Cortical microstructure in the amyotrophic lateral sclerosis–frontotemporal dementia continuum. *Neurology*, *95*(18), e2565–e2576. https://doi.org/10.1212/WNL.0000000000010727

Illman, M., Laaksonen, K., Liljeström, M., Jousmäki, V., Piitulainen, H., & Forss, N. (2020). Comparing MEG and EEG in detecting the ~20-Hz rhythm modulation to tactile and proprioceptive stimulation. *NeuroImage*, *215*, 116804. https://doi.org/10.1016/j.neuroimage.2020.116804

Iyer, P. M., Egan, C., Pinto-Grau, M., Burke, T., Elamin, M., Nasseroleslami, B., Pender, N., Lalor, E. C., & Hardiman, O. (2015). Functional Connectivity Changes in Resting-State EEG as Potential Biomarker for Amyotrophic Lateral Sclerosis. *PLoS ONE*, *10*(6). https://doi.org/10.1371/journal.pone.0128682

Iyer, P. M., Mohr, K., Broderick, M., Gavin, B., Burke, T., Bede, P., Pinto-Grau, M., Pender, N. P., McLaughlin, R., Vajda, A., Heverin, M., Lalor, E. C., Hardiman, O., & Nasseroleslami, B. (2017). Mismatch Negativity as an Indicator of Cognitive Sub-Domain Dysfunction in Amyotrophic Lateral Sclerosis. *Frontiers in Neurology*, *8*. https://www.frontiersin.org/articles/10.3389/fneur.2017.00395

Javitt, D. C., Siegel, S. J., Spencer, K. M., Mathalon, D. H., Hong, L. E., Martinez, A., Ehlers, C. L., Abbas, A. I., Teichert, T., Lakatos, P., & Womelsdorf, T. (2020). A roadmap for development of neuro-oscillations as translational biomarkers for treatment development in neuropsychopharmacology. *Neuropsychopharmacology*, *45*(9), Article 9. https://doi.org/10.1038/s41386-020-0697-9

Jayaram, V., Widmann, N., Förster, C., Fomina, T., Hohmann, M., vom Hagen, J. M., Synofzik, M., Schölkopf, B., Schöls, L., & Grosse-Wentrup, M. (2015). Brain-computer interfacing in amyotrophic lateral sclerosis: Implications of a resting-state EEG analysis. *2015 37th Annual International Conference of the IEEE Engineering in Medicine and Biology Society (EMBC)*, 6979–6982. https://doi.org/10.1109/EMBC.2015.7319998

Katayama, H., Gianotti, L. R. R., Isotani, T., Faber, P. L., Sasada, K., Kinoshita, T., & Lehmann, D. (2007). Classes of Multichannel EEG Microstates in Light and Deep Hypnotic Conditions. *Brain Topography*, *20*(1), 7–14. https://doi.org/10.1007/s10548-007-0024-3

Keon, M., Musrie, B., Dinger, M., Brennan, S. E., Santos, J., & Saksena, N. K. (2021). Destination Amyotrophic Lateral Sclerosis. *Frontiers in Neurology*, *12*. https://www.frontiersin.org/articles/10.3389/fneur.2021.596006

Kew, J. J. M., Leigh, P. N., Playford, E. D., Passingham, R. E., Goldstein, L. H., Frackowiak, R. S. J., & Brooks, D. J. (1993). Cortical function in amyotrophic lateral sclerosis: A positron emission tomography study. *Brain*, *116*(3), 655–680. https://doi.org/10.1093/brain/116.3.655

Khanna, A., Pascual-Leone, A., Michel, C. M., & Farzan, F. (2015). Microstates in resting-state EEG: Current status and future directions. *Neuroscience & Biobehavioral Reviews*, *49*, 105–113. https://doi.org/10.1016/j.neubiorev.2014.12.010

Kirschstein, T., & Köhling, R. (2009). What is the Source of the EEG? *Clinical EEG and Neuroscience*, *40*(3), 146–149. https://doi.org/10.1177/155005940904000305

Koenig, T., Lehmann, D., Merlo, M. C. G., Kochi, K., Hell, D., & Koukkou, M. (1999). A deviant EEG brain microstate in acute, neuroleptic-naive schizophrenics at rest. *European Archives of Psychiatry and Clinical Neuroscience*, *249*(4), 205–211. https://doi.org/10.1007/s004060050088

Koenig, T., Marti-Lopez, F., & Valdes-Sosa, P. (2001). Topographic Time-Frequency Decomposition of the EEG. *NeuroImage*, *14*(2), 383–390. https://doi.org/10.1006/nimg.2001.0825

Koopman, M. (2022). *From cellular vulnerability to altered circuit activity: A systems biology approach to study amyotrophic lateral sclerosis* [University of Groningen]. https://doi.org/10.33612/diss.248568722

Kotkowski, E., Price, L. R., DeFronzo, R. A., Franklin, C. G., Salazar, M., Garrett, A. S., Woolsey, M., Blangero, J., Duggirala, R., Glahn, D. C., & Fox, P. T. (2022). Metabolic syndrome predictors of brain gray matter volume in an age-stratified community sample of 776 Mexican- American adults: Results from the genetics of brain structure image archive. *Frontiers in Aging Neuroscience*, *14*. https://www.frontiersin.org/articles/10.3389/fnagi.2022.999288

Lagrange, E., de la Cruz, E., Esselin, F., Vernoux, J.-P., Pageot, N., Taieb, G., & Camu, W. (2022). Reversible sub-acute motor neuron syndrome after mushroom intoxication masquerading as amyotrophic lateral sclerosis. *Amyotrophic Lateral Sclerosis and Frontotemporal Degeneration*, *23*(7–8), 496–499. https://doi.org/10.1080/21678421.2021.2008453

Lehmann, D., Faber, P. L., Galderisi, S., Herrmann, W. M., Kinoshita, T., Koukkou, M., Mucci, A., Pascual-Marqui, R. D., Saito, N., Wackermann, J., Winterer, G., & Koenig, T. (2005). EEG microstate duration and syntax in acute, medication-naïve, first-episode schizophrenia: A multi-center study. *Psychiatry Research: Neuroimaging*, *138*(2), 141–156. https://doi.org/10.1016/j.pscychresns.2004.05.007

Lehmann, D., Ozaki, H., & Pal, I. (1987). EEG alpha map series: Brain micro-states by space-oriented adaptive segmentation. *Electroencephalography and Clinical Neurophysiology*, *67*(3), 271–288. https://doi.org/10.1016/0013-4694(87)90025-3

Lehmann, D., Strik, W. K., Henggeler, B., Koenig, T., & Koukkou, M. (1998). Brain electric microstates and momentary conscious mind states as building blocks of spontaneous

thinking: I. Visual imagery and abstract thoughts. *International Journal of Psychophysiology*, *29*(1), 1–11. https://doi.org/10.1016/S0167-8760(97)00098-6

Liu, H., Tang, H., Wei, W., Wang, G., Du, Y., & Ruan, J. (2021). Altered peri-seizure EEG microstate dynamics in patients with absence epilepsy. *Seizure*, *88*, 15–21. https://doi.org/10.1016/j.seizure.2021.03.020

Lloyd, C. M., Richardson, M. P., Brooks, D. J., Al-Chalabi, A., & Leigh, P. N. (2000). Extramotor involvement in ALS: PET studies with the GABAA ligand [11C]flumazenil. *Brain*, *123*(11), 2289–2296. https://doi.org/10.1093/brain/123.11.2289

Longo, F., Longo, F., Massa, S., & Massa, S. (2008). Small Molecule Modulation of p75 Neurotrophin Receptor Functions. *CNS & Neurological Disorders - Drug Targets*, *7*(1), 63–70. https://doi.org/10.2174/187152708783885093

Lopes da Silva, F. (2013). EEG and MEG: Relevance to Neuroscience. *Neuron*, *80*(5), 1112–1128. https://doi.org/10.1016/j.neuron.2013.10.017

Ludolph, A., Drory, V., Hardiman, O., Nakano, I., Ravits, J., Robberecht, W., & Shefner, J. (2015). A revision of the El Escorial criteria—2015. *Amyotrophic Lateral Sclerosis and Frontotemporal Degeneration*, *16*(5–6), 291–292. https://doi.org/10.3109/21678421.2015.1049183

Lulé, D., Böhm, S., Müller, H.-P., Aho-Özhan, H., Keller, J., Gorges, M., Loose, M., Weishaupt, J. H., Uttner, I., Pinkhardt, E., Kassubek, J., Del Tredici, K., Braak, H., Abrahams, S., & Ludolph, A. C. (2018). Cognitive phenotypes of sequential staging in amyotrophic lateral sclerosis. *Cortex*, *101*, 163–171. https://doi.org/10.1016/j.cortex.2018.01.004

Mahoney, C. J., Ahmed, R. M., Huynh, W., Tu, S., Rohrer, J. D., Bedlack, R. S., Hardiman, O., & Kiernan, M. C. (2021). Pathophysiology and Treatment of Non-motor

Dysfunction in Amyotrophic Lateral Sclerosis. *CNS Drugs*, *35*(5), 483–505. https://doi.org/10.1007/s40263-021-00820-1

Mai, R., Facchetti, D., Micheli, A., & Poloni, M. (1998). Quantitative electroencephalography in amyotrophic lateral sclerosis. *Electroencephalography and Clinical Neurophysiology*, *106*(4), 383–386. https://doi.org/10.1016/S0013-4694(97)00159-4

Mann, H. B., & Whitney, D. R. (1947). On a Test of Whether one of Two Random Variables is Stochastically Larger than the Other. *The Annals of Mathematical Statistics*, *18*(1), 50–60.

Mantini, D., Perrucci, M. G., Del Gratta, C., Romani, G. L., & Corbetta, M. (2007). Electrophysiological signatures of resting state networks in the human brain. *Proceedings of the National Academy of Sciences*, *104*(32), 13170–13175. https://doi.org/10.1073/pnas.0700668104

Marin, B., Boumédiene, F., Logroscino, G., Couratier, P., Babron, M.-C., Leutenegger, A. L., Copetti, M., Preux, P.-M., & Beghi, E. (2017). Variation in worldwide incidence of amyotrophic lateral sclerosis: A meta-analysis. *International Journal of Epidemiology*, *46*(1), 57–74. https://doi.org/10.1093/ije/dyw061

Maruyama, Y., Yoshimura, N., Rana, A., Malekshahi, A., Tonin, A., Jaramillo-Gonzalez, A., Birbaumer, N., & Chaudhary, U. (2021). Electroencephalography of completely locked-in state patients with amyotrophic lateral sclerosis. *Neuroscience Research*, *162*, 45–51. https://doi.org/10.1016/j.neures.2020.01.013

McLaughlin, R. L., Schijven, D., van Rheenen, W., van Eijk, K. R., O'Brien, M., Kahn, R. S., Ophoff, R. A., Goris, A., Bradley, D. G., Al-Chalabi, A., van den Berg, L. H., Luykx, J. J., Hardiman, O., & Veldink, J. H. (2017). Genetic correlation between

amyotrophic lateral sclerosis and schizophrenia. *Nature Communications*, *8*, 14774. https://doi.org/10.1038/ncomms14774

McMackin, R., Dukic, S., Broderick, M., Iyer, P. M., Pinto-Grau, M., Mohr, K., Chipika, R., Coffey, A., Buxo, T., Schuster, C., Gavin, B., Heverin, M., Bede, P., Pender, N., Lalor, E. C., Muthuraman, M., Hardiman, O., & Nasseroleslami, B. (2019). Dysfunction of attention switching networks in amyotrophic lateral sclerosis. *NeuroImage: Clinical*, *22*, 101707. https://doi.org/10.1016/j.nicl.2019.101707

McMackin, R., Dukic, S., Costello, E., Pinto-Grau, M., Fasano, A., Buxo, T., Heverin, M., Reilly, R., Muthuraman, M., Pender, N., Hardiman, O., & Nasseroleslami, B. (2020). Localization of Brain Networks Engaged by the Sustained Attention to Response Task Provides Quantitative Markers of Executive Impairment in Amyotrophic Lateral Sclerosis. *Cerebral Cortex*, *30*(9), 4834–4846. https://doi.org/10.1093/cercor/bhaa076

McMackin, R., Dukic, S., Costello, E., Pinto-Grau, M., Keenan, O., Fasano, A., Buxo, T., Heverin, M., Reilly, R., Pender, N., Hardiman, O., & Nasseroleslami, B. (2021). Sustained attention to response task-related beta oscillations relate to performance and provide a functional biomarker in ALS. *Journal of Neural Engineering*, *18*(2), 026006. https://doi.org/10.1088/1741-2552/abd829

McMackin, R., Dukic, S., Costello, E., Pinto-Grau, M., McManus, L., Broderick, M., Chipika, R., Iyer, P. M., Heverin, M., Bede, P., Muthuraman, M., Pender, N., Hardiman, O., & Nasseroleslami, B. (2021). Cognitive network hyperactivation and motor cortex decline correlate with ALS prognosis. *Neurobiology of Aging*, *104*, 57–70. https://doi.org/10.1016/j.neurobiolaging.2021.03.002

McMackin, R., Muthuraman, M., Groppa, S., Babiloni, C., Taylor, J.-P., Kiernan, M. C., Nasseroleslami, B., & Hardiman, O. (2019). Measuring network disruption in neurodegenerative diseases: New approaches using signal analysis. *Journal of*

Neurology, Neurosurgery & Psychiatry, *90*(9), 1011–1020. https://doi.org/10.1136/jnnp-2018-319581

Menke, R. A. L., Proudfoot, M., Talbot, K., & Turner, M. R. (2018). The two-year progression of structural and functional cerebral MRI in amyotrophic lateral sclerosis. *NeuroImage: Clinical*, *17*, 953–961. https://doi.org/10.1016/j.nicl.2017.12.025

Menon, V., & Crottaz-Herbette, S. (2005). Combined EEG and fMRI Studies of Human Brain Function. In *International Review of Neurobiology* (Vol. 66, pp. 291–321). Elsevier. https://doi.org/10.1016/S0074-7742(05)66010-2

Mertens, N., Sunaert, S., Van Laere, K., & Koole, M. (2022). The Effect of Aging on Brain Glucose Metabolic Connectivity Revealed by [18F]FDG PET-MR and Individual Brain Networks. *Frontiers in Aging Neuroscience*, *13*. https://www.frontiersin.org/articles/10.3389/fnagi.2021.798410

Michel, C. M., & Brunet, D. (2019). EEG Source Imaging: A Practical Review of the Analysis Steps. *Frontiers in Neurology*, *10*. https://www.frontiersin.org/article/10.3389/fneur.2019.00325

Michel, C. M., & Koenig, T. (2018). EEG microstates as a tool for studying the temporal dynamics of whole-brain neuronal networks: A review. *NeuroImage*, *180*, 577–593. https://doi.org/10.1016/j.neuroimage.2017.11.062

Miller, K. J., Weaver, K. E., & Ojemann, J. G. (2009). Direct electrophysiological measurement of human default network areas. *Proceedings of the National Academy of Sciences*, *106*(29), 12174–12177. https://doi.org/10.1073/pnas.0902071106

Milz, P., Faber, P. L., Lehmann, D., Koenig, T., Kochi, K., & Pascual-Marqui, R. D. (2016). The functional significance of EEG microstates—Associations with modalities of thinking. *NeuroImage*, *125*, 643–656. https://doi.org/10.1016/j.neuroimage.2015.08.023

Milz, P., Pascual-Marqui, R. D., Achermann, P., Kochi, K., & Faber, P. L. (2017). The EEG microstate topography is predominantly determined by intracortical sources in the alpha band. *NeuroImage*, *162*, 353–361. https://doi.org/10.1016/j.neuroimage.2017.08.058

Mishra, A., Englitz, B., & Cohen, M. X. (2020). EEG microstates as a continuous phenomenon. *NeuroImage*, *208*, 116454. https://doi.org/10.1016/j.neuroimage.2019.116454

Mohr, K. S., Nasseroleslami, B., Iyer, P. M., Hardiman, O., & Lalor, E. C. (2017). *EyeBallGUI: A Tool for Visual Inspection and Binary Marking of Multi-channel Bio-signals* [Preprint]. Neuroscience. https://doi.org/10.1101/129437

Münte, T. F., Tröger, M., Nusser, I., Wieringa, B. M., Matzke, M., Johannes, S., & Dengler, R. (1998). Recognition memory deficits in amyotrophic lateral sclerosis assessed with event-related brain potentials. *Acta Neurologica Scandinavica*, *98*(2), 110–115. https://doi.org/10.1111/j.1600-0404.1998.tb01728.x

Murray, M. M., Brunet, D., & Michel, C. M. (2008). Topographic ERP Analyses: A Step-by-Step Tutorial Review. *Brain Topography*, *20*(4), 249–264. https://doi.org/10.1007/s10548-008-0054-5

Musso, F., Brinkmeyer, J., Mobascher, A., Warbrick, T., & Winterer, G. (2010a). Spontaneous brain activity and EEG microstates. A novel EEG/fMRI analysis approach to explore resting-state networks. *NeuroImage*, *52*(4), 1149–1161. https://doi.org/10.1016/j.neuroimage.2010.01.093

Musso, F., Brinkmeyer, J., Mobascher, A., Warbrick, T., & Winterer, G. (2010b). Spontaneous brain activity and EEG microstates. A novel EEG/fMRI analysis approach to explore resting-state networks. *NeuroImage*, *52*(4), 1149–1161. https://doi.org/10.1016/j.neuroimage.2010.01.093

Nasseroleslami, B. (2018). An Implementation of Empirical Bayesian Inference and Non-Null Bootstrapping for Threshold Selection and Power Estimation in Multiple and Single Statistical Testing. *bioRxiv*, 342964. https://doi.org/10.1101/342964

Nasseroleslami, B., Dukic, S., Broderick, M., Mohr, K., Schuster, C., Gavin, B., McLaughlin, R., Heverin, M., Vajda, A., Iyer, P. M., Pender, N., Bede, P., Lalor, E. C., & Hardiman, O. (2019). Characteristic Increases in EEG Connectivity Correlate With Changes of Structural MRI in Amyotrophic Lateral Sclerosis. *Cerebral Cortex*, *29*(1), 27–41. https://doi.org/10.1093/cercor/bhx301

Neary, D., Snowden, J. S., Gustafson, L., Passant, U., Stuss, D., Black, S., Freedman, M., Kertesz, A., Robert, P. H., Albert, M., Boone, K., Miller, B. L., Cummings, J., & Benson, D. F. (1998). Frontotemporal lobar degeneration: A consensus on clinical diagnostic criteria. *Neurology*, *51*(6), 1546–1554. https://doi.org/10.1212/WNL.51.6.1546

Nishida, K., Morishima, Y., Yoshimura, M., Isotani, T., Irisawa, S., Jann, K., Dierks, T., Strik, W., Kinoshita, T., & Koenig, T. (2013). EEG microstates associated with salience and frontoparietal networks in frontotemporal dementia, schizophrenia and Alzheimer's disease. *Clinical Neurophysiology*, *124*(6), 1106–1114. https://doi.org/10.1016/j.clinph.2013.01.005

Nobili, F., Arbizu, J., Bouwman, F., Drzezga, A., Agosta, F., Nestor, P., Walker, Z., Boccardi, M., & Disorders, the E.-E. T. F. for the P. of F.-P. for D. N. (2018). European Association of Nuclear Medicine and European Academy of Neurology recommendations for the use of brain 18F-fluorodeoxyglucose positron emission tomography in neurodegenerative cognitive impairment and dementia: Delphi consensus. *European Journal of Neurology*, *25*(10), 1201–1217. https://doi.org/10.1111/ene.13728

Núñez, P., Poza, J., Gómez, C., Rodríguez-González, V., Hillebrand, A., Tewarie, P., Tola-Arribas, M. A., Cano, M., & Hornero, R. (2021). Abnormal meta-state activation of dynamic brain networks across the Alzheimer spectrum. *NeuroImage*, *232*, 117898. https://doi.org/10.1016/j.neuroimage.2021.117898

Ogawa, T., Tanaka, H., & Hirata, K. (2009). Cognitive deficits in amyotrophic lateral sclerosis evaluated by event-related potentials. *Clinical Neurophysiology*, *120*(4), 659–664. https://doi.org/10.1016/j.clinph.2009.01.013

Ogura, A., Watanabe, H., Kawabata, K., Ohdake, R., Tanaka, Y., Masuda, M., Kato, T., Imai, K., Yokoi, T., Hara, K., Bagarinao, E., Riku, Y., Nakamura, R., Kawai, Y., Nakatochi, M., Atsuta, N., Katsuno, M., & Sobue, G. (2019). Semantic deficits in ALS related to right lingual/fusiform gyrus network involvement. *eBioMedicine*, *47*, 506–517. https://doi.org/10.1016/j.ebiom.2019.08.022

Olbrich, S., & Arns, M. (2013). EEG biomarkers in major depressive disorder: Discriminative power and prediction of treatment response. *International Review of Psychiatry*, *25*(5), 604–618. https://doi.org/10.3109/09540261.2013.816269

Olsson, B., Portelius, E., Cullen, N. C., Sandelius, Å., Zetterberg, H., Andreasson, U., Höglund, K., Irwin, D. J., Grossman, M., Weintraub, D., Chen-Plotkin, A., Wolk, D., McCluskey, L., Elman, L., Shaw, L. M., Toledo, J. B., McBride, J., Hernandez-Con, P., Lee, V. M.-Y., … Blennow, K. (2019). Association of Cerebrospinal Fluid Neurofilament Light Protein Levels With Cognition in Patients With Dementia, Motor Neuron Disease, and Movement Disorders. *JAMA Neurology*, *76*(3), 318–325. https://doi.org/10.1001/jamaneurol.2018.3746

Oostenveld, R., Fries, P., Maris, E., & Schoffelen, J.-M. (2011). *FieldTrip: Open Source Software for Advanced Analysis of MEG, EEG, and Invasive Electrophysiological*

Data [Research Article]. Computational Intelligence and Neuroscience; Hindawi. https://doi.org/10.1155/2011/156869

O'Toole, O., Traynor, B. J., Brennan, P., Sheehan, C., Frost, E., Corr, B., & Hardiman, O. (2008). Epidemiology and clinical features of amyotrophic lateral sclerosis in Ireland between 1995 and 2004. *Journal of Neurology, Neurosurgery & Psychiatry*, *79*(1), 30–32. https://doi.org/10.1136/jnnp.2007.117788

Pal, A., Behari, M., Goyal, V., & Sharma, R. (2021). Study of EEG microstates in Parkinson's disease: A potential biomarker? *Cognitive Neurodynamics*, *15*(3), 463–471. https://doi.org/10.1007/s11571-020-09643-0

Pascual-Marqui, R. D., Lehmann, D., Faber, P., Milz, P., Kochi, K., Yoshimura, M., Nishida, K., Isotani, T., & Kinoshita, T. (2014). The resting microstate networks (RMN): Cortical distributions, dynamics, and frequency specific information flow. *arXiv:1411.1949 [q-Bio]*. http://arxiv.org/abs/1411.1949

Pascual-Marqui, R. D., Michel, C. M., & Lehmann, D. (1995). Segmentation of brain electrical activity into microstates: Model estimation and validation. *IEEE Transactions on Biomedical Engineering*, *42*(7), 658–665. https://doi.org/10.1109/10.391164

Paulus, K. S., Magnano, I., Piras, M. R., Solinas, M. A., Solinas, G., Sau, G. F., & Aiello, I. (2002). Visual and auditory event-related potentials in sporadic amyotrophic lateral sclerosis. *Clinical Neurophysiology*, *113*(6), 853–861. https://doi.org/10.1016/S1388-2457(02)00082-2

Pekkonen, E., Osipova, D., & Laaksovirta, H. (2004). Magnetoencephalographic evidence of abnormal auditory processing in amyotrophic lateral sclerosis with bulbar signs. *Clinical Neurophysiology*, *115*(2), 309–315. https://doi.org/10.1016/S1388-2457(03)00360-2

Pender, N., Pinto-Grau, M., & Hardiman, O. (2020). Cognitive and behavioural impairment in amyotrophic lateral sclerosis. *Current Opinion in Neurology*, *33*(5), 649–654. https://doi.org/10.1097/WCO.0000000000000862

Phukan, J., Elamin, M., Bede, P., Jordan, N., Gallagher, L., Byrne, S., Lynch, C., Pender, N., & Hardiman, O. (2012). The syndrome of cognitive impairment in amyotrophic lateral sclerosis: A population-based study. *Journal of Neurology, Neurosurgery & Psychiatry*, *83*(1), 102–108. https://doi.org/10.1136/jnnp-2011-300188

Piastra, M. C., Nüßing, A., Vorwerk, J., Clerc, M., Engwer, C., & Wolters, C. H. (n.d.). *A comprehensive study on electroencephalography and magnetoencephalography sensitivity to cortical and subcortical sources*.

Pinto-Grau, M., Burke, T., Lonergan, K., McHugh, C., Mays, I., Madden, C., Vajda, A., Heverin, M., Elamin, M., Hardiman, O., & Pender, N. (2017). Screening for cognitive dysfunction in ALS: Validation of the Edinburgh Cognitive and Behavioural ALS Screen (ECAS) using age and education adjusted normative data. *Amyotrophic Lateral Sclerosis and Frontotemporal Degeneration*, *18*(1–2), 99–106. https://doi.org/10.1080/21678421.2016.1249887

Poil, S.-S., De Haan, W., van der Flier, W., Mansvelder, H., Scheltens, P., & Linkenkaer-Hansen, K. (2013). Integrative EEG biomarkers predict progression to Alzheimer's disease at the MCI stage. *Frontiers in Aging Neuroscience*, *5*. https://www.frontiersin.org/articles/10.3389/fnagi.2013.00058

Polich, J. (2007). Updating P300: An Integrative Theory of P3a and P3b. *Clinical Neurophysiology : Official Journal of the International Federation of Clinical Neurophysiology*, *118*(10), 2128–2148. https://doi.org/10.1016/j.clinph.2007.04.019

Polverino, A., Lopez, E. T., Minino, R., Liparoti, M., Romano, A., Trojsi, F., Lucidi, F., Gollo, L. L., Jirsa, V., Sorrentino, G., & Sorrentino, P. (2022). *Flexibility of brain*

dynamics predicts clinical impairment in Amyotrophic Lateral Sclerosis [Preprint]. Neurology. https://doi.org/10.1101/2022.02.07.22270581

Poulsen, A. T., Pedroni, A., Langer, N., & Hansen, L. K. (2018). Microstate EEGlab toolbox: An introductory guide. *bioRxiv*, 289850. https://doi.org/10.1101/289850

Proudfoot, M., Bede, P., & Turner, M. R. (2019). Imaging Cerebral Activity in Amyotrophic Lateral Sclerosis. *Frontiers in Neurology*, *9*, 1148. https://doi.org/10.3389/fneur.2018.01148

Proudfoot, M., Colclough, G. L., Quinn, A., Wuu, J., Talbot, K., Benatar, M., Nobre, A. C., Woolrich, M. W., & Turner, M. R. (2018). Increased cerebral functional connectivity in ALS: A resting-state magnetoencephalography study. *Neurology*, *90*(16), e1418–e1424. https://doi.org/10.1212/WNL.0000000000005333

Raaphorst, J., Beeldman, E., Schmand, B., Berkhout, J., Linssen, W. H. J. P., Berg, L. H. van den, Pijnenburg, Y. A., Grupstra, H. F., Weikamp, J. G., Schelhaas, H. J., Papma, J. M., Swieten, J. C. van, Visser, M. de, & Haan, R. J. de. (2012). The ALS-FTD-Q: A new screening tool for behavioral disturbances in ALS. *Neurology*, *79*(13), 1377–1383. https://doi.org/10.1212/WNL.0b013e31826c1aa1

Raggi, A., Consonni, M., Iannaccone, S., Perani, D., Zamboni, M., Sferrazza, B., & Cappa, S. F. (2008). Auditory event-related potentials in non-demented patients with sporadic amyotrophic lateral sclerosis. *Clinical Neurophysiology*, *119*(2), 342–350. https://doi.org/10.1016/j.clinph.2007.10.010

Raggi, A., Iannaccone, S., & Cappa, S. F. (2010). Event-related brain potentials in amyotrophic lateral sclerosis: A review of the international literature. *Amyotrophic Lateral Sclerosis*, *11*(1–2), 16–26. https://doi.org/10.3109/17482960902912399

Rajagopalan, V., & Pioro, E. P. (2019). Longitudinal 18F-FDG PET and MRI Reveal Evolving Imaging Pathology That Corresponds to Disease Progression in a Patient

With ALS-FTD. *Frontiers in Neurology*, *10*. https://doi.org/10.3389/fneur.2019.00234

Rieger, K., Diaz Hernandez, L., Baenninger, A., & Koenig, T. (2016). 15 Years of Microstate Research in Schizophrenia - Where Are We? A Meta-Analysis. *Frontiers in Psychiatry*, *7*, 22. https://doi.org/10.3389/fpsyt.2016.00022

Rights, J. D., & Sterba, S. K. (2021). Effect size measures for longitudinal growth analyses: Extending a framework of multilevel model R-squareds to accommodate heteroscedasticity, autocorrelation, nonlinearity, and alternative centering strategies. *New Directions for Child and Adolescent Development*, *2021*(175), 65–110. https://doi.org/10.1002/cad.20387

Robinson, K. M., Lacey, S. C., Grugan, P., Glosser, G., Grossman, M., & McCluskey, L. F. (2006). Cognitive functioning in sporadic amyotrophic lateral sclerosis: A six month longitudinal study. *Journal of Neurology, Neurosurgery & Psychiatry*, *77*(5), 668–670. https://doi.org/10.1136/jnnp.2005.073403

Robinson, L. F., Atlas, L. Y., & Wager, T. D. (2015). Dynamic functional connectivity using state-based dynamic community structure: Method and application to opioid analgesia. *NeuroImage*, *108*, 274–291. https://doi.org/10.1016/j.neuroimage.2014.12.034

Rooney, J., Byrne, S., Heverin, M., Corr, B., Elamin, M., Staines, A., Goldacre, B., & Hardiman, O. (2013). Survival analysis of irish amyotrophic lateral sclerosis patients diagnosed from 1995-2010. *PloS One*, *8*(9), e74733. https://doi.org/10.1371/journal.pone.0074733

Ryan, M., Heverin, M., Doherty, M. A., Davis, N., Corr, E. M., Vajda, A., Pender, N., McLaughlin, R., & Hardiman, O. (2018). Determining the incidence of familiality in

ALS: A study of temporal trends in Ireland from 1994 to 2016. *Neurology. Genetics*, *4*(3), e239. https://doi.org/10.1212/NXG.0000000000000239

Schielzeth, H., & Nakagawa, S. (2022). Conditional repeatability and the variance explained by reaction norm variation in random slope models. *Methods in Ecology and Evolution*, *13*(6), 1214–1223. https://doi.org/10.1111/2041-210X.13856

Schiller, B., Koenig, T., & Heinrichs, M. (2019). Oxytocin modulates the temporal dynamics of resting EEG networks. *Scientific Reports*, *9*(1), Article 1. https://doi.org/10.1038/s41598-019-49636-6

Schmidt, R., de Reus, M. A., Scholtens, L. H., van den Berg, L. H., & van den Heuvel, M. P. (2016). Simulating disease propagation across white matter connectome reveals anatomical substrate for neuropathology staging in amyotrophic lateral sclerosis. *NeuroImage*, *124*, 762–769. https://doi.org/10.1016/j.neuroimage.2015.04.005

Schmitt, L. I., Wimmer, R. D., Nakajima, M., Happ, M., Mofakham, S., & Halassa, M. M. (2017). Thalamic amplification of cortical connectivity sustains attentional control. *Nature*, *545*(7653), Article 7653. https://doi.org/10.1038/nature22073

Schwab, S., Koenig, T., Morishima, Y., Dierks, T., Federspiel, A., & Jann, K. (2015). Discovering frequency sensitive thalamic nuclei from EEG microstate informed resting state fMRI. *NeuroImage*, *118*, 368–375. https://doi.org/10.1016/j.neuroimage.2015.06.001

Scotter, E. L., Chen, H.-J., & Shaw, C. E. (2015). TDP-43 Proteinopathy and ALS: Insights into Disease Mechanisms and Therapeutic Targets. *Neurotherapeutics*, *12*(2), 352–363. https://doi.org/10.1007/s13311-015-0338-x

Secco, A., Tonin, A., Rana, A., Jaramillo-Gonzalez, A., Khalili-Ardali, M., Birbaumer, N., & Chaudhary, U. (2020). EEG power spectral density in locked-in and completely

locked-in state patients: A longitudinal study. *Cognitive Neurodynamics*. https://doi.org/10.1007/s11571-020-09639-w

Seeber, M., Cantonas, L.-M., Hoevels, M., Sesia, T., Visser-Vandewalle, V., & Michel, C. M. (2019). Subcortical electrophysiological activity is detectable with high-density EEG source imaging. *Nature Communications*, *10*(1), Article 1. https://doi.org/10.1038/s41467-019-08725-w

Seeber, M., & Michel, C. M. (2021). Synchronous Brain Dynamics Establish Brief States of Communality in Distant Neuronal Populations. *eNeuro*, *8*(3). https://doi.org/10.1523/ENEURO.0005-21.2021

Senda, J., Kato, S., Kaga, T., Ito, M., Atsuta, N., Nakamura, T., Watanabe, H., Tanaka, F., Naganawa, S., & Sobue, G. (2011). Progressive and widespread brain damage in ALS: MRI voxel-based morphometry and diffusion tensor imaging study. *Amyotrophic Lateral Sclerosis*, *12*(1), 59–69. https://doi.org/10.3109/17482968.2010.517850

Shen, D., Hou, B., Xu, Y., Cui, B., Peng, P., Li, X., Tai, H., Zhang, K., Liu, S., Fu, H., Gao, J., Liu, M., Feng, F., & Cui, L. (2018). Brain Structural and Perfusion Signature of Amyotrophic Lateral Sclerosis With Varying Levels of Cognitive Deficit. *Frontiers in Neurology*, *9*. https://www.frontiersin.org/articles/10.3389/fneur.2018.00364

Smitha, K., Akhil Raja, K., Arun, K., Rajesh, P., Thomas, B., Kapilamoorthy, T., & Kesavadas, C. (2017). Resting state fMRI: A review on methods in resting state connectivity analysis and resting state networks. *The Neuroradiology Journal*, *30*(4), 305–317. https://doi.org/10.1177/1971400917697342

Stam, C. J. (2005). Nonlinear dynamical analysis of EEG and MEG: Review of an emerging field. *Clinical Neurophysiology*, *116*(10), 2266–2301. https://doi.org/10.1016/j.clinph.2005.06.011

Strong, M. J., Abrahams, S., Goldstein, L. H., Woolley, S., Mclaughlin, P., Snowden, J., Mioshi, E., Roberts-South, A., Benatar, M., HortobáGyi, T., Rosenfeld, J., Silani, V., Ince, P. G., & Turner, M. R. (2017). Amyotrophic lateral sclerosis - frontotemporal spectrum disorder (ALS-FTSD): Revised diagnostic criteria. *Amyotrophic Lateral Sclerosis and Frontotemporal Degeneration*, *18*(3–4), 153–174. https://doi.org/10.1080/21678421.2016.1267768

Taga, A., & Maragakis, N. J. (2018). Current and emerging ALS biomarkers: Utility and potential in clinical trials. *Expert Review of Neurotherapeutics*, *18*(11), 871–886. https://doi.org/10.1080/14737175.2018.1530987

Tait, L., Tamagnini, F., Stothart, G., Barvas, E., Monaldini, C., Frusciante, R., Volpini, M., Guttmann, S., Coulthard, E., Brown, J. T., Kazanina, N., & Goodfellow, M. (2020). EEG microstate complexity for aiding early diagnosis of Alzheimer's disease. *Scientific Reports*, *10*(1), 17627. https://doi.org/10.1038/s41598-020-74790-7

Tang, J., Yang, Y., Gong, Z., Li, Z., Huang, L., Ding, F., Liu, M., & Zhang, M. (2021). Plasma Uric Acid Helps Predict Cognitive Impairment in Patients With Amyotrophic Lateral Sclerosis. *Frontiers in Neurology*, *12*. https://www.frontiersin.org/articles/10.3389/fneur.2021.789840

Tarailis, P., Koenig, T., Michel, C. M., & Griškova-Bulanova, I. (2023). The Functional Aspects of Resting EEG Microstates: A Systematic Review. *Brain Topography*. https://doi.org/10.1007/s10548-023-00958-9

Tekin, S., & Cummings, J. L. (2002). Frontal–subcortical neuronal circuits and clinical neuropsychiatry: An update. *Journal of Psychosomatic Research*, *53*(2), 647–654. https://doi.org/10.1016/S0022-3999(02)00428-2

Temp, A. G. M., Dyrba, M., Büttner, C., Kasper, E., Machts, J., Kaufmann, J., Vielhaber, S., Teipel, S., & Prudlo, J. (2021). Cognitive Profiles of Amyotrophic Lateral Sclerosis

Differ in Resting-State Functional Connectivity: An fMRI Study. *Frontiers in Neuroscience*, *15*, 682100. https://doi.org/10.3389/fnins.2021.682100

Teplan, M. (2002). FUNDAMENTALS OF EEG MEASUREMENT. *MEASUREMENT SCIENCE REVIEW*, *2*.

Terpou, B. A., Shaw, S. B., Théberge, J., Férat, V., Michel, C. M., McKinnon, M. C., Lanius, R. A., & Ros, T. (2022). Spectral decomposition of EEG microstates in post-traumatic stress disorder. *NeuroImage: Clinical*, *35*, 103135. https://doi.org/10.1016/j.nicl.2022.103135

Tewarie, P., Liuzzi, L., O'Neill, G. C., Quinn, A. J., Griffa, A., Woolrich, M. W., Stam, C. J., Hillebrand, A., & Brookes, M. J. (2019). Tracking dynamic brain networks using high temporal resolution MEG measures of functional connectivity. *NeuroImage*, *200*, 38–50. https://doi.org/10.1016/j.neuroimage.2019.06.006

The MathWorks, I. (2019). *MATLAB and Computer Vision System Toolbox* [Computer software]. The MathWorks, Inc.

Tibshirani, R., Walther, G., & Hastie, T. (2001). Estimating the number of clusters in a data set via the gap statistic. *Journal of the Royal Statistical Society: Series B (Statistical Methodology)*, *63*(2), 411–423. https://doi.org/10.1111/1467-9868.00293

Traynor, B. J., Alexander, M., Corr, B., Frost, E., & Hardiman, O. (2003). Effect of a multidisciplinary amyotrophic lateral sclerosis (ALS) clinic on ALS survival: A population based study, 1996–2000. *Journal of Neurology, Neurosurgery & Psychiatry*, *74*(9), 1258–1261. https://doi.org/10.1136/jnnp.74.9.1258

Trojsi, F., Di Nardo, F., Siciliano, M., Caiazzo, G., Femiano, C., Passaniti, C., Ricciardi, D., Russo, A., Bisecco, A., Esposito, S., Monsurrò, M. R., Cirillo, M., Santangelo, G., Esposito, F., & Tedeschi, G. (2020). Frontotemporal degeneration in amyotrophic

lateral sclerosis (ALS): A longitudinal MRI one-year study. *CNS Spectrums*, 1–10. https://doi.org/10.1017/S109285292000005X

Trojsi, F., Nardo, F. D., Siciliano, M., Caiazzo, G., Femiano, C., Passaniti, C., Ricciardi, D., Russo, A., Bisecco, A., Esposito, S., Monsurrò, M. R., Cirillo, M., Santangelo, G., Esposito, F., & Tedeschi, G. (undefined/ed). Frontotemporal degeneration in amyotrophic lateral sclerosis (ALS): A longitudinal MRI one-year study. *CNS Spectrums*, 1–10. https://doi.org/10.1017/S109285292000005X

Turner, M. R., & Kiernan, M. C. (2012). Does interneuronal dysfunction contribute to neurodegeneration in amyotrophic lateral sclerosis? *Amyotrophic Lateral Sclerosis*, *13*(3), 245–250. https://doi.org/10.3109/17482968.2011.636050

Tzourio-Mazoyer, N., Landeau, B., Papathanassiou, D., Crivello, F., Etard, O., Delcroix, N., Mazoyer, B., & Joliot, M. (2002). Automated anatomical labeling of activations in SPM using a macroscopic anatomical parcellation of the MNI MRI single-subject brain. *NeuroImage*, *15*(1), 273–289. https://doi.org/10.1006/nimg.2001.0978

Van Den Broek, S. P., Reinders, F., Donderwinkel, M., & Peters, M. J. (1998). Volume conduction effects in EEG and MEG. *Electroencephalography and Clinical Neurophysiology*, *106*(6), 522–534. https://doi.org/10.1016/S0013-4694(97)00147-8

van den Heuvel, M. P., Mandl, R. C. W., Kahn, R. S., & Hulshoff Pol, H. E. (2009). Functionally linked resting-state networks reflect the underlying structural connectivity architecture of the human brain. *Human Brain Mapping*, *30*(10), 3127–3141. https://doi.org/10.1002/hbm.20737

Van Der Burgh, H. (2020). *A multimodal longitudinal study of structural brain involvement in amyotrophic lateral sclerosis* (Version 3, p. 6635133 bytes) [dataset]. Dryad. https://doi.org/10.5061/DRYAD.8931ZCRKV

van Diessen, E., Numan, T., van Dellen, E., van der Kooi, A. W., Boersma, M., Hofman, D., van Lutterveld, R., van Dijk, B. W., van Straaten, E. C. W., Hillebrand, A., & Stam, C. J. (2015). Opportunities and methodological challenges in EEG and MEG resting state functional brain network research. *Clinical Neurophysiology*, *126*(8), 1468–1481. https://doi.org/10.1016/j.clinph.2014.11.018

Varela, F., Lachaux, J.-P., Rodriguez, E., & Martinerie, J. (2001). The brainweb: Phase synchronization and large-scale integration. *Nature Reviews Neuroscience*, *2*(4), Article 4. https://doi.org/10.1038/35067550

Vellante, F., Ferri, F., Baroni, G., Croce, P., Migliorati, D., Pettoruso, M., De Berardis, D., Martinotti, G., Zappasodi, F., & Giannantonio, M. D. (2020). Euthymic bipolar disorder patients and EEG microstates: A neural signature of their abnormal self experience? *Journal of Affective Disorders*, *272*, 326–334. https://doi.org/10.1016/j.jad.2020.03.175

Verstraete, E., Heuvel, M. P. van den, Veldink, J. H., Blanken, N., Mandl, R. C., Pol, H. E. H., & Berg, L. H. van den. (2010). Motor Network Degeneration in Amyotrophic Lateral Sclerosis: A Structural and Functional Connectivity Study. *PLOS ONE*, *5*(10), e13664. https://doi.org/10.1371/journal.pone.0013664

Verstraete, E., Veldink, J. H., van den Berg, L. H., & van den Heuvel, M. P. (2014). Structural brain network imaging shows expanding disconnection of the motor system in amyotrophic lateral sclerosis. *Human Brain Mapping*, *35*(4), 1351–1361. https://doi.org/10.1002/hbm.22258

Vidaurre, D., Abeysuriya, R., Becker, R., Quinn, A. J., Alfaro-Almagro, F., Smith, S. M., & Woolrich, M. W. (2018). Discovering dynamic brain networks from big data in rest and task. *NeuroImage*, *180*, 646–656. https://doi.org/10.1016/j.neuroimage.2017.06.077

Vidaurre, D., Hunt, L. T., Quinn, A. J., Hunt, B. A. E., Brookes, M. J., Nobre, A. C., & Woolrich, M. W. (2018). Spontaneous cortical activity transiently organises into frequency specific phase-coupling networks. *Nature Communications*, *9*(1), Article 1. https://doi.org/10.1038/s41467-018-05316-z

Vidaurre, D., Quinn, A. J., Baker, A. P., Dupret, D., Tejero-Cantero, A., & Woolrich, M. W. (2016). Spectrally resolved fast transient brain states in electrophysiological data. *NeuroImage*, *126*, 81–95. https://doi.org/10.1016/j.neuroimage.2015.11.047

Vieregge, P., Wauschkuhn, B., Heberlein, I., Hagenah, J., & Verleger, R. (1999). Selective attention is impaired in amyotrophic lateral sclerosis—A study of event-related EEG potentials. *Cognitive Brain Research*, *8*(1), 27–35. https://doi.org/10.1016/S0926-6410(99)00004-X

Ville, D. V. D., Britz, J., & Michel, C. M. (2010). EEG microstate sequences in healthy humans at rest reveal scale-free dynamics. *Proceedings of the National Academy of Sciences*, *107*(42), 18179–18184. https://doi.org/10.1073/pnas.1007841107

von Wegner, F., Knaut, P., & Laufs, H. (2018). EEG Microstate Sequences From Different Clustering Algorithms Are Information-Theoretically Invariant. *Frontiers in Computational Neuroscience*, *12*, 70. https://doi.org/10.3389/fncom.2018.00070

von Wegner, F., Tagliazucchi, E., & Laufs, H. (2017). Information-theoretical analysis of resting state EEG microstate sequences—Non-Markovianity, non-stationarity and periodicities. *NeuroImage*, *158*, 99–111. https://doi.org/10.1016/j.neuroimage.2017.06.062

Vucic, S., & Kiernan, M. C. (2017). Transcranial Magnetic Stimulation for the Assessment of Neurodegenerative Disease. *Neurotherapeutics*, *14*(1), 91–106. https://doi.org/10.1007/s13311-016-0487-6

Wackermann, J., Lehmann, D., Michel, C. M., & Strik, W. K. (1993). Adaptive segmentation of spontaneous EEG map series into spatially defined microstates. *International Journal of Psychophysiology*, *14*(3), 269–283. https://doi.org/10.1016/0167-8760(93)90041-M

Wang, G. (2019). High Temporal-Resolution Dynamic PET Image Reconstruction Using a New Spatiotemporal Kernel Method. *IEEE Transactions on Medical Imaging*, *38*(3), 664–674. https://doi.org/10.1109/TMI.2018.2869868

Wang, J., Barstein, J., Ethridge, L. E., Mosconi, M. W., Takarae, Y., & Sweeney, J. A. (2013). Resting state EEG abnormalities in autism spectrum disorders. *Journal of Neurodevelopmental Disorders*, *5*(1), 24. https://doi.org/10.1186/1866-1955-5-24

Ward, J. H. (1963). Hierarchical Grouping to Optimize an Objective Function. *Journal of the American Statistical Association*, *58*(301), 236–244. https://doi.org/10.2307/2282967

Wechsler, D. (2003). *WISC-IV: Administration and Scoring Manual* (4th ed). Psychological Corp.

West, B. T., Welch, K. B., & Ga, A. T. (2007). *A Practical Guide Using Statistical Software*. 348.

Witten, D. M., & Tibshirani, R. (2010). A framework for feature selection in clustering. *Journal of the American Statistical Association*, *105*(490), 713–726. https://doi.org/10.1198/jasa.2010.tm09415

Wong, L.-W., Wang, Z., Ang, S. R. X., & Sajikumar, S. (2022). Fading memories in aging and neurodegeneration: Is p75 neurotrophin receptor a culprit? *Ageing Research Reviews*, *75*, 101567. https://doi.org/10.1016/j.arr.2022.101567

Yuan, H., Zotev, V., Phillips, R., Drevets, W. C., & Bodurka, J. (2012). Spatiotemporal dynamics of the brain at rest—Exploring EEG microstates as electrophysiological

signatures of BOLD resting state networks. *NeuroImage*, *60*(4), 2062–2072. https://doi.org/10.1016/j.neuroimage.2012.02.031

Zanesco, A. P., King, B. G., Skwara, A. C., & Saron, C. D. (2020). Within and between-person correlates of the temporal dynamics of resting EEG microstates. *NeuroImage*, *211*, 116631. https://doi.org/10.1016/j.neuroimage.2020.116631

Zanesco, A. P., Skwara, A. C., King, B. G., Powers, C., Wineberg, K., & Saron, C. D. (2021). Meditation training modulates brain electric microstates and felt states of awareness. *Human Brain Mapping*, *42*(10), 3228–3252. https://doi.org/10.1002/hbm.25430

Zhang, S., Cao, C., Quinn, A., Vivekananda, U., Zhan, S., Liu, W., Sun, B., Woolrich, M., Lu, Q., & Litvak, V. (2021). Dynamic analysis on simultaneous iEEG-MEG data via hidden Markov model. *NeuroImage*, *233*, 117923. https://doi.org/10.1016/j.neuroimage.2021.117923

Zhang, S., Vladimir Litvak, Tian, S., Zhongpeng Dai, Hao Tang, Wang, X., Yao, Z., & Lu, Q. (2022). Spontaneous transient states of fronto-temporal and default-mode networks altered by suicide attempt in major depressive disorder. *European Archives of Psychiatry and Clinical Neuroscience*. https://doi.org/10.1007/s00406-021-01371-8

Zisk, A. H., Borgheai, S. B., McLinden, J., Deligani, R. J., & Shahriari, Y. (2022). Improving longitudinal P300-BCI performance for people with ALS using a data augmentation and jitter correction approach. *Brain-Computer Interfaces*, *9*(1), 49–66. https://doi.org/10.1080/2326263X.2021.2014678

XI. Appendices

1. Appendix – Chapter IV

1.1. Supplementary note 1: Brain networks

To define neurophysiologically-meaningful networks, we used the five anatomical lobes: frontal, temporal, centro-parietal, occipital and subcortical with the separation of the centro-parietal lobe into parietal and motor networks as this last brain region is a hallmark of atrophy in ALS. Each network is described in terms of the AAL regions in Table 9.

Table 9: Subgroups of brain regions according to the AAL atlas.

Motor network	Precentral gyrus, Rolandic operculum, Supplementary motor area, Paracentral lobule
Frontal lobe	Superior frontal gyrus, dorsolateral, Superior frontal gyrus, orbital, Middle frontal gyrus, Middle frontal gyrus, orbital, Inferior frontal gyrus, opercular, Inferior frontal gyrus, triangular, Inferior frontal gyrus, orbital, Superior frontal gyrus, medial, Superior frontal gyrus, medial orbital, Gyrus rectus
Temporal lobe	Fusiform gyrus, Heschl gyrus, Superior temporal gyrus, Temporal pole: superior temporal gyrus, Middle temporal gyrus, Temporal pole: middle temporal gyrus Inferior temporal gyrus,
Occipital lobe	Calcarine fissure and surrounding cortex, Cuneus, Lingual gyrus, Superior occipital lobe, Middle occipital lobe, Inferior occipital lobe
Parietal lobe	Postcentral gyrus, Superior parietal gyrus, Inferior parietal gyrus, Supramarginal gyrus, Angular gyrus, Precuneus,
Subcortical	Amygdala, Caudate nucleus,

	Cingulate gyrus, anterior part, Cingulate gyrus, mid part, Cingulate gyrus, posterior part, Hippocampus, Insula, Olfactory cortex, Pallidum, Parahippocampus, Putamen, Thalamus

2. Appendix – Chapter V

2.1. Supplementary note 2: Fixed-effects statistics of the EEG measures models

Spectral power

For each frequency band of the spectral power with ROI-specific significant changes over time (significance determined by bootstrapping analysis on the LME models per ROI), the F-tests were computed with the null hypothesis H_0 of all fixed-effects being null. The corresponding F-statistics can be observed in Table 10.

Table 10: Spectral power model F-statistics performed for each frequency band of interest. Each rejected null hypothesis ($p<0.05$) reveals the existence of non-zero fixed-effects.

	All		ALSbi		ALSncbi
Frequencies	δ	γl	γ_l	γ_h	β
p-values	0.2	0.2	0.2	0.2	0.5
F-statistics	1.8	1.5	1.5	1.6	0.5

For each frequency-band model of interest, the fixed-effects and their related statistics are detailed in Table 11. It describes the estimated effects of time (since disease onset) on the EEG power. Depending on the frequency band, the effects differ, but no overall significant temporal effect was observed in any model.

Table 11: ALSci - spectral power models fixed-effects and related t-statistics for each frequency band of interest. For each fixed-effect, is given the estimate and its standard error as well as the t-statistic with p-value and confidence intervals. Significant effects are represented in bold. No significant overall time effect was observed for any of the six frequency-band.

	θ	**(Intercept)**	**0.082**	**0.0073**	**11**	**2E-29**	**0.068**	**0.096**
		Time	-0.0003	0.0002	-1.3	0.18	-0.0007	0.0001
	γ_l	**(Intercept)**	**0.1**	**0.012**	**8.9**	**6E-19**	**0.081**	**0.13**
		Time	0.00033	0.00027	1.2	0.22	-0.0002	0.00085
	γ_l	**(Intercept)**	**0.095**	**0.014**	**6.7**	**2E-11**	**0.067**	**0.12**
		Time	0.00061	0.0005	1.2	0.22	-0.0004	0.0016
	γ_h	**(Intercept)**	**0.17**	**0.032**	**5.2**	**2E-07**	**0.1**	**0.23**
		Time	0.0015	0.0011	1.3	0.2	-0.0008	0.0037
	γ_l	**(Intercept)**	**0.11**	**0.015**	**7.2**	**7E-13**	**0.078**	**0.14**
		Time	0.0002	0.0003	0.71	0.48	-0.0004	0.0007

Amplitude envelope correlation (AEC)

For each frequency band of the spectral power with ROI-specific significant changes over time, the F-tests were computed with the null hypothesis H_0 of all fixed-effects being null. The corresponding F-statistics can be observed in Table 12.

Table 12: Co-modulation model F-statistics performed for each frequency band of interest. Each rejected null hypothesis ($p<0.05$) reveals the existence of non-zero fixed-effects.

	ALSci				ALSbi	ALSncbi	
Frequencies	**δ**	**θ**	α	β	α	δ	θ
p-values	**0.0009**	**0.01**	0.4	0.6	0.7	0.2	0.09
F-statistic	**11**	**11**	0.68	3.6	0.16	1.5	2.8

For each frequency-band model, the fixed-effects and their related statistics are detailed in Table 13. It describes the estimated effects of time (since disease onset) on the EEG power. Depending on the frequency band, the effects differ but overall significant temporal effects were observed in the δ and θ-bands, in ALSci patients.

Table 13: Co-modulation models fixed-effects and related t-statistics for each frequency band of interest. For each fixed-effect, is given the estimate and its standard error as well as the t-statistic with p-value and confidence intervals. Significant effects are represented in bold.

	Freq	Fixed-effect name	Estimate	SE	tStat	pValue	Lower	Upper
ALSci	$\boldsymbol{\delta}$	**(Intercept)**	**-1.7**	**0.57**	**-3**	**0.0026**	**-2.8**	**-0.6**
		Time	**0.065**	**0.02**	**3.3**	**0.0009**	**0.027**	**0.1**
	$\boldsymbol{\theta}$	**(Intercept)**	**-1**	**0.33**	**-3**	**0.0026**	**-1.7**	**-0.35**
		Time	**0.042**	**0.01**	**3.3**	**0.0011**	**0.017**	**0.067**

	α	(Intercept)	-0.023	0.46	-0.05	0.96	-0.92	0.87
		Time	0.012	0.02	0.82	0.41	-0.017	0.042
	β	(Intercept)	-0.44	0.4	-1.1	0.27	-1.2	0.35
		Time	0.03	0.02	1.9	0.057	-0.0009	0.061
ALSbi	α	(Intercept)	0.16	0.34	0.47	0.64	-0.5	0.82
		Time	-0.0053	0.01	-0.4	0.69	-0.03	0.021
ALSncbi	δ	(Intercept)	-0.048	0.5	-0.096	0.92	-1	0.93
		Time	0.016	0.013	1.2	0.23	-0.0097	0.041
	θ	(Intercept)	-0.4	0.5	-0.79	0.43	-1.4	0.58
		Time	0.025	0.015	1.7	0.094	-0.0043	0.054

Imaginary coherence (iCoh)

Significant fixed-effects were observed for non-cognitively impaired patients in β-band, in the synchrony model (Table 14).

Table 14: Synchrony model F-statistics performed for each frequency band of interest. Each rejected null hypothesis ($p<0.05$) reveals the existence of non-zero fixed-effects.

	ALSci	ALSbi		ALSncbi		
Frequencies	β	δ	α	δ	$\boldsymbol{\beta}$	γ_h
p-values	0.9	0.2	0.4	0.1	**0.003**	0.2
F-statistic	0.02	1.9	0.7	2.3	**8.8**	1.4

For each frequency-band model, the fixed-effects and their related statistics are detailed in Table 15. It describes the estimated effects of time (since disease onset) on the EEG power. Depending on the frequency band, the effects differ, but whole brain β-band synchrony significantly decreased over time in ALSncbi patients.

Table 15: Synchrony models fixed-effects and related t-statistics for each frequency band of interest. For each fixed-effect, is given the estimate and its standard error as well as the t-statistic with p-value and confidence intervals. Significant effects are represented in bold. A significant overall time effect was observed in β-band for ALSncbi patients.

	Freq	Fixed-effect name	Estimate	SE	tStat	pValue	Lower	Upper
ALSci	β	(Intercept)	-0.6	0.89	-0.68	0.5	-2.3	1.1
		Time	0.0073	0.007	1	0.3	-0.007	0.021
ALSbi	δ	(Intercept)	-0.27	0.21	-1.3	0.2	-0.69	0.14
		Time	0.0067	0.006	1.1	0.29	-0.006	0.019
		(Intercept)	-0.15	0.18	-0.9	0.4	-0.51	0.2

	α	Time	0.0046	0.005	0.85	0.39	-0.006	0.015
ALSncbi	δ	**(Intercept)**	**-0.3**	**0.14**	**-2.2**	**0.028**	**-0.57**	**-0.033**
		Time	0.0074	0.005	1.5	0.13	-0.002	0.017
	β	**(Intercept)**	**0.45**	**0.16**	**2.8**	**0.005**	**0.14**	**0.77**
		Time	**-0.013**	**0.004**	**-3**	**0.003**	**-0.021**	**-0.0043**
	γ_h	(Intercept)	0.23	0.2	1.1	0.25	-0.16	0.61
		Time	-0.0054	0.005	-1.2	0.23	-0.014	0.0035

2.2. Supplementary note 3: Longitudinal models of motor and cognitive clinical measures

We estimated the longitudinal changes in functional clinical scores (ALSFRS-R and neuropsychological scores) using linear mixed-effects models. The goodness-of-fit was estimated using the negative log-likelihood of the fitted model: the lower the value, the best the model fits the dataset. On average across participants, an ALSFRS-R score decreases by 0.72 points per month. The estimated variance of the random slope $\hat{\sigma}_0$ was of 0.5 and that of random intercept $\hat{\sigma}_1$ was 8. The ALSFRS-R subscores and neuropsychology models can be interpreted similarly. For the ECAS scores models questionnaire version fixed-effects and level of education random-effects were additionally estimated.

*Table 16: Longitudinal models of the clinical measures of functional disability and neuropsychology. Fixed- and random-effects of the linear mixed-effects models describing clinical scores (ALSFRS, ECAS, BBI) progressions over the time of the disease. Standard errors were added in parenthesis. *p < 0.05; ***p < 0.001*

		ALSFRS-R		**Neuropsychology**		
		total ALSFRS-R	upper limbs	total ECAS	fluency	BBI
Negative log-likelihood		-3120	-2107	-1200	-950	-993
Fixed-effects						
Intercept		50 (0.8) ***	12 (0.3) ***	102 (2) ***	16 (0.7) ***	11 (1.6) ***
Version B		-	-	2 (0.9)	0.4 (0.4)	-
Version C		-	-	1 (1)	0.6 (0.5)	-
Time (per months)		**-0.7 (0.05)** ***	**-0.2 (0.01)** ***	**0.2 (0.07)** *	0.04 (0.02)	-0.05 (0.05)
Random-effects						
Participant	**Intercept variance**	8	3	14	4	12
	Time variance (per months^2)	0.5	0.2	0.2	0.01	0.07

Education	**Intercept variance**	-	-	8	2	-
	Time variance (per months^2)			0.02	0.04	
Residual		2	1	5	2	8

The linearity of ALSFRS-scores progression has been discussed, with the hypothesis of a curvilinear evolution proposed (Gordon et al., 2010), but a linear regression remains a valid estimation. In our model, while the rate of disease progression was expected to be participant-specific, the variability in the initial ALSFRS-R score across participants was larger than predicted. This may be due to uncertainty in the estimated onset time. Similarly, the ECAS scores (total and fluency) have already been demonstrated to have a linear progression over time (Costello et al., 2021), and our results supported this hypothesis.

2.3. Supplementary note 4: Checks for potential confounding factors

To evaluate the effect of age, gender or medication on the observed EEG measures progressions, additional statistical tests were performed.

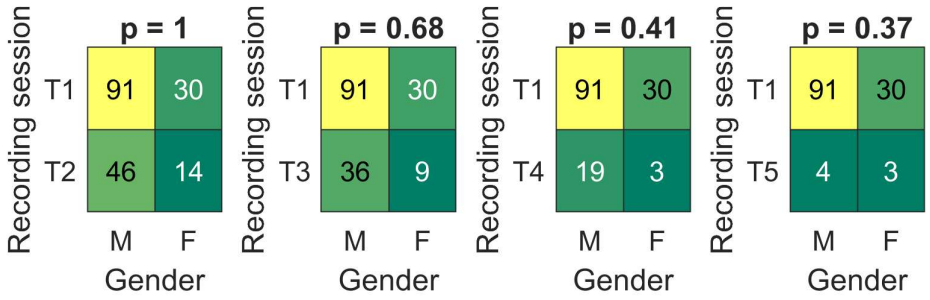

(a) Gender distributions in different recording sessions (T1-T5). Fisher's exact test (α=0.05, two-tailed) did not reveal any non-random association between gender and recording sessions.

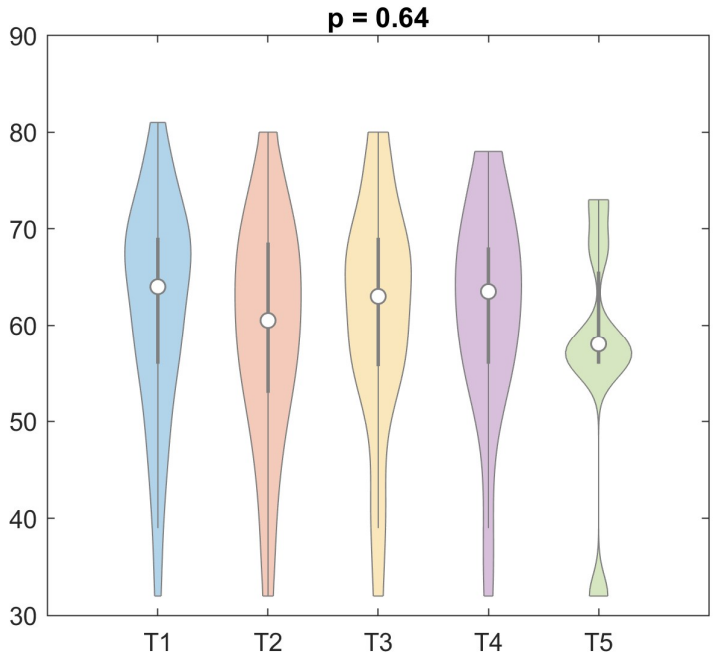

(b) Age distributions in patients' different recording sessions (T1-T5). Kruskal-Wallis's one-way analysis of variance revealed no statistical difference in age distribution between recording sessions. (Bechtold, 2016/2022)

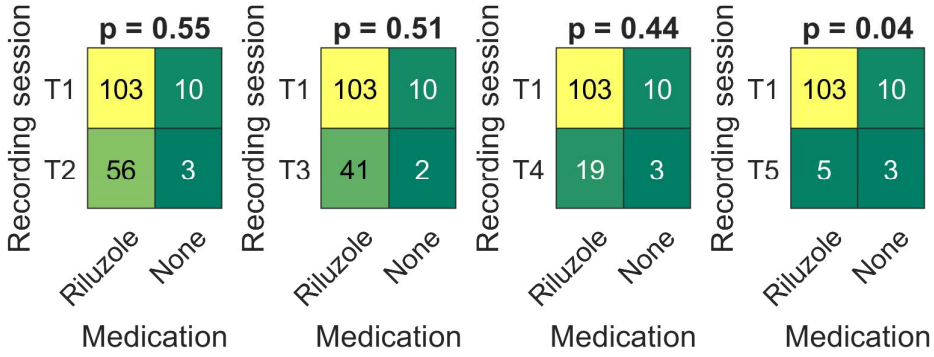

(c) Medication distributions in different recording sessions (T1-T5). Fisher's exact test (α=0.05, two-tailed) did not reveal any non-random association between medication and recording sessions T1 to T4. Unfortunately, the sample size for T5 was too small to be conclusive.

2.4. Supplementary note 5: Additional analyses on the linearity of the EEG measures

To test whether the longitudinal changes of the EEG measures can be estimated by a linear model, we applied a quadratic model to the participants with more than two recording sessions (N=37). For each observed longitudinal change, we assessed potential quadratic time effects, (i.e. EEG ~ Time + Time^2, expressed in Wilkinson notation). For connectivity measures, the inverse normal transformation was used to transform EEG data to a standard normal distribution. The linearity assumption was verified for the majority of the participants ($q<.05$).

In case of a significant quadratic effect, we inspected the patterns of change over time to ensure that despite the non-linearity, the patterns were still monotonic.

2.5. Supplementary note 6: Localisation of significant longitudinal changes of EEG spectral power and functional connectivity in participants with normal and impaired cognition/behaviour

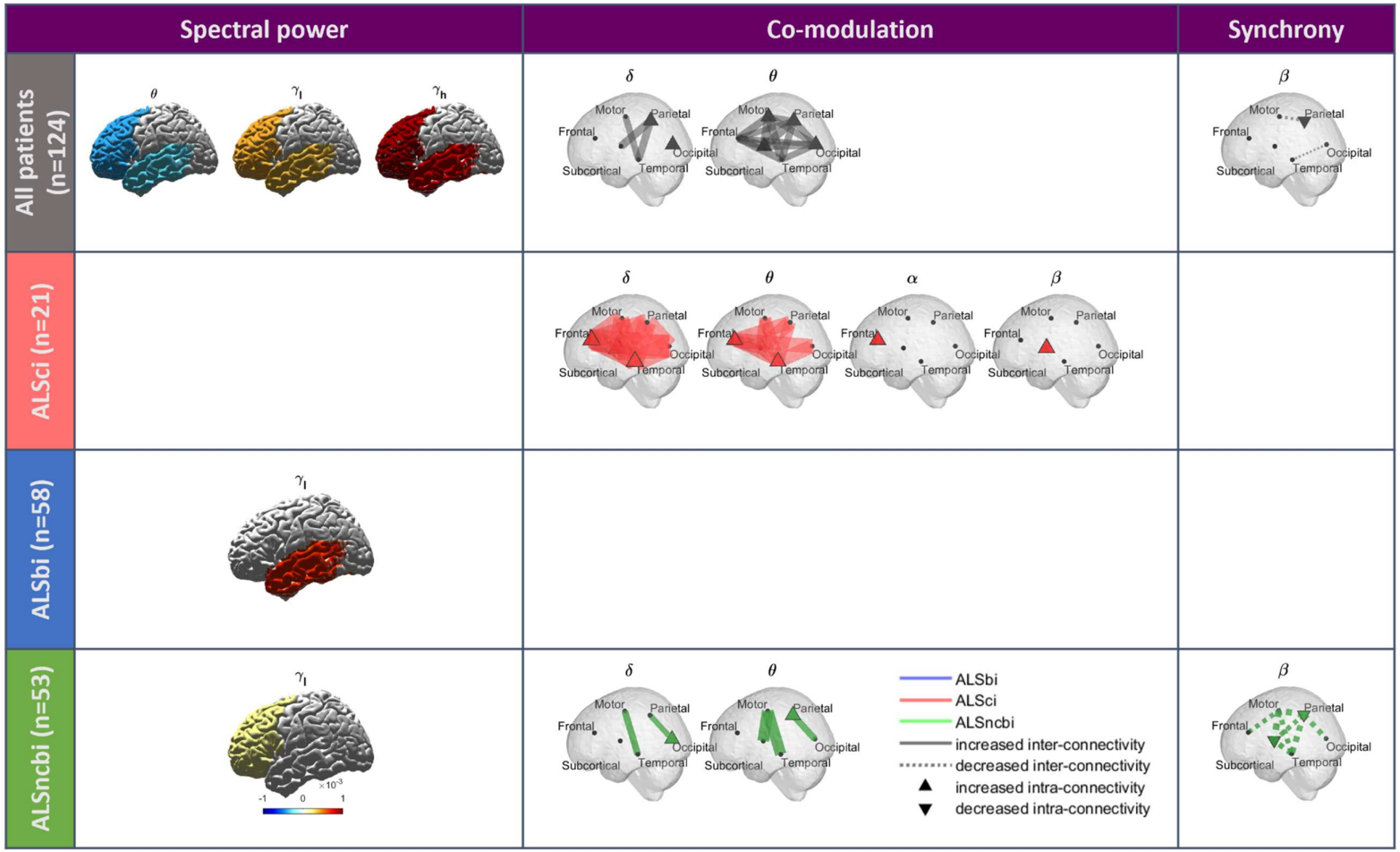

Figure 28: ***Left.*** *Longitudinal changes of EEG spectral power in participants with normal and impaired cognition/behaviour. The significant temporal spectral power variations, in terms of the time fixed-effect and the time ROI-specific random-effects (Bootstrapping, $p<0.05$), were mapped to get a spatial visualisation.* ***Middle-Right.*** *Localisation of longitudinal changes of EEG co-modulation and synchrony in ALS, ALSci, ALSbi and ALSncbi groups. The significant temporal connectivity changes were mapped to get a spatial visualisation of their magnitudes. The temporal variations represent the combined estimated slope (significance by bootstrapping, $q<0.1$). The dashed lines represent a decrease while the solid lines represent an increase in connectivity. A filled node represents significant intra-lobe connectivity.*

3. Appendix – Chapter VI

3.1. Supplementary note 1: Longitudinal analysis of the clinical assessments

*Table 17: Model parameter estimates from longitudinal analyses of clinical scores. Fixed and random-effects of the models describing clinical scores (ALSFRS, ECAS, BBI) progressions over the time of the disease. Standard errors were added in parenthesis. *p < 0.05; ***p < 0.001.*

		bulbar ALSFRS	**lower limbs ALSFRS**	**upper limbs ALSFRS**	**respiratory ALSFRS**	**total ECAS**	**BBI**
log-likelihood		-1883	-2125	-2107	-2259	-1200	-1053
Fixed-effects							
Intercept		12 (0.2) ***	12 (0.3) ***	12 (0.3) ***	12 (0.3) ***	102 (3) ***	11 (1.5) ***
Version B		-	-	-	-	1 (1)	-
Version C		-	-	-	-	0.2 (1)	-
Time (per months)		**-0.1 (0.01)** ***	**-0.2 (0.01)** ***	**-0.2 (0.01)** ***	**-0.1 (0.01)** ***	**0.2 (0.06)** *	-0.06 (0.05)
Random-effects							
Subject	*Intercept variance*	2	4	3	3	13	11
	Time variance (per months^2)	0.1	0.1	0.2	0.1	0.1	0.07
Education	*Intercept variance*	-	-	-	-	8	-
	Time variance (per months^2)					0.02	
Residual		0.9	2	1	1	5	8